

## *1. INTRODUCTION*

The High Enthalpy Geothermal Energy for the production of electric energy, has got a growing projection of the 27.9 % for 2035 at a global level, in agreement with data of the International Energy Agency (IEA).

The same IEA, established that in 2012, two thousands of millions of dollars were invested in this activity.

Among the most relevant advantages of geothermics, the low technology cost for power generation, with respect of others RES, is worth to mention. In fact, an average cost of 52 dollars for each MWh has been determined, opposite to the 280 dollars required by solar energy, the 100 dollars of marine aeolian energy generation and the 131 dollars required by biomass energy production. (SENER, 2012).

A number of technologies have existed for almost a century to extract this virtually inexhaustible source of power, and today many countries in the world are investing heavily in developing high-temperature geothermal plants. Countries around the Pacific Rim are especially well placed geographically for high-temperature geothermal power, and the United States, Indonesia and the Philippines are world leaders in this field.

In this context, Mexico is ranked fourth in geothermal power generation worldwide, with the 2.02 % of electric energy generated with this technology, which corresponds to about 7,047 GWh per year (Gutierrez-Negrín, 2010). The total national consume of electric energy reached 229,318 GWh in 2011, which represented a 7.2% increase with respect of 2010. (SENER, 2012).

As a matter of fact, in Mexico the geothermal resources have become more and more important with the passing of time. There, the geothermal resources are present all around the country, and 4 geothermal Fields are operating since decades. For the Mexicans, Geothermal resources represent a strategic opportunity for supporting the national energy consume. Therefore, researches and applications on this energy sector have been developing and improving with the passing of time,

making Mexico to become one of the best developed countries in the Geothermal energy sector.

In 2014, a collaboration program was started between the main electric energy company of Mexico, the Comisión Federal of Electricidad (CFE), and the University of Padua, in order to share knowledge and information about the exploitation in Geothermal Fields.

On this purpose, the present work have been realized, in collaboration with CFE personal, at the Los Azufres Geothermal Field in Mexico, for the developing and improvement of the local geothermal reservoir exploitation. The goal of the work was to verify how the multidisciplinary method of work that is adopted there (which includes geological, structural, geophysical, petrographic, geochemical and engineer skills), for the identification of the drilling depth of a new production well, has the capacity of reducing the drilling risk, and its applicability in other geothermal fields of the World.

## 2. RENEWABLE ENERGY RESOURCES AND GEOTHERMICS MARKET

### 2.1 GLOBAL ENERGY SUPPLY

According to the US Energy Information Administration's 2011 report, the current global electric energy consumption is estimated at 471.8 Exajoules ( $EJ = 1 \cdot 10^{18} J$ ) with fossil fuels supplying 78% (oil, coal and natural gas) [1]. The largest consumption of fossil fuels involves the Pacific Region, especially China, Japan, India and South Korea where the 35 % of the worldwide total electrical energy consumption occurs.

However the fossil fuels reserves are limited and their exploitation contributes more or less directly to the worsening of environmental conditions, such as acid precipitation, depletion of stratospheric ozone barrier and global climate change.

In this global context, Renewable Energy Resources (RES) play a major role in sustaining the global energy demand, supplying about 19% of the request in 2011, and in the environment protection, as they are defined as *sustainable resources available over the long term, at a reasonable cost, that can be used without negative effects* (Alemán-Nava et al., 2014). RES include biomass, hydropower, wind, solar, geothermal and biofuels. (Figure 1 - Alemán-Nava et al., 2014).

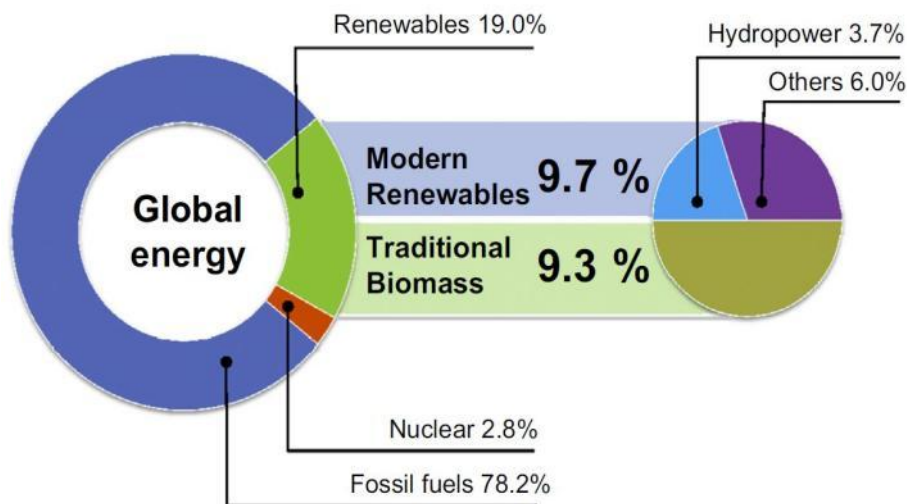


Figure 1: Global energy supply diagram, showing the dominance of fossil fuels compared with renewable energy sources (modified from Alemán-Nava et al., 2014).

The amount of 19% supplied by RES is divided as follows: traditional biomass accounts for 9.3%, while modern renewable resources for the remaining 9.7%. In this 9.7% they are included hydropower (3.7%) and wind, solar, geothermal and biofuels (6%).

In terms of power generation installed capacity, RES contribution on a global scale reached about 1470 GW in 2012. Hydropower stations accounts for 67% of the total installed capacity of RES and 33% is accounted by the non-hydro renewable sources, including Geothermics (Alemán-Nava et al., 2014)..

The RES sector has developed a lot in the last years, thanks to global new investments and research in renewable sources (Figure 2), and it is expected to continue growing while the cost of production is expected to decrease due to accelerated technologies development and scientific progresses in the research of renewable energy sources and equipment improvements. (Alemán-Nava et al., 2014).

*G.S. Alemán-Nava et al. / Renewable and Sustainable Energy Reviews 32 (2014) 140–153*

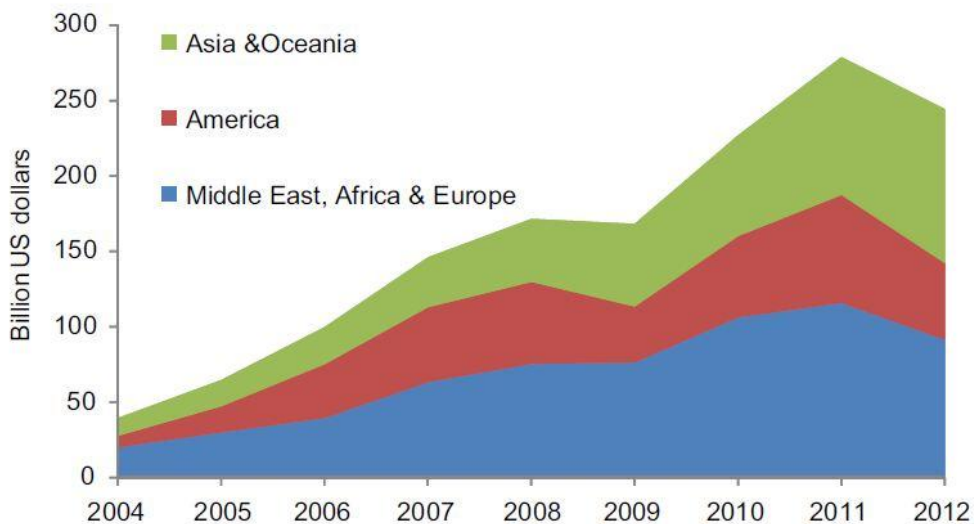


*Figure 2: Diagram showing the trend of investments in renewable resources for each area of the World, during the period 2004-2012 (from Alemán-Nava et al., 2014).*

## 2.2 MEXICO'S GLOBAL ENERGY SUPPLY

In 2011 in Mexico, the use of hydrocarbon fuels accounted for 88.7% of the total primary energy supply, while that of renewable energy sources about 6.7% (Figure 3 - Alemán-Nava et al., 2014).

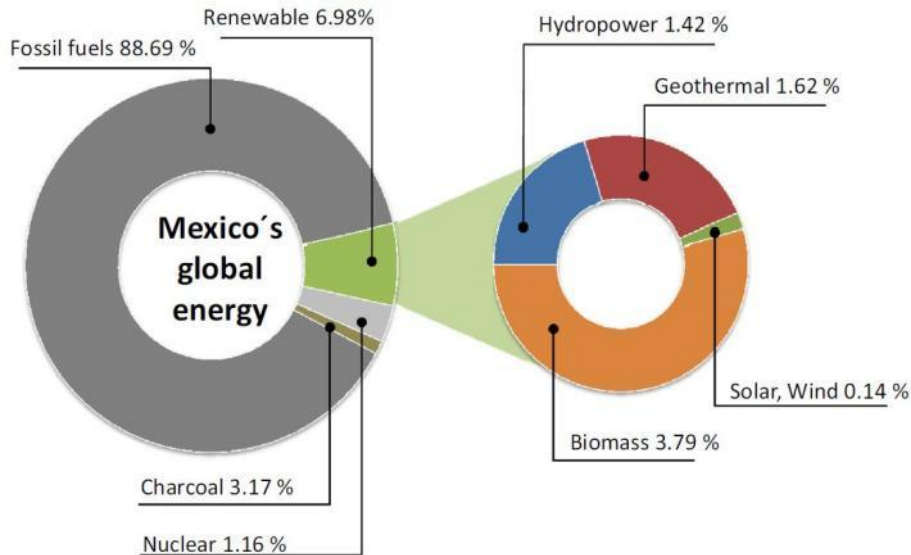


Figure 3: Pie chart showing Mexico's percentages in the internal energy supply with the different type of sources (from Alemán-Nava et al., 2014).

Concerning the mere production of electricity (including both internal use and export use), data updated to 2011 show a total of 76.47% of electric energy produced with fossil fuels, while the 4.44% is produced with charcoal and nuclear sources, and the 19.09% is produced with RES. In particular, geothermal energy contributes for the 2.17% of the Mexico's electric energy production (CFE, 2011).

Definitely, the dependence on fossil fuels is really problematic for Mexico, because the national reserves of hydrocarbon in 2007 were considered sufficient to support the annual oil and gas production just for 9.6 and 8.9 years respectively (that is why Mexico increased the energy imports, which in 2008 was 15% of Diesel, 40% of gasoline and 15% for natural gas), In addition, fossil fuels contributes to an annual non-biogenic CO<sub>2</sub> emissions of 4.3% in Mexico, that is one of the highest in the world (Alemán-Nava et al., 2014).

The good thing for Mexico, which had an estimated population of 112.3 million in 2010 with a growth rate of 0.9%, is that about 56.5% of all public investment is directed to energy projects, employing around 250,000 workers. The CFE (Comisión Federal de Electricidad) is the 6<sup>th</sup> largest power company in the world and electricity generation covers about 95% of national population. Mexico itself is the 16<sup>th</sup> producer of electricity (Alemán-Nava et al., 2014).

In fact, Mexico experienced a series of reforms in the energy sector since the 1990's. Recently the Congress of the Union approved the Energy Reform where the articles 25, 26 and 27 of the Constitution were modified to allow the participation of private companies in the energy sector (mainly power generation), in order to share technology and expertise. Indeed, in the recent presidential period from 2006 to 2012, renewable resources were given an important role in the National Strategic Plan for Development (NDP). Mexico adopted the Law for Climate Change in May 2012, setting the goal of 35% of energy generation coming from renewable resources by 2024. Furthermore, the Law for the Use of Renewable Energy and Finance of the Energy transition was recently modified and approved, establishing the legal aspects for the use of renewable sources and clean technologies, and creating a Fund for the support of energy transition, energy saving, clean technologies and renewable energy. So, Mexico has the legal instruments for a future green economy (Alemán-Nava et al., 2014).

Power generation installed capacity from RES in Mexico was 14357 MW in 2012. From this capacity, 80.8% belongs to hydropower, 8.5% to wind energy, 6.7% to geothermal energy and 0.2% to solar energy (Alemán-Nava et al., 2014).

Concerning Geothermal energy, Mexico ranks 4<sup>th</sup> in geothermal power generation worldwide. The geothermal installed capacity at present time is 959.50 MW (CFE 2011), but its potential in Mexico has not been fully evaluated.

It is worth saying that, for example, an installed capacity of 228 MW, approximately generates 1736 GWh (equivalent to 6250 TJ), which saves about 3 millions of equivalent oil barrels each year (CFE, 2011).

In 2000, The Electric Investigation Institute (Instituto de Investigación Eléctrica) published the Geothermal Chart of Mexico at scale 1:2,000,000 (Torres-Rodríguez, 2000), as the result of geological and geochemical analysis of 1451 thermal sources known until 1999 in Mexico (Figure 4).

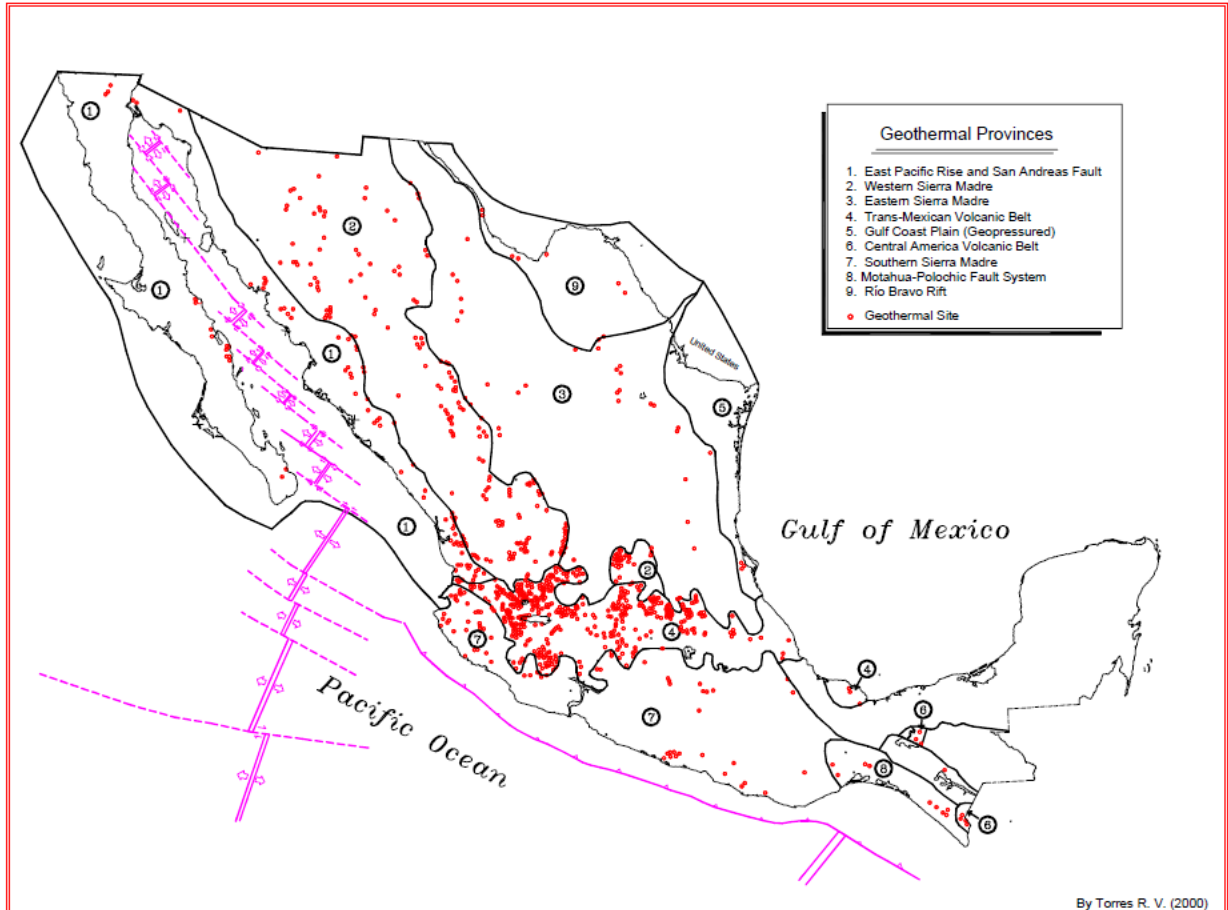


Figure 4: the geothermal chart of Mexico (from Torres-Rodríguez, 2000).

In Figure 4 it is possible to observe that the highest concentration of geothermal sites is, without any doubt, in the geothermal province called Trans-Mexican Volcanic Belt (see Chapter 4.3).

There are in Mexico four geothermal fields in operation (Cerro Prieto, Las Tres Vírgenes, Los Azufres and Los Humeros), all managed by CFE, while another one (Cerritos Colorados), is still under study (Ormad, 2014) (Figure 5). The Cerro Prieto field, the biggest and oldest in Mexico, still has an installed capacity of 720 MW, but the two oldest units of 37.5 MW, are currently out of operation.



Figure 5: the geothermal fields active in Mexico (modified from Gutierrez-Negrin, 2012)

CFE has planned to increase the installed capacity in three of the geothermal fields. In table 1 geothermal projects planned by CFE in 2011, referred to three of the geothermal fields at disposal, such as Los Humeros, Los Azufres and Cierro Prieto, are shown. (Table 1 - Gutierrez-Negrin, 2012).

Field	Project (and Planned Date of Commissioning)	Under Construction or Planned Capacity (net MW)		
		New	Retirements	Additional
Cerro Prieto	Cerro Prieto V (2017)	100	75	25
Los Azufres	Los Azufres IIIa (2014-15)	50	20	30
	Los Azufres IIIb (2018)	25	15	10
Los Humeros	Los Humeros II (2013)	50	15	35
	Los Humeros III (2016)	50	25	25
Total		275	150	125

Table 1: Geothermal projects reported in the CFE's master plan known as POISE (Programa de Obras e Inversiones del Sector Eléctrico, 2011) (from Gutierrez-Negrin, 2012).

The unit Los Humeros II was completed in 2013 with the installation of a 50 MW unit of electric power generation. The projects named Los Azufres IIIa (50 MW) and Los Humeros III (50 MW) will be completed by 2015 and 2016 respectively. Further, Cerro Prieto V (100 MW) will be built by 2017 and Los Azufres IIIb (25 MW) by 2018. Totally 275 MW will be installed, and, at the same time, some of the oldest and technologically underdeveloped geothermal plants would be dismantled, subtracting 150 MW. So, as a whole, 125 MW would be added to the national electric line.

### 3. *GEOTHERMAL ENERGY*

#### 3.1 *THE GEOTHERMAL ENERGY RESOURCE*

The term Geothermal originates from two Greek words ‘GEO’ and ‘THERME’. The Greek word ‘geo’ can be translated as ‘the earth’, while the word ‘therme’ means ‘heat’. So, in general terms, Geothermal Energy is energy derived from the heat which exists inside the Earth.

To form a Geothermal systems are essentially required heat, a permeable rock formation and water. The heat is transmitted to the water and rock forming what is called a “Geothermal Reservoir”.

The classification of Geothermal Energy is based on the temperature (or Enthalpy) of the reservoir (Figure 6 – IGC, 2011):

- Very Low temperature (or Enthalpy): Energy is produced by extracting heat (at a maximum of 40°C) from the subsoil or in near-surface aquifers at depths of a few meters to 200-300 meters. In this case, the underground is used as a heat exchanger, by means of heat pumps arranged as closed or open circuit. These applications can be used for heating, cooling and producing domestic hot water in individual housing, but also in the tertiary sector and in collective housing. These kinds of reservoirs may be anywhere, because their efficiency is just determined by the underground thermal inertia in normal (average) geothermal gradient conditions.
- Low temperature (or Enthalpy): The temperature of these reservoirs is between 100 and 40 °C. They are located in areas with a favorable geological context including deep aquifers; the geothermal gradient is like the average in the region. Their exploitation involves pumping hot groundwater from the aquifer and re-injecting it after it has delivered the heat and is cold again. These are used in direct applications and for district heating systems and industrial processes.

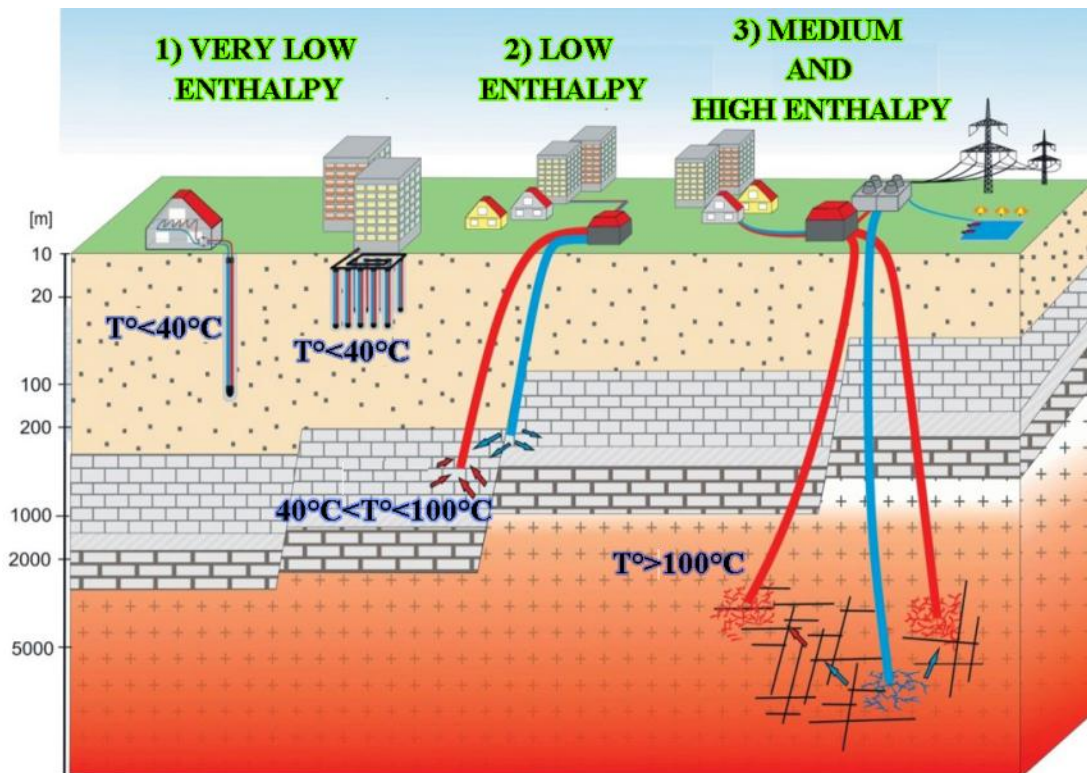


Figure 6: Examples of different types of geothermal reservoirs: 1) **Very low temperature**: Ground thermal inertia is exploited through different types of buried heat exchangers that provide a stable fluid temperature to heat a house or a building in winter and cold it in summer. 2) **Low temperature**: Groundwater is drawn from a deep aquifer to exchange heat within an urban district heating system, and cold water is re-injected. 3) **Medium and High temperature**: In a deep granitic basement beneath a sedimentary cover, hot water is extracted in such a way that it directly generates hot steam for electricity production (High temperature). Otherwise, cold water is injected and hot water is extracted to directly produce electric energy (Medium temperature - EGS technique) or to produce it through the use of a secondary fluid circuit (Binary cycle technique) (IGC, 2011).

- **Medium Temperature (or Enthalpy)**: The reservoirs usually reach temperatures between 100 and 150 °C. Heat is transported by conduction through the crustal rocks, with an average gradient of 30°C/km and peak values of 60°C/km (*Hydrothermal Conduction System*). Those types of systems are Warm Groundwater Basins, Deep Sedimentary Aquifers, Warm Springs Fracture and Fault Systems, Geopressed Systems and Engineered Geothermal Systems (Grant et Bixley., 2011). Despite these reservoirs have a lower temperature compared to the high temperature ones, they allow extracting sufficient heat to produce electricity (but with lower performances) using a volatile fluid. Moreover, those types of reservoir can be used also for heating, and their main applications are in district heating systems and industrial processes.

- **High Temperature (or Enthalpy):** Heat is extracted from subsurface areas where temperatures greater than 150-200°C, are detected, which made it possible to produce electric energy power. In this context, there is usually heat, generated by a magma, which doesn't reach the surface as lava, but it remains below the Earth's crust, heating nearby rock and water, and increasing the geothermal gradient. The geothermal reservoir is formed by hot water or steam trapped in permeable and porous rocks under a layer of impermeable ones (see below: *Hydrothermal Convective Systems*). This hot geothermal water can manifest itself on the surface as hot springs or geysers, but most of it stays deep underground, trapped in cracks and porous rock. (Figure 6 – IGC, 2011).

In this work, the *High Enthalpy* Geothermal Energy Systems are taken into account.

In particular, we are dealing with *Hydrothermal Convective Systems*, which are geothermal systems with high temperatures, geothermal gradient higher than the average and usually surface activity, where the flow of hot fluid goes through the rock system and determines the temperature and fluid distribution. Fluids ascend through fractures towards less deep zones to form the geothermal fields. As it has been said, High-temperature hydrothermal convective systems demand some additional heat above the normal conductive gradient, which is usually given by close contact with some magmatic body (Figure 7) (Grant et Bixley., 2011).

At the present time, all major geothermal power stations in Mexico operate on such hydrothermal convective system, which is constituted by:

- a) The large heat source;
- b) A permeable reservoir;
- c) A supply of water;
- d) An overlying layer of impervious rock;
- e) A reliable recharge mechanism;

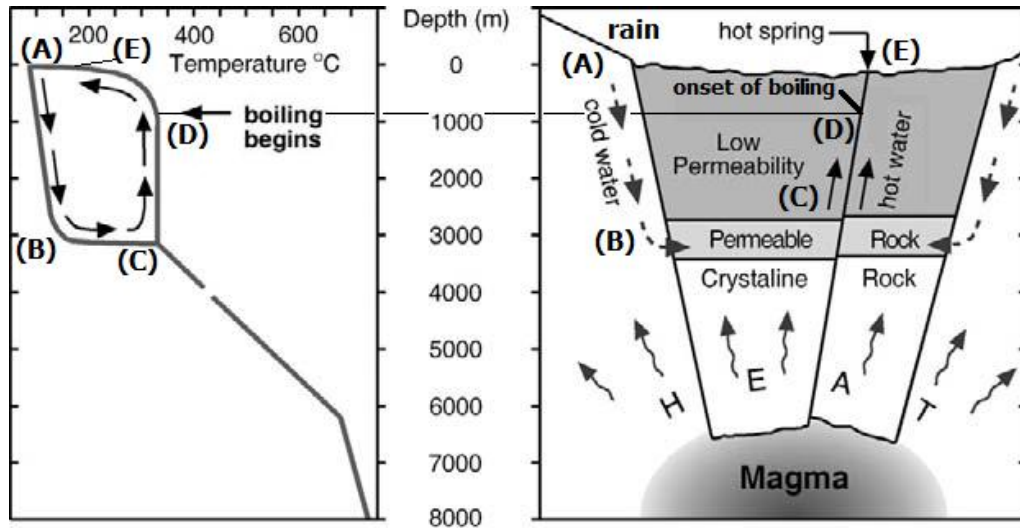


Figure 7: Cold recharge water is given as rain water (point A), percolating through faults and fractures down into the formation where it comes in contact with heated rocks. The permeable layer allows water to spread into the rock formation (point B) and, as the liquid heats, it becomes less dense and tends to rise within the formation. If it encounters a major fault (point C) it will ascend toward the surface, losing pressure as it rises until it reaches the boiling point for its temperature (point D). There it flashes into steam which can emerge as a fumarole, a hot spring, a mud pot, or a steam-heated pool (point E) (modified from Grant et Bixley, 2011).

It is not possible to have a High-Temperature Hydrothermal Convective System without (a) and (d) and there are no artificial methods to make it possible. On the other hand, insufficient permeability (b) can sometimes be overcome by hydraulic fracturing (called “hydrofracking”) in which high-pressure liquid is injected from the surface through wells to open fractures by means of stress cracking. If little water (c) is present in the formation or recharge is lacking, all unused geofluid from the plant can be reinjected. Furthermore, external fluids can be brought to the site and injected into the formation (Di Pippo, 2007).

High-Temperature Hydrothermal Convective Systems are generally found in regions of relatively recent volcanism. This explains the large number of geothermal fields associated with volcanic arc and crustal rifting. The fractures are the flow paths for the water circulation, and they appear to be associated with structures at regional scale, such as rift zones or calderas. (Grant et Bixley, 2011). Without any doubt, trenching or subduction is one of the most important mechanisms that give rise to high-temperature geothermal regions. Furthermore, another important

mechanism is tension, and in this case the plate can relieve the stress by cracking and rifting, by down-dropping, and by thinning (Figure 8 – Di Pippo, 2007).

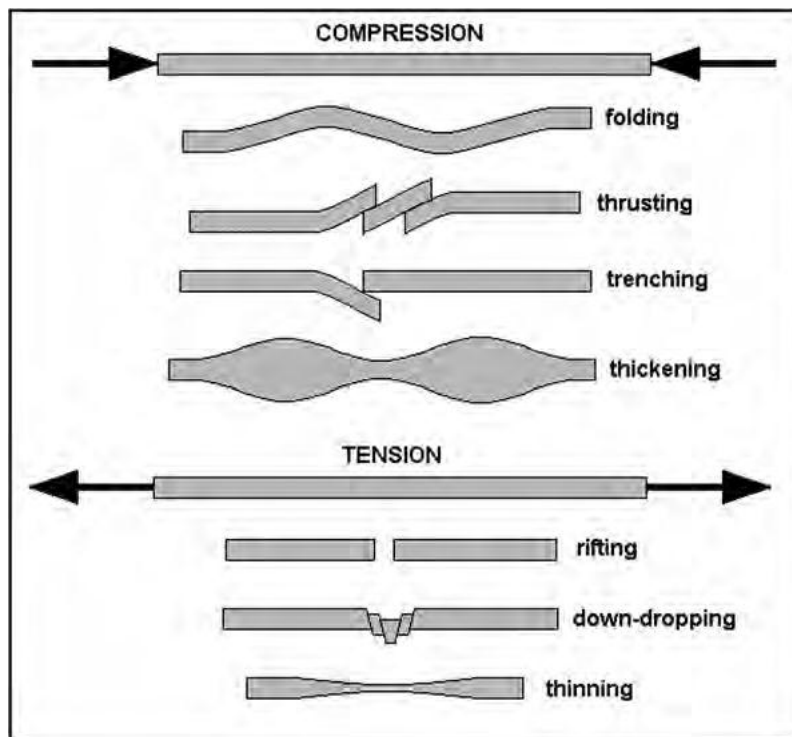


Figure 8: image showing the plate response to compression and tension. All of these responses to compression and tension lead to anomalous geothermal regions that may be conducive to exploitation (Di Pippo, 2007).

Two plates may also slide past each other along what is called a *transform fault*. Perhaps the most famous one is the San Andreas Fault running along much of the length of California in the United States. This fault, and others related to it, have caused immeasurable harm and financial loss from numerous earthquakes, but also has given rise to several commercial geothermal resources.

From the viewpoint of geothermal exploitation, the most important interaction between plates boundaries occur along the edges of the gigantic Pacific plate, in what is called the “Pacific Ring of Fire”. If we include the two adjacent eastern plates, the Cocos and the Nazca plates, as well as the western one, the Philippine plate, then the following countries (in clockwise order) are affected: United States, Mexico, Guatemala, El Salvador, Honduras, Nicaragua, Costa Rica, Panama, Colombia, Ecuador, Peru, Bolivia, Chile, New Zealand, Micronesia, Papua New Guinea, Indonesia, Philippines, China, Japan, and Russia. All 21 of these countries

have exploitable geothermal resources and 13 of them have geothermal power plants in operation as of mid-2007. Generally speaking, subduction zones exist beneath all land masses in contact with the Pacific, Cocos and Nazca plates, except in the contiguous California and Baja California of United States and Mexico, where transform boundaries exist. (Figure 9, Di Pippo, 2007)

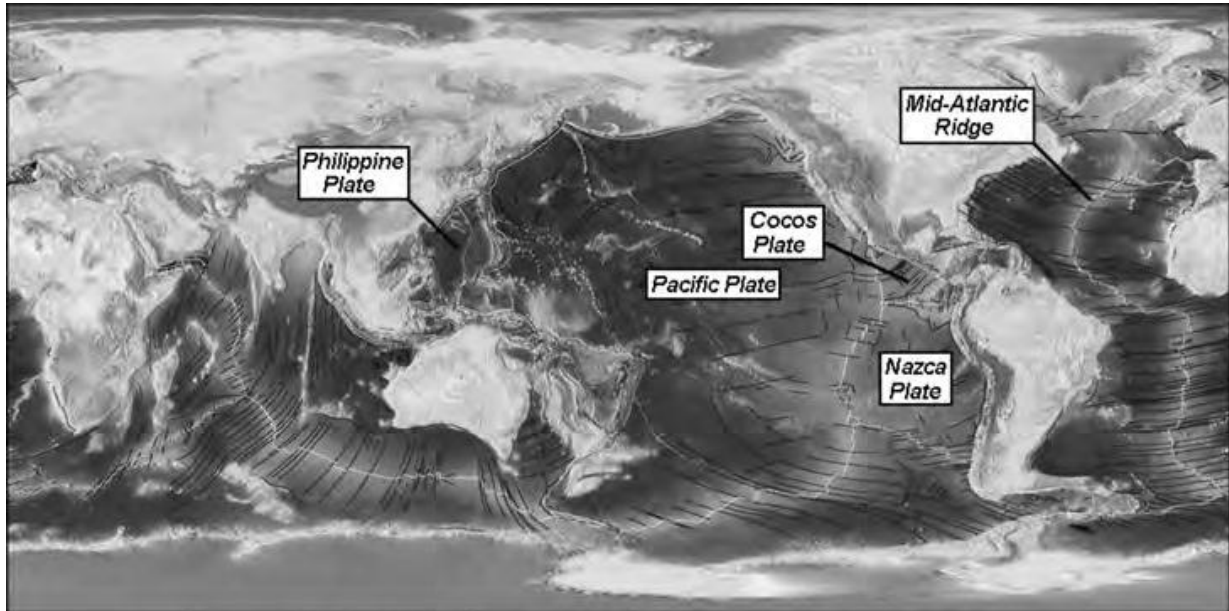


Figure 9: Collocation of main tectonic plate boundaries of the Pacific Ring of Fire (Di Pippo, 2007).

### 3.2 HIGH ENTHALPY RESERVOIR EXPLOITATION

The denomination *Geothermal Field* implies the presence of a Geothermal Reservoir with relatively high heat flow, whom Profitable exploitation is practicable or viable (Salas, 1988).

Geothermal reservoirs can produce a mixture of water and vapor (which is the most common circumstance), dry vapor, overheated vapor, or hot water alone. So, as a consequence, Geothermal Reservoir can be defined as *Liquid-Dominant* or *Vapor-Dominant*, depending on the percentages of liquid and vapor which are found in it. Another type of reservoir is that which is called *Compressed Liquid-Dominant*, where the water is exposed to a pressure that is greater than the saturation pressure for the given temperature.

In the generation of electric energy in a geothermal process, hot pressurized water can pass to vapor phase very rapidly by artificial methods through the pipes of geothermal wells. The technology used for the construction of geothermal wells is similar to that of oil wells, though in general geothermal wells are less deep and with a larger diameter. The deep at which geothermal fluids are stored is variable, from a few meters to 4500m approximately, changing from zone to zone (Di Pippo, 2007).

A Geothermal Well is a: a) *Production Well*, if it presents optimum conditions of Pressure and Temperature, and thus the utilization of the geothermal resource is feasible for the generation of electric energy; b) *Injection well*, if the residual exhaust water produced in the geothermal field is discharged there; the residual exhausted water can derive from water separated from vapor, if the reservoir is composed of a gas-water mixture, from water circulating through condensates formed into pipelines and into the *back-pressure* generation units (see below), and from cooling water of cooling towers *condensation* units (see below); in other words, wells which do not present appropriate conditions of pressure and temperature to be used as producers, but are confined in deep and permeable geological formations, connected with the geothermal reservoir, are used as injectors; c) *Exploratory Well*, if it is utilized to investigate the thermodynamic characteristics of a possible exploitable zone (CFE, 2011).

In order to understand where exactly a new well would be drilled, several analyses belonging to different areas of investigation (geology, geophysics, geochemistry, reservoir engineering, environmental science) have to be carried out, of whom this work is an example. Once the location of a Production well is defined, the perforation can be done and the extraction of the geothermal fluids can start. At this point, different engineering solution can be adopted to produce electrical energy. The production cycles employed in the Units of Electric Power Generation using geothermal sources can be summarized as follow:

- Back-pressure Cycle (Figure 10): this is the simplest and cheapest in initial investment among all geothermal cycles. Vapor from wells, either coming directly from dry wells or after having passed through a separator in the case of wet wells, passes through a turbine and then it is discharged directly in the

atmosphere. Back-pressure cycles have their applications in pilot plant, reserve plant, in little local supply for isolated wells and also (even though in little degree) to cover maximum charges. In addition, this cycle is employed if non-condensable gas content exceeds 10%, due to the high energy required to extract those gases in a condenser. (Flores-Alcalá, 2012).

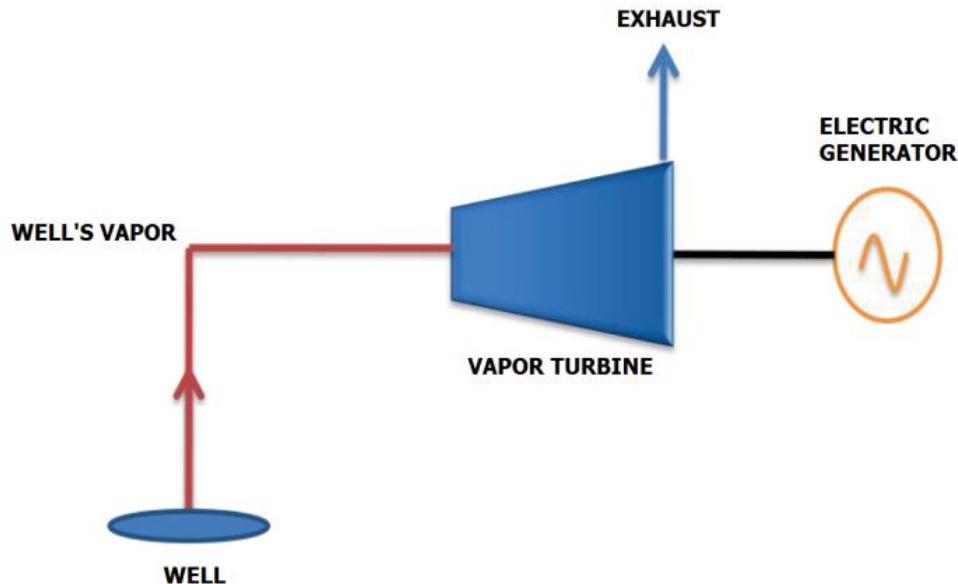


Figure 10: diagram of back-pressure cycle (modified from Flores-Alcalá, 2012).

- Condensation Cycle (Figure 11): in this cycle the vapor from wells (separated from water through a separator equipment of cyclonic type installed in the platform of the well<sup>1</sup>) enters in the turbine and generates electric energy, then it goes to a condenser (normally a Direct-Contact condenser or Surface Condenser<sup>2</sup>) to become partially liquid and finally is pumped to the cooling tower where a pool of condensed vapor forms and it can be reinjected.

<sup>1</sup> *Cyclonic Type Separator*: The mixture enters in this separator following a tangential trajectory in relation to the equipment body, inducing a centrifugal force that allows phases to separate. Water gains more inertia because it has more density than vapor, and so it tends to stick on the walls of the separator and to fall down in the lower part of the equipment.

<sup>2</sup> *Direct-Contact Condenser*: a device

in which a vapor, such as steam, is brought into direct contact with a cooling liquid, such as water, and is condensed by giving up its latent heat to the liquid (from The Free Dictionary by Farlex)

*Surface Condenser*: an apparatus for condensing steam, especially the exhaust of a steam engine, by bringing it into contact with metallic surface cooled by water or air (from the Webster Dictionary).

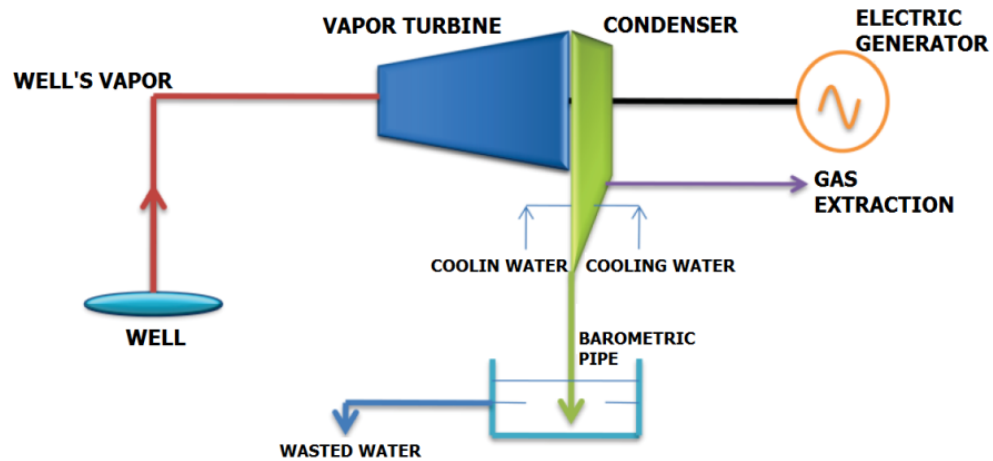


Figure 11: diagram showing the Condensation Cycle type (modified from Flores-Alcalá) 2012).

- Binary Cycle (Figure 12): in this cycle, part of the heat of the geothermal fluid is transferred to a Heat Exchanger working with a secondary fluid, which in general is a refrigerant like isobutene or isopentene, whose boiling point is low,  $-12$  and  $28^{\circ}\text{C}$  respectively. The secondary fluid passes through a closed circuit. After its evaporation it can pass through the turbine, achieving Work and then it's cooled in the Condenser until it reaches again the liquid phase, in order to be pumped and re-injected again in the cycle. Water used in the condenser is proportioned for one cooling tower, and the geothermal fluid that lost its heat is sent to a reinjection well. In many geothermoelectric plants of Los Azufres, the residual energy of hot liquid water is utilized from those types of units. (Flores-Alcalá, 2012).

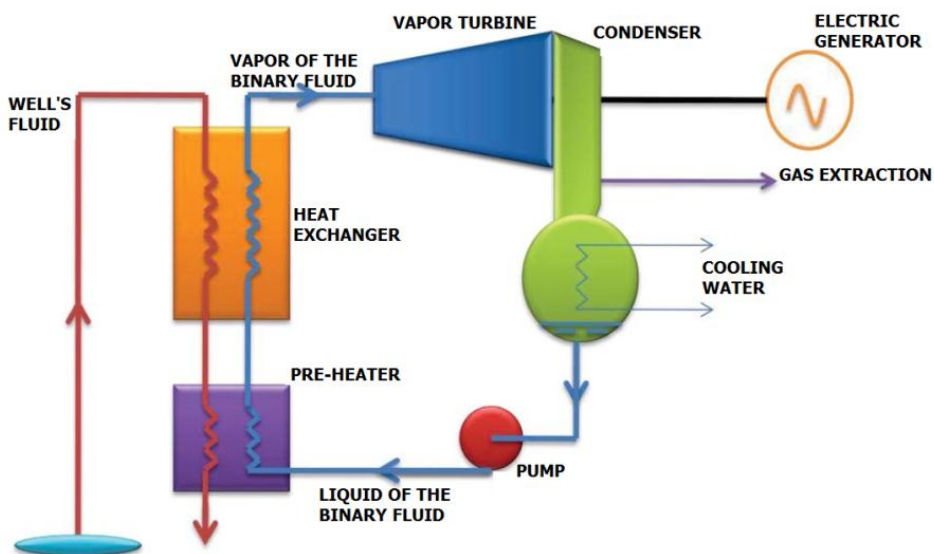


Figure 12: diagram showing the Binary-Cycle type (modified from Flores-Alcalá, 2012).

It is important to mention that *Back-pressure cycle* is a technology which is considered to be obsolete, because it can consume more or less twice the vapor (for the same pressure of entrance and generated power) than Condensation Cycles. So, the number of wells necessary to produce the same amount of electrical energy is higher than that for Condensation Cycles, as well as the costs for the operations. By the way, in a *Condensation cycle*, the use of a condenser allows to extract more energy from the fluid and to increase the efficiency of the plant. So, this technology is currently the most employed in Geothermal Fields. Steam temperatures necessary for the functioning of Back-pressure and Condensation Cycles are the same, usually above 200°C. For what concerning the *Binary Cycle*, the advantages are that a water-steam mixture can be used without any separation process, chemical aggressiveness is confined only in the heat exchanger and temperatures of the reservoir can be lower than 200°C. On the other hand, disadvantages of this cycle are that heat-exchangers are expensive and refrigerant fluids are toxic (Flores-Alcalá, 2012).

As it has been mentioned before, the exploitation of geothermal resources is supported by scientific tools, and nowadays they are easily available and routinely used. The scientific research precedes the costly phase of deep well drilling, and is based on geological, volcanological, geophysical, geochemical and reservoir engineering studies. The purpose is to determine a reliable position of drilling sites, increasing the probability of success. For the research on new possible geothermal fields, the ultimate exploration tool is the drilling of deep wells based on the findings of the scientific surveys (see definition above: *Exploration Well*). This is the best way to obtain precise information of the subsurface nature, planning a good exploration program that should give a reasonable estimate for the properties of the reservoir. For the research on geothermal fields which are already operative, information about a new area of study can be given by the correlation between information of already drilled wells. (Di Pippo, 2007).

In this particular thesis work, it is presented an example of scientific research conducted preliminarily in geothermal resources exploitation.

### 3.3 EXPLOITATION AT THE LOS AZUFRES GEOTHERMAL FIELD

The Los Azufres Geothermal Field (Figure 13) occupies the second place in Mexican Republic rank of electric power generation by geothermal energy. It is located in the State of Michoacán, 80 km east from the city of Morelia and 16 km north-west from Ciudad Hidalgo. The field is located above a hydrothermal volcanic complex at an elevation ranging from 2500 to 3000 m above sea level.

The extraction of the natural resource for business purposes began in 1982, with the installation and the putting into service of five back-pressure units of 5 MW, and it had been gradually growing until the activation of 4 units of 25 MW in 2003 (Los Azufres II Geothermoelectric Project) with an annual supply of 1779 t/h of vapor.

The perforation of the first well began in august 1977 and the production in the field has been maintaining active since that time uninterruptedly.

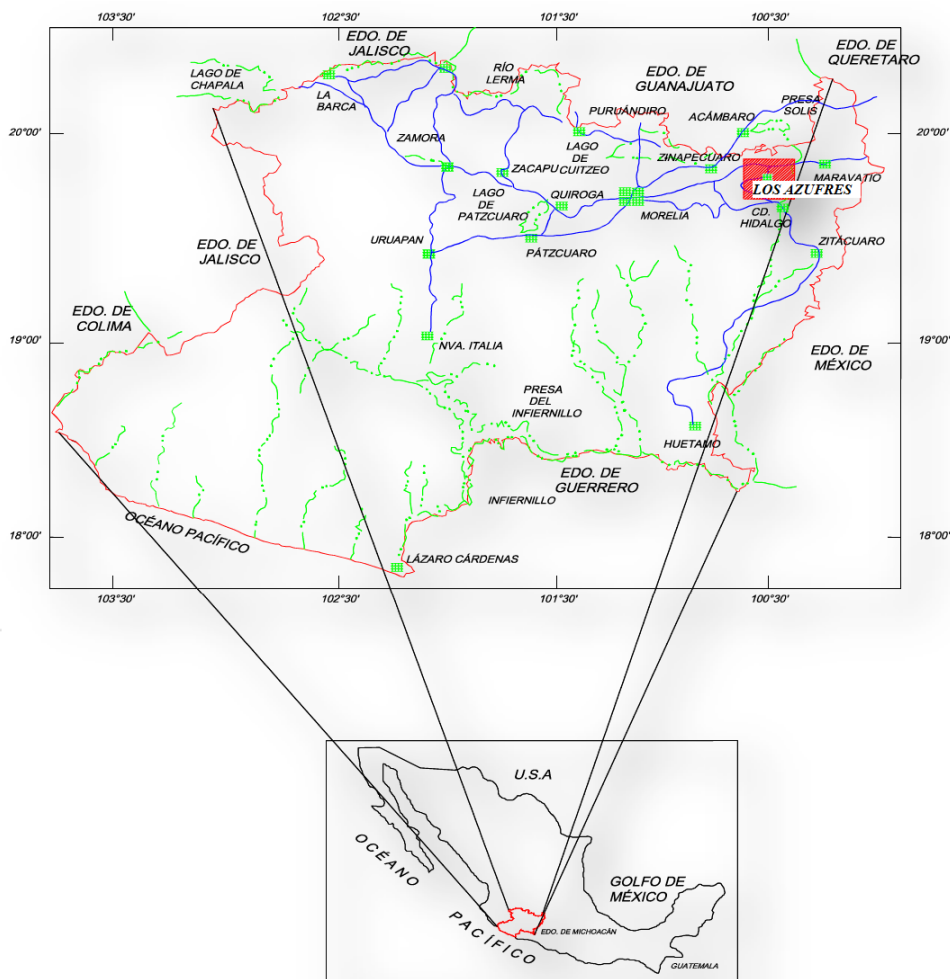


Figure 13: Geographical map showing the location of the Los Azufres geothermal field within the Mexican Republic (modified from Gutierrez-Gomez, 2005).

The Los Azufres geothermal field reservoir was thought to be *liquid-dominant* in its natural state, but different studies discovered that there are three thermodynamically different zones: *vapor-dominant* in the shallowest part of the reservoir, *liquid dominant* in its saturation state and *compressed liquid-dominant* in the deepest part; wells that are integrated into the electric power generation system extract the fluid by these last two zones.

So far, in the Los Azufres geothermal field 82 wells have been drilled (Figure 14).

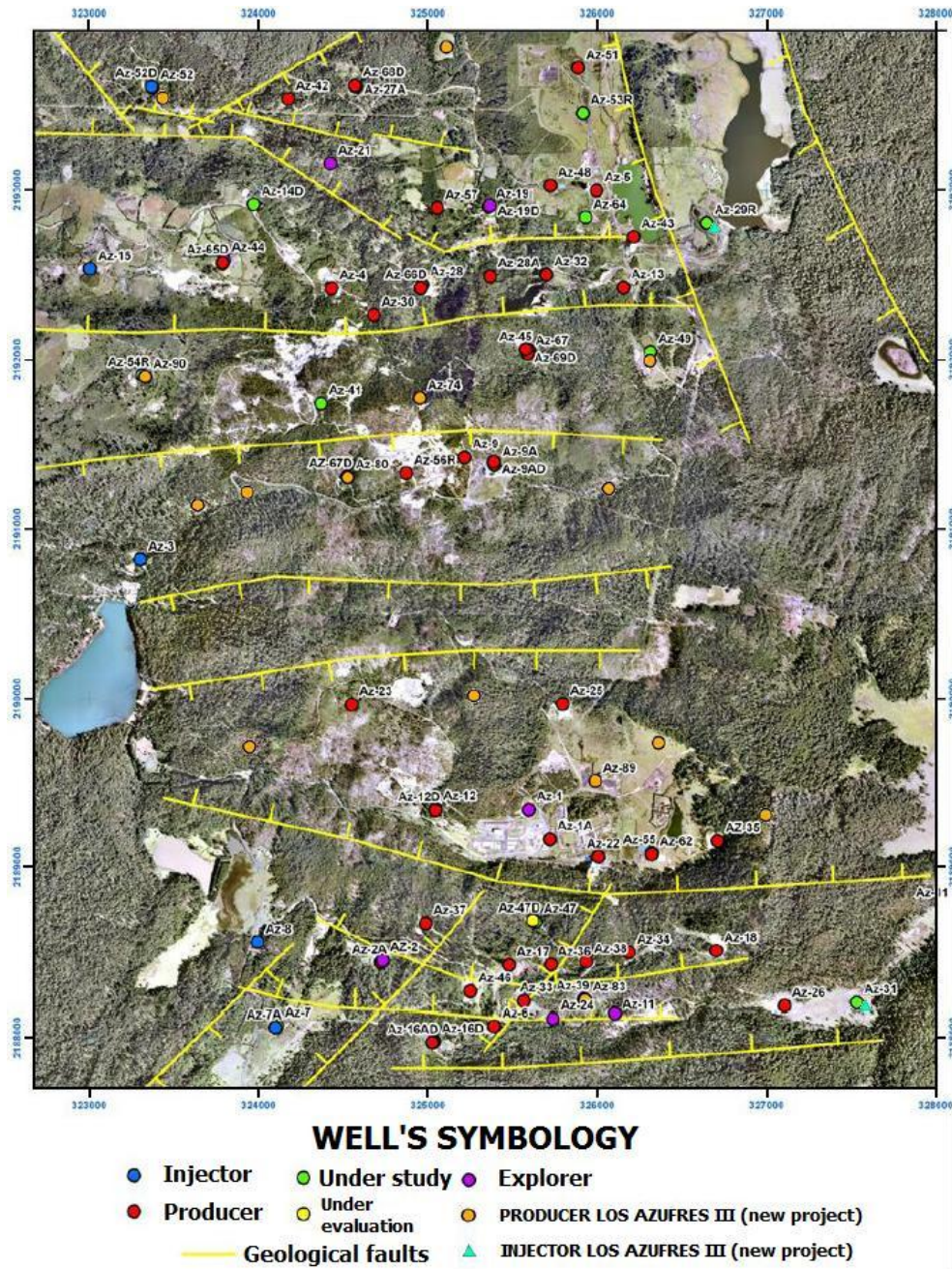


Figure 14: geographic map of the Los Azufres Geothermal Field's area, showing all wells and main geological faults (modified from CFE, 2011).



- Four back-pressure units of 5MW each and three condensation units of 25 MW each in the north zone, supplied by the separated vapor of 22 wells (Figure 15).

The Los Azufres III Geothermoelectric Project is a new plan consisting in exploiting more efficiently the geothermal fluid which is currently extracted for the generation of electric energy at Los Azufres geothermal field. In order to do so, the CFE has planned to substitute seven back-pressure Units of 5 MW (U-2 (Figure 15 and 16), U-6 and U-10 of the south zone, U-3 (Figure 15 and 17), U-4, U-5, U-9 in the north zone, for a sum of 35 MW) with two condensation units of 25 (example in Figure 18) and 50 MW (example in Figure 19) respectively for a sum of 75 MW, which are more efficient in the vapor exploitation. In fact, at Los Azufres, to generate 1 MW with back-pressure units, more or less 14 tons of separated vapor are required, while about 7.5 tons of separated vapor are required to generate 1 MW with condensation units. (M.I.A. Proyecto Geotermoelectrico Los Azufres III, 2011).



*Figure 16: Unit 2, located in the south zone of LAGF, producing 5 MW of electrical energy, to be dismantled in 2015.*



*Figure 17: Unit 3, located in the north zone of LAGF, producing 5 MW of electrical energy, to be dismantled in 2015.*



*Figure 18: Unit-13, in the south zone, as an example of a 25 MW unit.*



*Figure 19: Unit-7 (Tejamaniles Central), in the south zone, as an example of a 50 MW unit.*

#### 4. GEOLOGICAL OVERVIEW

##### 4.1 GEOLOGY OF MEXICO

A Geologic Province has been defined as “the whole mappable part of the solid surface of the planet, with an extension varying from hundreds to millions of square kilometers, characterized for its rocks, geologic structures and for a sequence of events such that it integrates a singular evolution history different from that of adjacent areas, from which it is separated by stratigraphic and/or tectonic limits” (Ortega-Gutiérrez et al., 1992). This definition is, therefore, independent from tectonic, morphotectonic, physiographic, metalogenic, tectonostratigraphic provinces, etc... although it could coincide with any of them. According to this definition, and with an accurate analysis of the geological information about the country, the Map of the Geological Provinces of Mexico could have been produced (Ortega-Gutiérrez et al., 1992), and 35 geological provinces have been identified (scale 1:2'000'000 - Figure 20).

For its extension, the biggest Geological Province of Mexico is the Ignimbritic Mexican Belt, extended to more or less 300,000 km<sup>2</sup>, 1600 km of longitude and an average width of 250 km, while the smallest one is Juchateca, which is a volcanosedimentary province of submarine arc, in the south of Mexico, with only ~3 hundreds square kilometers of amplitude.

The Geological Provinces Map of Mexico, identifies 35 different geological provinces, taking also into account age, origin and structural features of the territory. In detail, from a chronological point of view each geological province belongs to Precambrian (2), Paleozoic (3), Mesozoic (13), Cenozoic (16) and Cenozoic-Mesozoic (1) units. Concerning the geological origin, the provinces are subdivided in plutonic (6), volcanic (5), marine-sedimentary (10), continental-sedimentary (4), volcano-sedimentary (5) and complex origin (5). Finally, the structural tectonic characterization allow to recognize subduction complexes (1 province), arc root areas (6), submarine arc zones (4), continental arc zones (5), platform areas (4), orogenetic areas (2), geoclines (8) and complex structural zones (5) (Ortega-Gutiérrez et al., 1991).



Figure 20: GEOLOGIC PROVINCES OF MEXICO (in brackets it's indicated the age, origin and geotectonic dominant environment, with this order): 1. Yucatán Platform (C. sm, p); 2, Deltaic basin of Tabasco (C, sc, g); 3, Folds and Faults Belt of Chiapas (C, sm, or); 4, Batholith of Chiapas (P, p, ra); 5. Igneous Massif of Soconusco (C. p, ra); 6. Basin of Tehuantepec (C, sm, g); 7 Deltaic Basin of Veracruz (C, sc, g); 8, Volcanic Massif of the Tuxtlas (C, v, ac); 9, Cuicateca (M, vs, as); 10. Zapoteca (pC, c, co); 11, Mixteca (PC, c, co); 12, Chalina (M, p, ra); 13, Juchateca (P, vs, as); 14, Platform of the Morelos (M, sm, p); 15, Trans-Mexican volcanic Belt (C, v, ac); 16, Orogenetic Complex of Guerrero-Colima (M, vs, as); 17. Batholith of Jalisco (M, p, ra); 18. Igneous Massif of Palma Sola (C, v, ac); 19. Miogeocline of the Gulf of México (C, sm, g); 20, Folds and Faults Mexican Belt (M, sm, or); 21, Platform of Coahuila (M, sm, p); 22, Zacatecana (M, c, co); 23, Platform of San Luis Potosi Valley (M, sm, p); 24, Ignimbritic Mexican Belt (C, v, ac); 25. Sinaloa Orogenic Belt (M, vs, as); 26, Chihuahuense (C-M, c, co); 27, Basin of Nayarit (C, sm, g); 28, Deltaic Basin of Sonora-Sinaloa (C. sc, g); 29. Sonorense (p-C, c, co); 30. Delta of Colorado (C, sc, g); 31. Batholith of Juárez-San Pedro Mártir (M, p, ra); 32, Basin of Vizcaíno-Purísima (C, sm, g); 33. Cedros-Margarita Orogenic Belt (M, vs, cs); 34, La Giganta Volcanic Belt (C, v, ac); 35, La Paz Plutonic Complex (M, p, ra) **Explication:** Age: p-C- Precambrian ; P - Paleozoic; M - Mesozoic; C - Cenozoic. **Origen:** m - metamorphic; p - plutonic; v - volcanic; vs - volcanosedimentary; sm - marine sedimentary; sc - continental sedimentary; c-complex. **Geotectonic Environment:** es - Subduction complex; ra - Arc root; as - submarine arc; ac - continental arc; g - geoclinal; or - orogen; p - platform; co - compound. (Ortega-Gutiérrez et al., 1991).

In addition, since the 70s, a Geological Map of Mexico has been produced and updated until 2007 by the UNAM (Universidad Nacional Autónoma de México) (Ferrari et al., 2007 - Figure 21-22). Looking through this map, the national territory shows its most distinctive features, that is almost three quarters of the national

geologic provinces characterized by rocks of Mesozoic or Cenozoic age (in other words, rocks of the last 225 million years), while Precambrian rocks only outcrops in the 12% of the country. Another distinctive characteristic of Mexican geology is the asymmetric distribution of sedimentary and magmatic/metamorphic provinces, that are concentrated the former in the oriental part of the country, while the latter in the western part.

The distinctive dichotomy of Mexican geology can be explained by the passive nature owned by the oriental margin of Mexico since the Jurassic Period, in contrast with the occidental margin which has been, since the same period, convergent and active. The convergence of oceanic plates of the Pacific against the occidental edge of the American continent, including Mexico, has gone on from the Paleozoic to the present. As a consequence of this geological history, metallic and geothermal resources of deep origin are concentrated in the western half of the territory, while energetic resources of superficial origin (oil, natural gas and charcoal) are localized in the eastern half.

### ***Sedimentary rocks***

Without any doubt, the predominant Mesozoic-Cenozoic age of the national territory and its geological constitution associated with the evolution of the two continental margins of the American continent, have given a prominent role in the generation and conservation of the sedimentary rocks, as it can be seen in the geological map of Mexico.

For a better comprehension, sedimentary stratigraphic units have been classified into three paleo-environmental groups (Ortega-Gutiérrez et al., 1992): continental, mixed and marine. It's clear that, for their economic-oil importance, sedimentary rocks are the most studied and mapped group of the country. Continental Sedimentary Rocks units are 7, distributed as follows (scale 1:2'000'000): 1 of Paleozoic age (Psc), 3 of Mesozoic age (Jc, Jmc and Ksc) and 4 of Cenozoic age (Pgc, Csc, Qc and Qe) (continue at page 30)

MAPA GEOLÓGICO DE MÉXICO

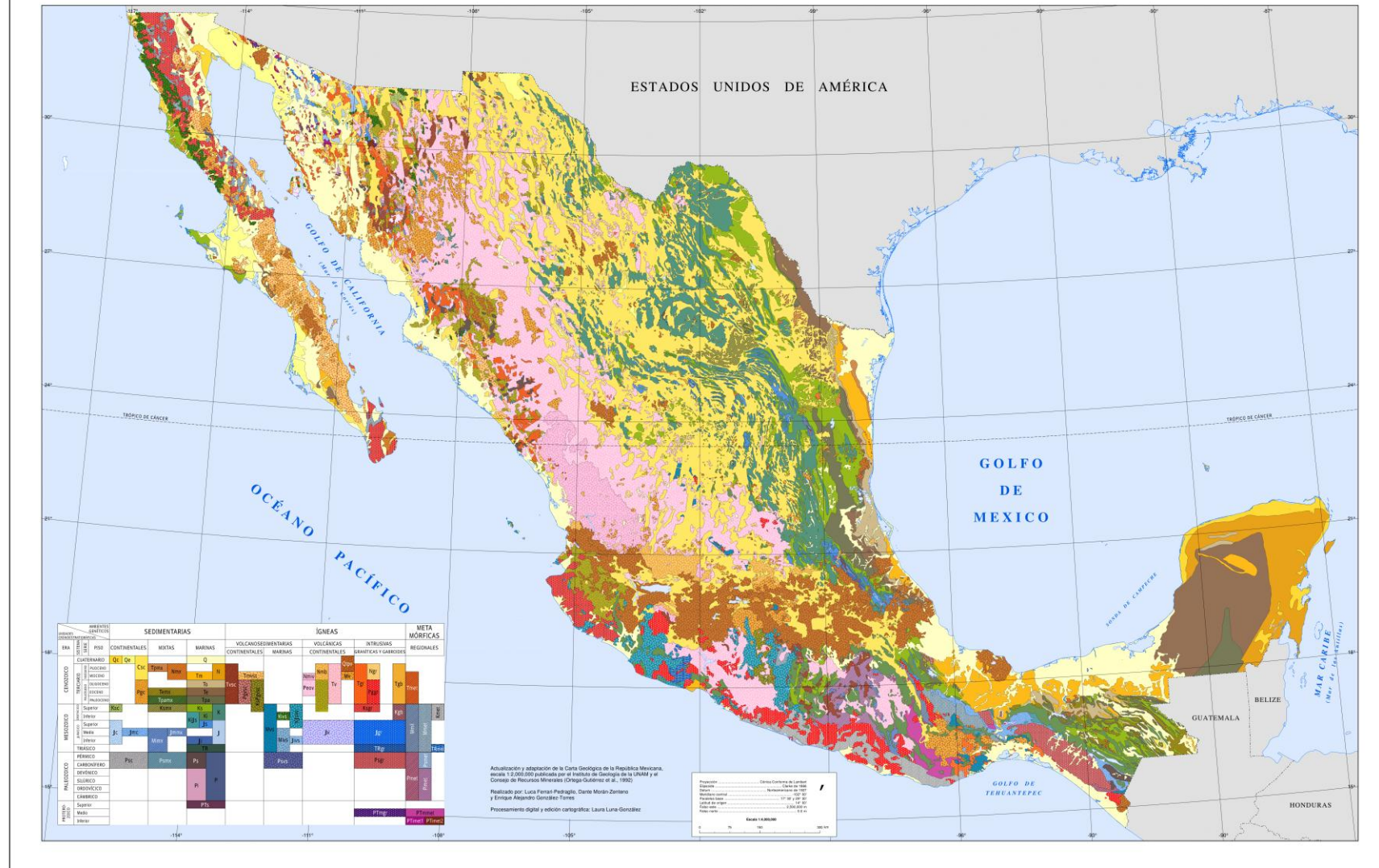


Figure 21: Geologic Map of Mexico (Ferrari et al., 2007).

GENETIC ENVIRONMENT				SEDIMENTARY			IGNEOUS				META MORPHYC		
CHRONOSTRATIGRAPHIC UNITS							VOLCANOSEDIMENTARY		VOLCANIC	INTRUSIVE	REGIONAL		
ERA	SYSTEM	SERIES	STAGE	CONTINENTAL	MIXED	MARINE	CONTINENTAL	MARINE	CONTINENTAL	GRANITIC AND GABBROID			
CENOZOIC	TERTIARY	QUATERNARY		Qc	Qe	Q							
		PALEOGENE	PLIOCENE		Csc	Tpmx	Nmx						
			MIOCENE										
			OLIGOCENE										
			EOCENE										
			PALEOCENE										
MESOZOIC	CRETACEOUS	UPPER		Ksc									
		LOWER											
	JURASSIC	UPPER											
		MIDDLE	Jc	Jmc									
		LOWER											
		TRIASSIC											
	PALEOZOIC	PERMIAN											
		CARBONIFEROUS		Psc	Psmx	Ps							
		DEVONIAN											
		SILURIAN											
ORDOVICIAN					Pi	P							
CAMBRIAN													
PROTERO-ZOIC	Upper					PTs							
	Middle									PTmgr	PTmmet		
	Lower										PTimet1	PTimet2	

Figure 22: Legend of the Geologic Map of Mexico (Ferrari et al., 2007).

Mixed Sedimentary rocks units are 8, 1 of Paleozoic age (Psmx), 3 of Mesozoic age (Mimx, Jmmx and Ksmx) and 4 of Cenozoic age (Tpamx, Temx, Nmx, Tpmx). Marine Sedimentary Rocks units are 18, 1 of Proterozoic age (PTs), 3 of Paleozoic age (Pi, P, Ps), 8 of Mesozoic age (TR, J, Ji, Js, KiJs, K, Ki, Ks) and 5 of Cenozoic age (Tpa, Te, To, Tm, N).

The separation between volcano-sedimentary and sedimentary units was particularly difficult where volcanic rocks exist over marine or continental sedimentary deposits. Nevertheless, in the majority of cases, the presence of volcanic rocks like pyroclastic material or lava effusions is exiguous, and it doesn't constitute an adequate factor to diminish the preponderance of marine or continental sedimentological processes which acted during the deposit of the units, therefore classified as sedimentary.

#### ***Volcanic and volcano-sedimentary rocks***

Those groups of rocks are, maybe, the most important for the country for their extension and mineral richness. In the geologic map of Mexico (Scale 1:2'000'000) they have been separated into 21 stratigraphic units, of which 1 is of Quaternary age, 10 of Tertiary age, 6 of Mesozoic age and 1 of Paleozoic age. Regarding their origin, 10 are volcanosedimentary (4 of continental origin and 6 of marine origin) and the last 8 are of volcanic origin and continental environment.

#### ***Intrusive rocks***

Intrusive rocks in Mexico are abundant; for the majority, they have a sensu-lato-granitic character. With respect to Mafic rocks, at the scale of the Map, only three rock bodies of gabbroic composition have been delimited: Sierra de la Trinchera, in the Crystalline Complex of La Paz in the South Baja California (Kgb in the map), and two little bodies, still without denomination, in the south of the State of Guerrero (Tgb). (Ortega-Gutiérrez et al., 1991)

In total, 10 intrusive units have been identified, with the following temporal distribution: 1 Proterozoic unit (PTmgr), 1 Paleozoic unit (Psgr), 4 Mesozoic units (Ksgr, Kgb, Jgr, TRgr) and 4 Tertiary units (Tgr, Tgb, Pggr, Ngr). In the most of cases, the volume of intrusive rocks is integrated in plutons which stand in the

occidental margin of Mexico, and the age is 90-40 Ma. For scale reasons, a big number of plutonic and subvolcanic intrusions couldn't be added to the map; however, is important to say that those rocks are so important for metallogenic and geothermal purposes, since a big number of metallic (Fe, Cu, Mo, W, Zn, Pb, Ag and Graphite) and geothermal reservoirs of the country are associated with them.

### ***Metamorphic rocks***

The geodynamic and tectonic vigor that the country suffered, had meant that rocks transformed by heat, pressure, stress and chemical activity of the fluids that persist within the Earth, arise to the surface as extensive metamorphic formations, whose age in Mexico is comprised from Precambrian to Tertiary. To express properly those fundamental events of the Mexican geologic evolution, it has been necessary to utilize 11 stratigraphic units (Ortega-Gutiérrez et al., 1991), distributed as follows: 3 of Proterozoic age (PTimet1, PTimet1, PTmmet), 3 of Paleozoic age (Pimet, Pmet, Psmet), 4 of Mesozoic age (TRmet, kmet, Mmet, Mmil) and one of Cenozoic age (Tmet) (Ortega-Gutiérrez et al., 1991).

## ***4.2 THE TRANS-MEXICAN VOLCANIC BELT (TMVB)***

The Trans-Mexican Volcanic Belt (TMVB) o Cinturón Volcánico Transmexicano (CVT) is a crustal fractures system, where volcanic rocks coming from the fusion of the Cocos Plate's oceanic crust are expelled (Figure 23). It's major magmatic activity manifested during the Pliocene-Quaternary. However, there are evidences of a previous volcanism in different sector of the volcanic complex itself. (Aguayo et Trápaga, 1996).

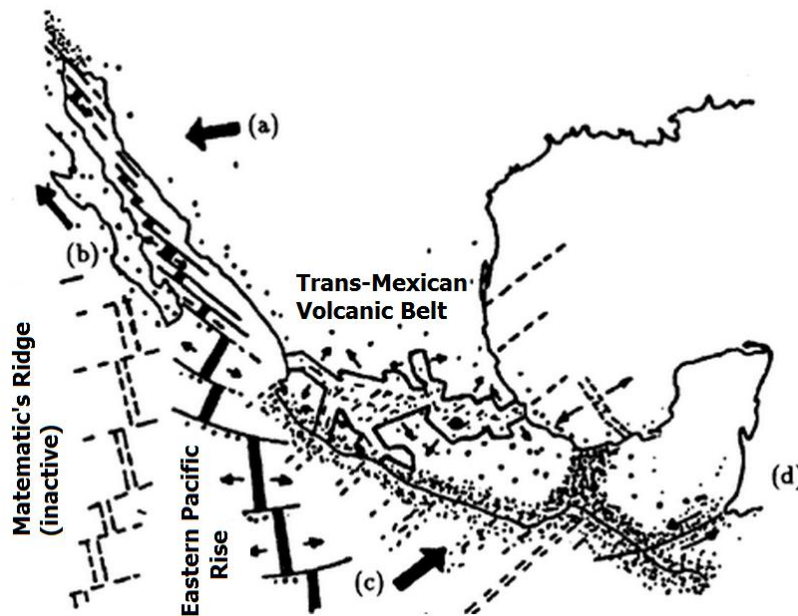


Figure 23: Diagram showing the Trans-Mexican volcanic Belt (TMVB) o Cinturón Volcánico Transmexicano (CVT) within the Mexican territory. In it, there can be seen the movements of plates which originated the TMVB, which are: a) the North American, toward the South-West, b) The oriental Pacific, toward the North-West; c) the Cocos Plate, toward North-East; d) the Carribean Plate toward the East (Aguayo et Trápaga, 1996).

In a recent publication, an integrative review of the main geophysical, geological and geochemical features of the Trans-Mexican Volcanic Belt (TMVB) has been carried out (Ferrari et al., 2012).

First of all, it is certain that the TMVB is the largest Neogene volcanic arc in North America, covering 160,000 km<sup>2</sup> and a length of almost 1000 km between 18°30' and 21°30'N in central Mexico. Moreover, it has a variable width, ranging between 90 and 230 km, and east of 102°W is not parallel to the Middle America trench (Figure 24-25).

Furthermore, it has been confirmed that the TMVB is built upon Cretaceous and Cenozoic magmatic provinces (Figure 24) and a heterogeneous basement made of tectonostratigraphic terranes of different age and lithology (Figure 25). In a geodynamic frame, the TMVB is built on the southern edge of the North America plate, which overrides the Rivera microplate and the northern part of the Cocos plate.

So, the TMVB represents the most recent episode of long-lasting continental magmatic activity that, since the Jurassic, produced a series of partially overlapping arcs as a result of the eastward subduction of the oceanic plate beneath western Mexico. Since the Late Cretaceous arc magmatism was entirely continental and the geographic distribution of the arcs has been reconstructed with reasonable precision. (Ferrari et al., 2012).



Figure 24: Geodynamic setting and main continental magmatic provinces of Mexico (Ferrari et al, 2012)

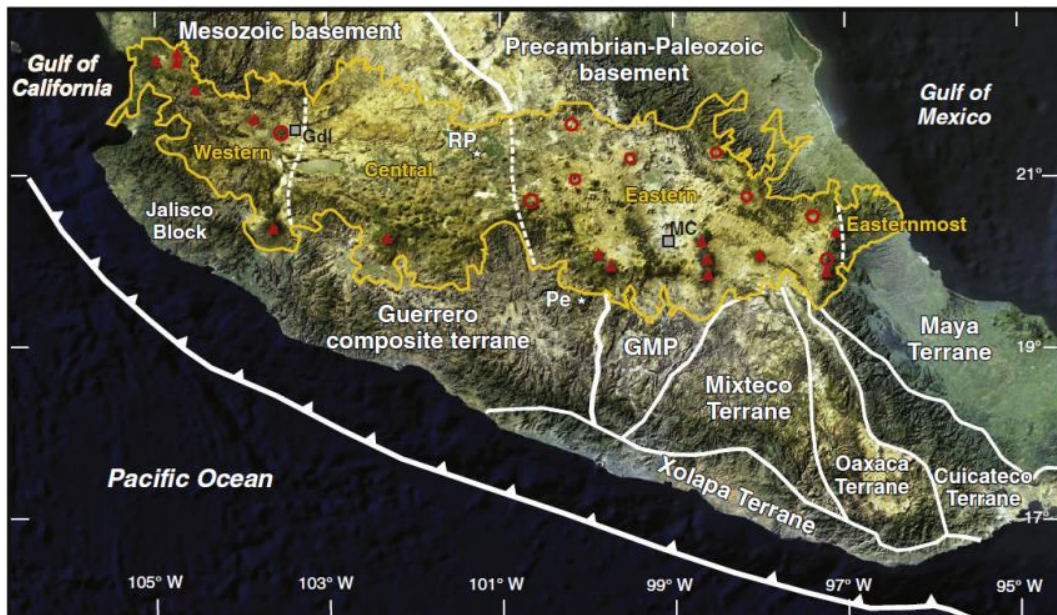


Figure 25: Satellite image of central Mexico outlining the Trans-Mexican Volcanic Belt (yellow line) with the main stratovolcanoes (red triangles) and calderas (red circles) as well as its four sectors (thin dashed white lines). The main crustal units are outlined with thick white lines. The Jalisco block is part of the Guerrero composite terrane and might be also underlain by pre-Mesozoic crust according to the ages of its Cretaceous granitoid batholiths. MC: Mexico City; Gdl: Guadalajara (from Ferrari et al., 2012).

As a whole, the magmatic belts of the TMVB maintained a general NNW orientation until the Eocene but since Oligocene began a counter-clockwise rotation, eventually reaching its present transverse E–W orientation typical of the TMVB in the middle Miocene.

Because the TMVB is oriented oblique to the trend of Mexican tectonic provinces, its pre-Cretaceous basement is highly heterogeneous (Figure 26). The eastern half of the TMVB, east of 101° W, is built on Precambrian terranes, grouped into the so called Oaxaca microcontinent, as well as on the Mixteco terrane of Paleozoic age. West of 101°W, the TMVB is underlain by the Guerrero composite terrane, an assemblage of Jurassic to Cretaceous marine marginal arcs built on Triassic–Early Jurassic siliciclastic turbidites. The westernmost Guerrero composite terrane is the Jalisco block, dominated by a late Cretaceous to Paleocene batholith intruding mid to late Jurassic schists, and covered by Late Cretaceous to Eocene subaerial ignimbrites and lavas.

In order to know in details either the thickness of the upper plate (Figure 28), the depth of the subducting plate (Figure 29) and its geometry (Figure 30), three joint US–Mexico seismic experiments have been accomplished between 2006 and 2010: the Mapping the Rivera Subduction Zone (MARS), the Middle America Subduction Experiment (MASE) and the Veracruz-Oaxaca seismic line (VEOX) (Figure 26) (Ferrari et al., 2012).

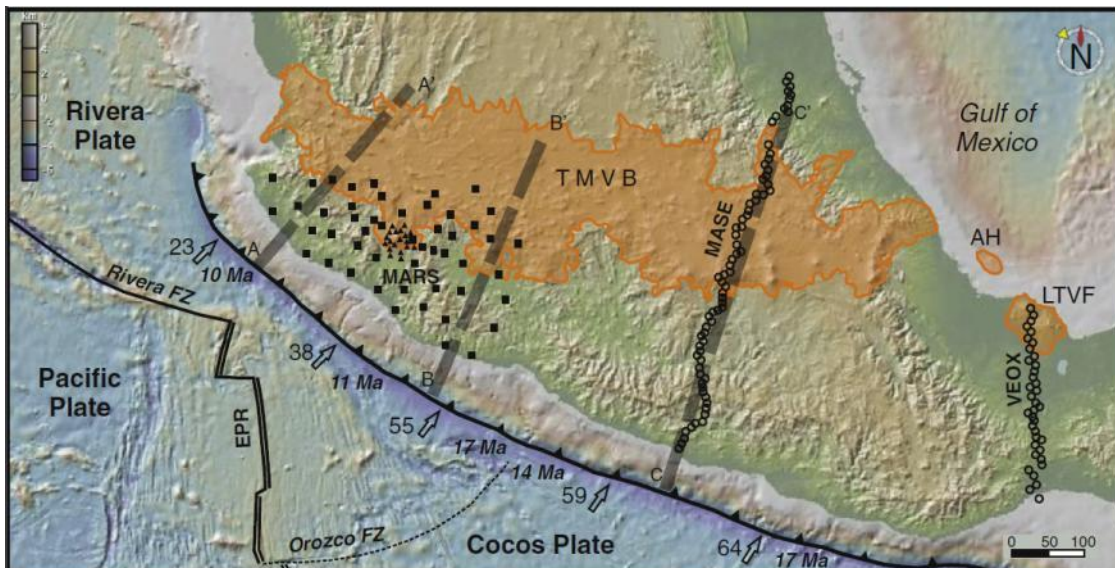


Figure 26: Location of broadband seismic stations used in the MARS experiment (black squares), MASE and VEOX profiles (open circles). The boundaries of the Pacific, Rivera and Cocos oceanic plates, as well as the age of the subducting plate at the trench, are indicated. Small arrows show direction and relative convergence rate (mm/yr) at the trench. FZ = Fracture Zone; EPR= East Pacific Rise; AH= Anegada High; LTVF= Los Tuxtlas volcanic field (from Ferrari et al., 2012).

The MARS experiment, led by the University of Texas at Austin with the collaboration of UNAM (Universidad Autónoma de México) and University of New Mexico, deployed a seismic network of 50 broadband stations in the Jalisco and Michoacán states, covering a region between the coast and the northwestern TMVB (Figure 26 – Profiles A-A' and B-B'). The MASE experiment, led by the California Institute of Technology with the collaboration of University of California at Los Angeles and UNAM, deployed 100 broadband stations at ~5 km intervals along a profile orthogonal to the trench, from Acapulco to the northern Veracruz state, crossing the TMVB near Mexico City (Profile C-C'). Half of these stations were subsequently employed along the VEOX profile, located in the western part of the Isthmus of Tehuantepec, with the same inter-station distance.

Using the results of receiver functions studies from the MARS, MASE and VEOX data, combined with the estimation from gravimetric data of Urrutia-Fucugauchi and Flores-Ruiz (1996) for areas where seismic information was not available, some important features of the TMVB have been understood. First of all, the thickness of the crust have been deeply understood (Figure 27, Ferrari et al., 2012).

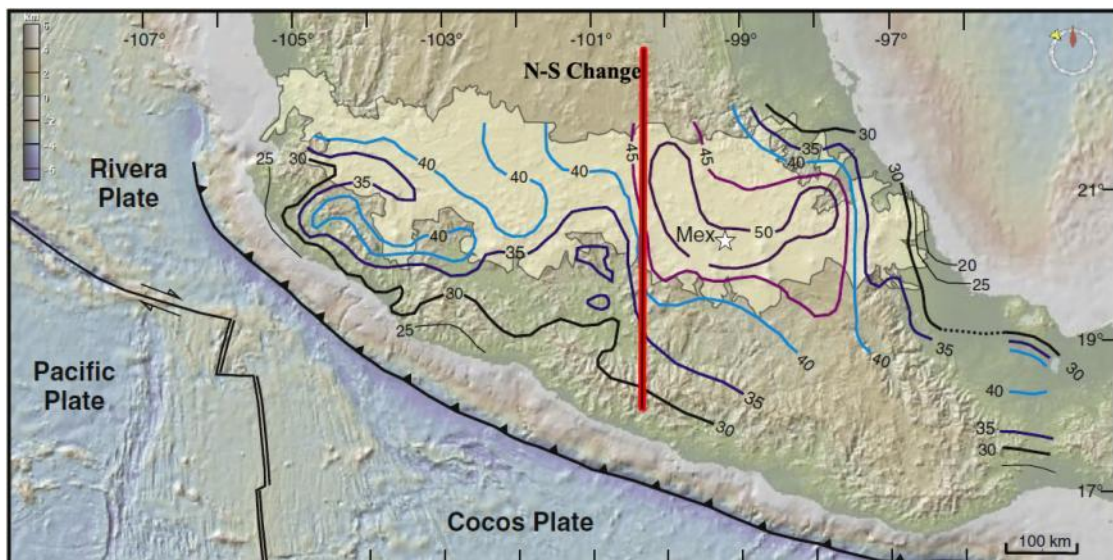


Figure 27: Map showing the thickness of the crust beneath and south of the TMVB (in km), in other words the Moho depth is shown (from Ferrari et al., 2012).

The map of Figure 27 shows a first order ~N–S change in thickness of the crust beneath the TMVB, just east of 101°W. The region to the east has thicker crust with maxima over 50 km, whereas to the west the thickness is 40 km or less. After this, the depth of the subducted slab of oceanic crust has been reconstructed (Figure 28).

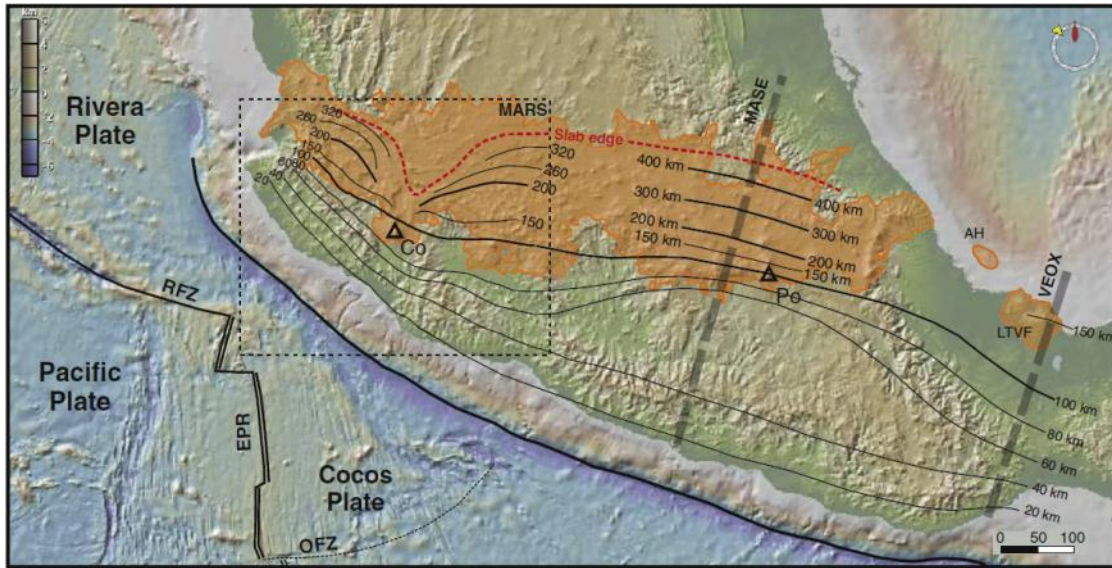


Figure 28: Depth of the subducted slab beneath central Mexico compiled using the results of receiver function and tomography studies from the MARS, MASE and VEOX experiments. (Ferrari et al., 2012.)

Therefore, the geometry of the slab, along with the estimated temperatures at the trench, has been described and pictured in a series of 2d profiles (A-A', B-B' and C-C' of figure 26). (Figure 29).

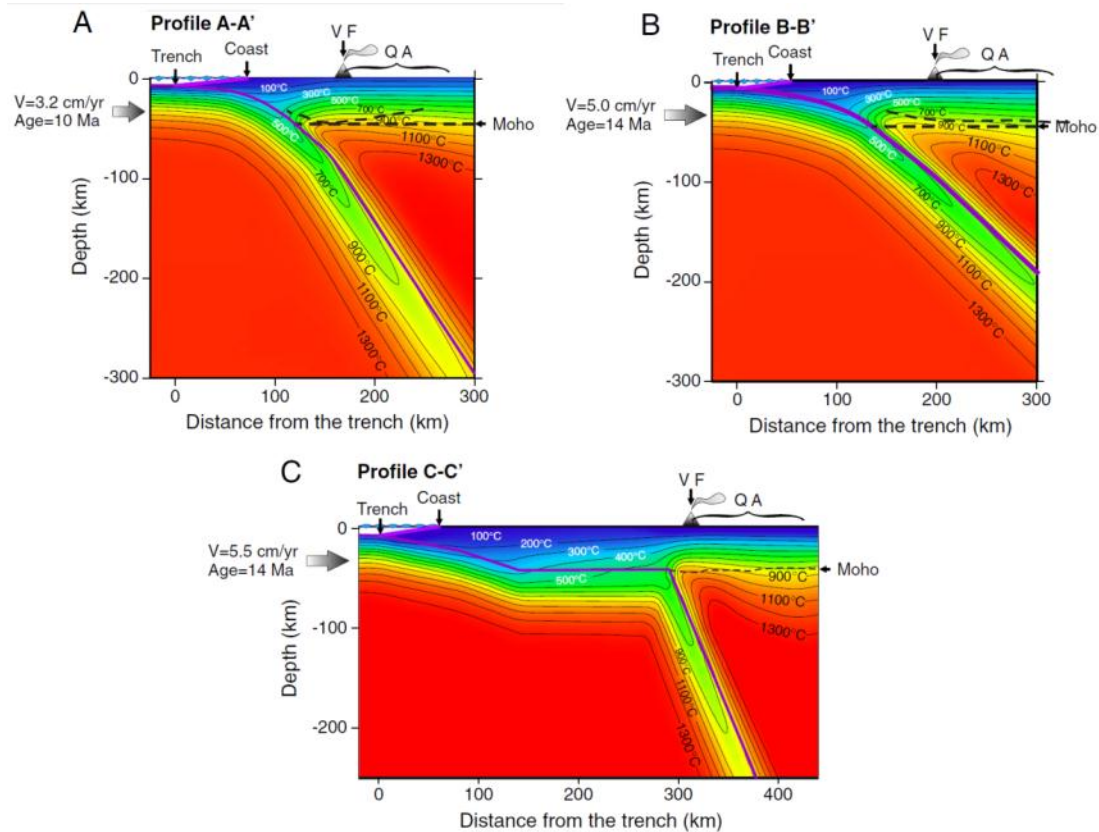


Figure 29: profiles representing the shape of the oceanic crust slab under subduction, along with 2D instantaneous thermal models. Profiles A-A' and BB' obtained from MARS experiment. Profile C-C' obtained from MASE experiments (see Figure 34) (modified from Ferrari et al., 2012).

According to the results exposed in Figure 28 and 29, it can be affirmed that the Rivera plate dips at  $40^\circ$  beneath the forearc region and then dips  $\sim 70^\circ$  beneath the TMVB. The westernmost Cocos slab dips slightly less, either beneath the forearc and the TMVB. The two plates are separated by a trench-orthogonal tear starting just north of the Colima volcano (Co) and broadening northwards. East of  $101^\circ\text{W}$ , the dip of the Cocos plate decreases markedly. Receiver function results along the MASE profile show that the plate initially dips at  $15^\circ$  until 80 km from the coast and then flattens at 50 km depth. The flat slab extends inland for 200 km just below the Moho of the upper plate. However, results provided by the seismic tomography, show that beneath the volcanic front the Cocos plate abruptly plunges with a  $75^\circ$  dip. East of  $96^\circ\text{W}$ , the flat subduction segment shortens and eventually disappears beneath the Isthmus of Tehuantepec, where the VEOX profile imaged the Cocos plate subducting with an almost constant  $26^\circ$  dip between 140 and 310 km from the trench.

From the volcanological and rock-compositional point of view, the evolution of the TMVB has been divided into four stages, on the basis of the spatial distribution and composition of volcanism in the whole area (Figure 30) (Ferrari et al., 2012):

- (1) The first stage was that of the initiation of the TMVB, which started in the early to Mid-Miocene, with predominantly effusive volcanism. Those rock formations are exposed inside an area localized at east of  $101^\circ\text{W}$ . The composition of the rocks emplaced during this first stage is sub-alkaline, with predominant andesite to dacite composition.
- (2) The second stage started in the late Miocene and was an episode of eastward-migrating mafic volcanism, located to the north of the previous arc. Plateau of basaltic lava erupted through fissures, or less often from small shield volcanoes and lava cones. The radiometric age indicates that this pulse migrated from west to east, between 11.5 and 7-3 Ma. This episode is thought to be linked with a scenario of oceanic crust slab detachment propagating eastward.

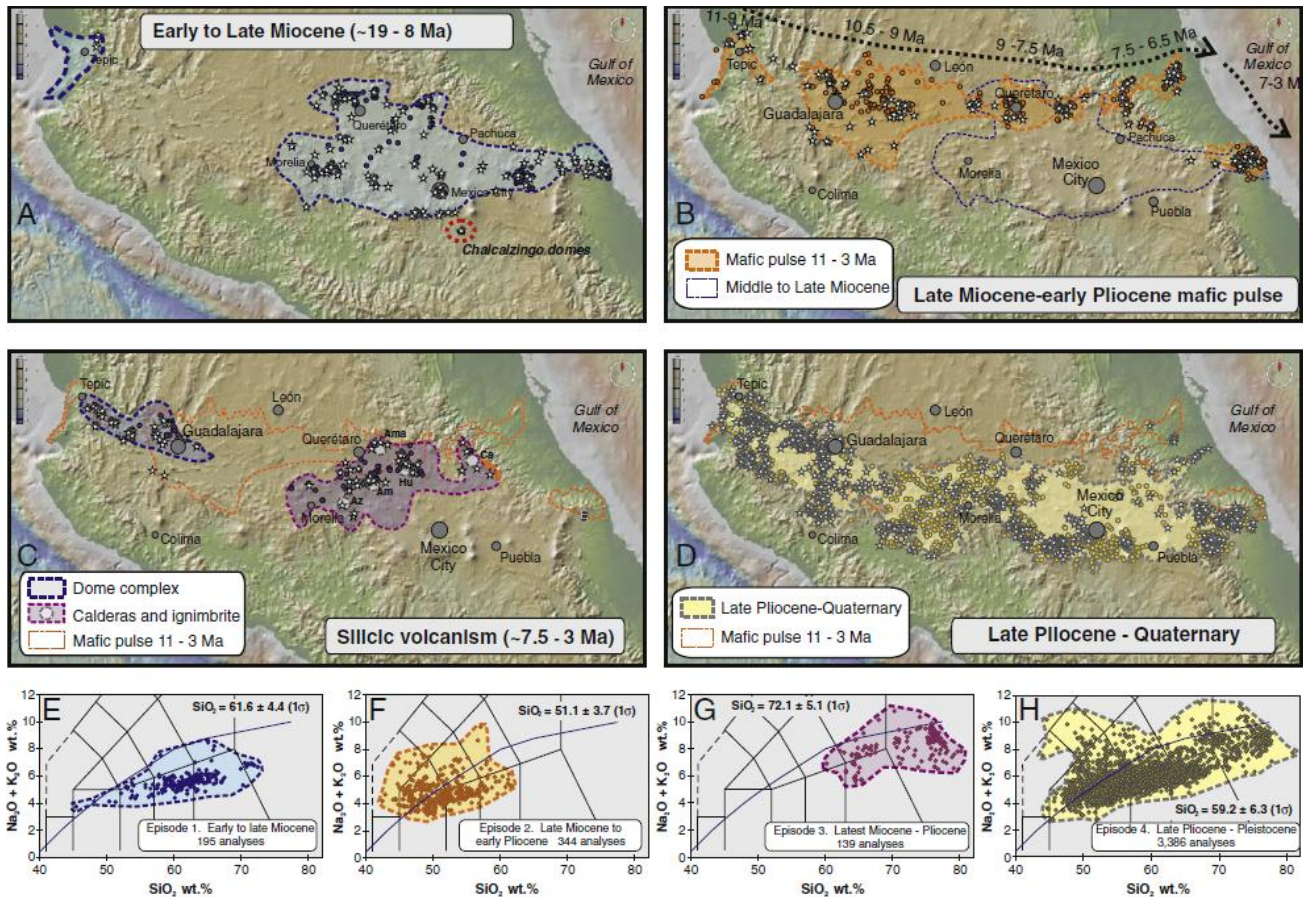
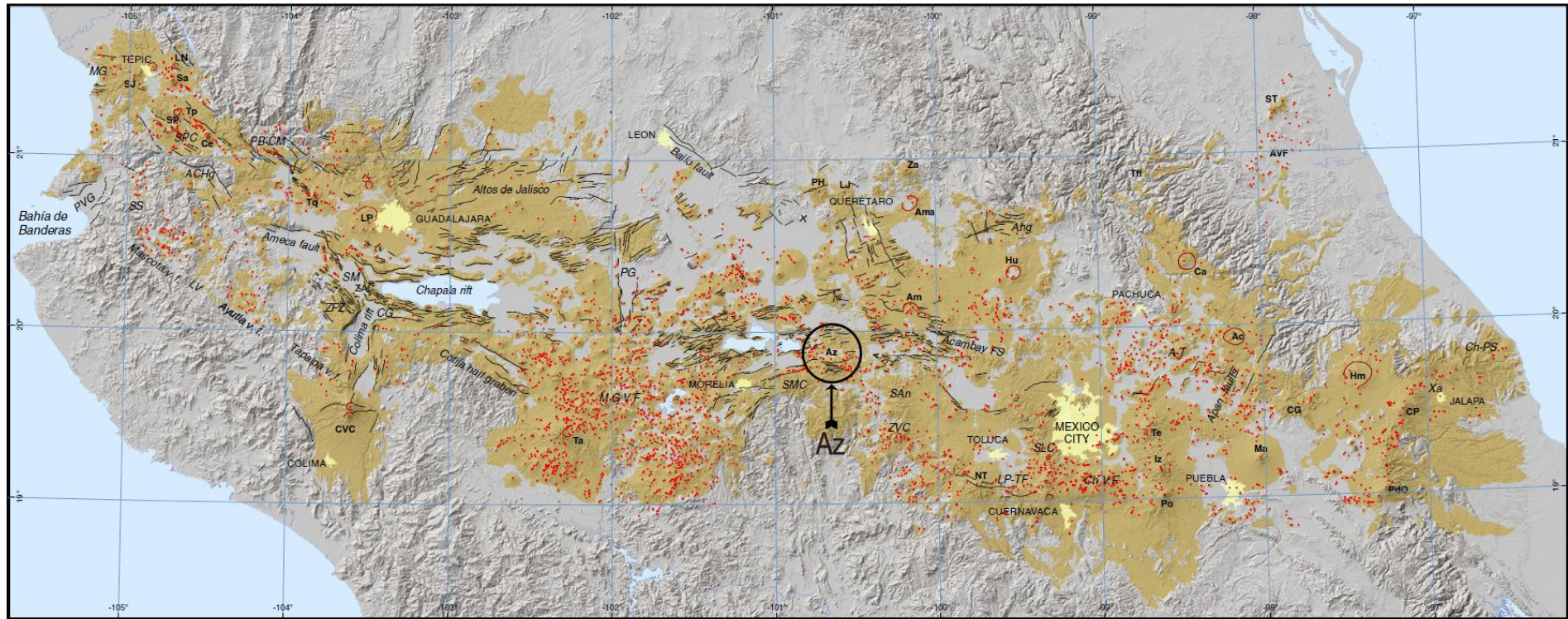


Figure 30: The four magmatic episodes of the Trans-Mexican Volcanic Belt. There are also shown the total alkalis vs. silica diagrams for each episode, included average SiO<sub>2</sub> values. A) and E) The early TMVB of early to late Miocene; B) and F) The eastward migrating mafic pulse of the late Miocene to early Pliocene; C) and G) The silicic episode of the late Miocene to early Pliocene; D) and H) The modern TMVB of late Pliocene to Pleistocene (Ferrari et al., 2012).

(3) In the latest Miocene, volcanism changed along the arc, with an initial silicic episode that became bimodal (mafic–silicic) in the early Pliocene and marked the beginning of the trenchward migration of volcanism. East of 101°W, volcanism was characterized by the formation of large calderas that produced large volumes of ignimbrites (>50 km<sup>3</sup>). and associated pyroclastic deposits. Caldera products are characterized by intermediate to silicic compositions in contrast to the bimodal compositions of rocks unrelated to calderas. This episode of is thought to be linked with the slab rollback. In this scenario, silicic volcanism may have originated by partial melting of the lower crust due to its progressive exposure to asthenospheric mantle as the slab retreated. In other words, the continental crust participated in the genesis of silicic magmas.

4) Since the late Pliocene, the style and composition of volcanism of the TMVB became more diverse: volumetric dominant calc-alkaline rocks are associated in time and space with modest volumes of intraplate-like lavas and/or with lamprophyres and other potassium-rich rocks; besides, Quaternary volcanic centers are of rhyolitic-peralkaline composition. In the last million of years, large stratovolcanoes have been built. In the western sector, they are located in a WNW-ESE oriented belt, while in toward the east they form a ~E-W belt and they localize at the volcanic front (Figure 31). Also characteristic for this episode is the formation of monogenetic volcanic fields. The most prominent is the Michoacán–Guanajuato volcanic field (MGVF) with ca. 1000 volcanic centers distributed over 40,000 km<sup>2</sup> in the central TMVB sector, but many other smaller monogenetic volcanic fields occur along the arc (Figure 31) (Ferrari et al., 2012).



**LEGEND**

- Vent
- Fault
- Collapse crater
- Trans-Mexican Volcanic Belt
- City
- Lake



- |                                                                                                                                                                                                                                                                                                                                                                                                                                                                                                                                                                                                                                                                                              |                                                                                                                                                                                                                                                                                                                                                                                                                                                                                                                                                                                                                                                                                                                                                             |                                                                                                                                                                                                                                                                                                                                                                                                                                                                                                                                                                                                                      |
|----------------------------------------------------------------------------------------------------------------------------------------------------------------------------------------------------------------------------------------------------------------------------------------------------------------------------------------------------------------------------------------------------------------------------------------------------------------------------------------------------------------------------------------------------------------------------------------------------------------------------------------------------------------------------------------------|-------------------------------------------------------------------------------------------------------------------------------------------------------------------------------------------------------------------------------------------------------------------------------------------------------------------------------------------------------------------------------------------------------------------------------------------------------------------------------------------------------------------------------------------------------------------------------------------------------------------------------------------------------------------------------------------------------------------------------------------------------------|----------------------------------------------------------------------------------------------------------------------------------------------------------------------------------------------------------------------------------------------------------------------------------------------------------------------------------------------------------------------------------------------------------------------------------------------------------------------------------------------------------------------------------------------------------------------------------------------------------------------|
| <ul style="list-style-type: none"> <li>A-T: Apan-Tezontepec volcanic field</li> <li>Ac: Acoculco caldera</li> <li>ACHg: Amatlán de Cañas half-graben</li> <li>Ahg: Aljibes half-graben</li> <li>Am: Amealco caldera</li> <li>Ama: Amazcala caldera</li> <li>AVF: Álamo volcanic field</li> <li>Az: Los Azufres caldera</li> <li>Ca: Carboneros caldera</li> <li>Ce: Ceboruco volcano</li> <li>Ch-PS: Chiconquiaco-Palma Sola</li> <li>ChVF: Chichinautzin volcanic field</li> <li>CG: Citlala graben</li> <li>CP: Cofre de Perote volcano</li> <li>CVC: Colima volcanic complex</li> <li>Hm: Los Humeros caldera</li> <li>Hu: Huichapan caldera</li> <li>Iz: Iztaccihuatl volcano</li> </ul> | <ul style="list-style-type: none"> <li>LJ: La Joya volcano</li> <li>LN: Las Navajas volcano</li> <li>LP: La Primavera caldera</li> <li>LP-TF: La Pera-Tenango fault system</li> <li>LV: Los Volcanes volcanic field</li> <li>Ma: La Malinche volcano</li> <li>MG: Mecatán graben</li> <li>MGVF: Michoacán-Guanajuato volcanic field</li> <li>NT: Nevado de Toluca volcano</li> <li>PB-CM: Plan de Barrancas-Cinco Minas graben</li> <li>PdO: Pico de Orizaba volcano</li> <li>PG: Penajmillo graben</li> <li>PH: Palo Huérfano volcano</li> <li>PH: Palo Huérfano volcano</li> <li>Po: Popocatepetl volcano</li> <li>PVG: Puerto Vallarta graben</li> <li>SA: Sangangüey volcano</li> <li>SAn: Sierra de Angangueo</li> <li>SJ: San Juan volcano</li> </ul> | <ul style="list-style-type: none"> <li>SLC: Sierra de Las Cruces</li> <li>SM: San Marcos fault</li> <li>SMC: Sierra de Mil Cumbres</li> <li>SP: San Pedro volcano</li> <li>SS: San Sebastián volcanic field</li> <li>ST: Sierra de Tantima</li> <li>Ta: Tancitaro volcano</li> <li>Te: Telapón volcano</li> <li>Tq: Tequila volcano</li> <li>Tfi: Tlanchinol flows</li> <li>Tp: Tepeltitico volcano</li> <li>VCG: Cerro Grande volcano</li> <li>Xa: Xalapa volcanic field</li> <li>Za: Zamorano volcano</li> <li>ZAC: Zacoalco</li> <li>ZFZ: Zacoalco fault zone</li> <li>ZVC: Zitácuaro volcanic complex</li> </ul> |
|----------------------------------------------------------------------------------------------------------------------------------------------------------------------------------------------------------------------------------------------------------------------------------------------------------------------------------------------------------------------------------------------------------------------------------------------------------------------------------------------------------------------------------------------------------------------------------------------------------------------------------------------------------------------------------------------|-------------------------------------------------------------------------------------------------------------------------------------------------------------------------------------------------------------------------------------------------------------------------------------------------------------------------------------------------------------------------------------------------------------------------------------------------------------------------------------------------------------------------------------------------------------------------------------------------------------------------------------------------------------------------------------------------------------------------------------------------------------|----------------------------------------------------------------------------------------------------------------------------------------------------------------------------------------------------------------------------------------------------------------------------------------------------------------------------------------------------------------------------------------------------------------------------------------------------------------------------------------------------------------------------------------------------------------------------------------------------------------------|

Figure 31: tectonic and volcanic structures of the TMVB. The Los Azufres Geothermal field is visible (Az). (Ferrari et al., 2012).

### 4.3 THE LOS AZUFRES VOLCANIC COMPLEX

The Los Azufres Geothermal Field (LAGF) is located at 3000 m above sea level (m.a.s.l.), in the northeastern part of the Michoacán State, close to the Guanajuato State, at 90 km from the city of Morelia, and between the cities of Ciudad Hidalgo to the south and Zinapécuaro to the north (Figure 32). It is situated in the central sector of the TMVB (see Figure 31). One of the most peculiar skills of the LAGF within the TMVB is the presence of very recent and active faults with E-W direction, even though at Los Azufres there are also faults with N-S, NE-SW and NW-SE directions.

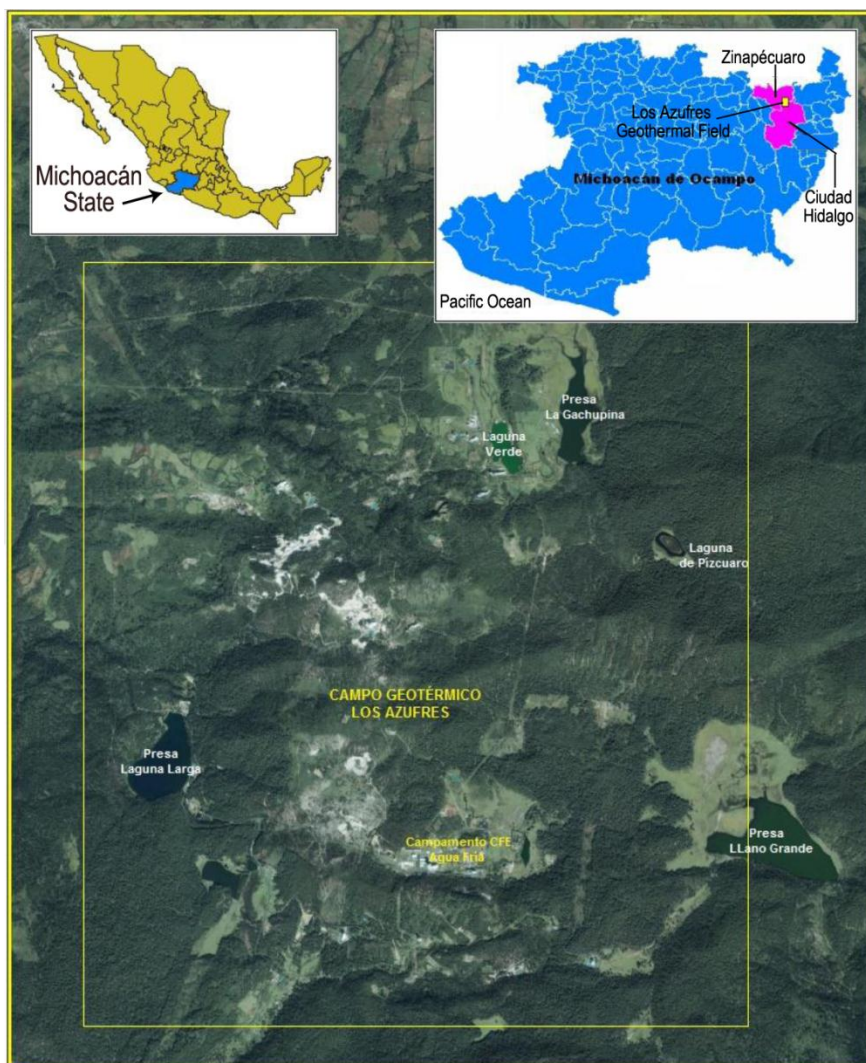


Figure 32: Location of the Los Azufres Geothermal Field, by Google Earth.

In the past, Los Azufres has been object of numerous studies (Ferrari et al., 1991; Robin and Pradal, 1993), and others that were realized by the CFE for the geothermal exploration and development. As the progress went on, it became

necessary a better understanding of the geothermal reservoir, because the space for drilling new wells, without affecting contiguous zones of production or injection, is restricted, due to the exploitation and decline of the wells. So, a precise and updated knowledge of the field's geology is required, in order to finally determine the structure and shape of the reservoir under exploitation. It's for that reason that Pérez-Esquívias et al. (2010) recently realized a work, whereby it has been possible to describe the Los Azufres geology in a really good way. The main results which are useful for this work are summarized here after .

From the structural geology point of view, the results of the structural measuring performed all over the area highlights an intense fracturing and faulting with three principal trends: NNW-SSE (~N-S), NE-SW and E-W (Figure 33).

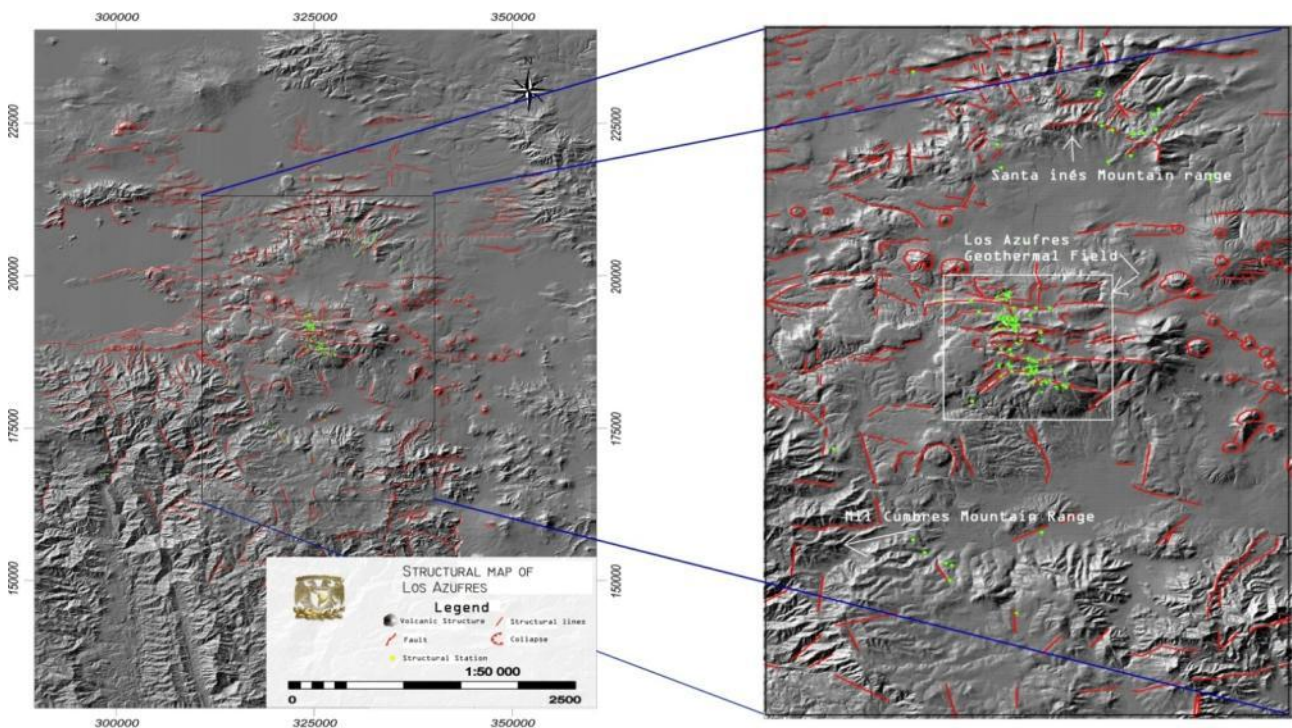


Figure 33: On the left, structural map comprising the LAGF and the Sierra de Inés and the Mil Cumbres Mountain ranges. On the right, a zoom centered in the LAGF (Pérez-Esquívias et al. 2010). For the location of the LAGF within the TMVB, see Figure 31.

Structures with NNW-SSE trend are related to the deformation which occurred between the Oligocene (33.7-23.8 Ma) and Miocene (23.8-5 Ma) and, through their structural features they were identified as lateral faults induced by the basement deformation. Structures with NE-SW and E-W orientation originated during the formation of the TMVB. In particular, structures with NE-SW

direction are scarce, and they are characterized by almost-vertical fault planes, even though some of them are 45° inclined. Meanwhile, structures with E-W orientation are the most abundant and they have got a lot of importance, because they affect all the lithological units and lacustrine sequences of Holocene (<0.01 M.a) and historical age in the Los Azufres field, and also because they include the greater part of field's hydrothermal alteration. A clear example of those structures is the Agua Fría fault, which have morphological evidences of recent seismic activity. Agua Fría has been the main fault on which this work focused (see Chapter 5). Both the fracturing in reservoir-stocking andesitic rocks and that of recent-deformed rhyolitic rock is semi-vertical. Precisely, the inclination goes from 70° to 80° in the first case and from 80° to 90° in the second one.

From the volcanological point of view, seven volcanic units are defined, which are, from the oldest to the youngest: Mil Cumbres Mountain Range, Pucato ignimbrite, Santa Inés Mountain Range, Santa Inés Ignimbrite, El Fraile Mountain Range, Los Azufres Geothermal Field and the Basalts-Andesites of the Michoacán-Guanajuato Volcanic Field (MGVF), which makes part of the western section of the TMVB (Figure 34). Meanwhile, the volcanological history of the LAGF can be resumed in the following eight stages:

- The volcanic activity began since the early Miocene more or less at 23 Ma, with the emplacement of thick complex sequence of welded ignimbrites, breaches, pyroclastic flows and falls, and lava effusions (*Mil Cumbre Sequence*), in the central and south part of the area shown in Figure 33 on the left.
- The volcanic activity continued until the end of the Early Miocene (17 Ma). At all the effects, this zone is probably associated to the volcanism of the Sierra Madre Occidental or to the beginning of the TMVB (Ferrari et al, 1999 and 2012). From the structural point of view, the rocks of the Mil Cumbres Range were cut by Faults, of NW-SE direction and were displaced at major deep, so that consequently they appear between 700 and 1000 meters deep in the Los Azufres' Wells (see figure 36).

SECUENCIAS VOLCANICAS

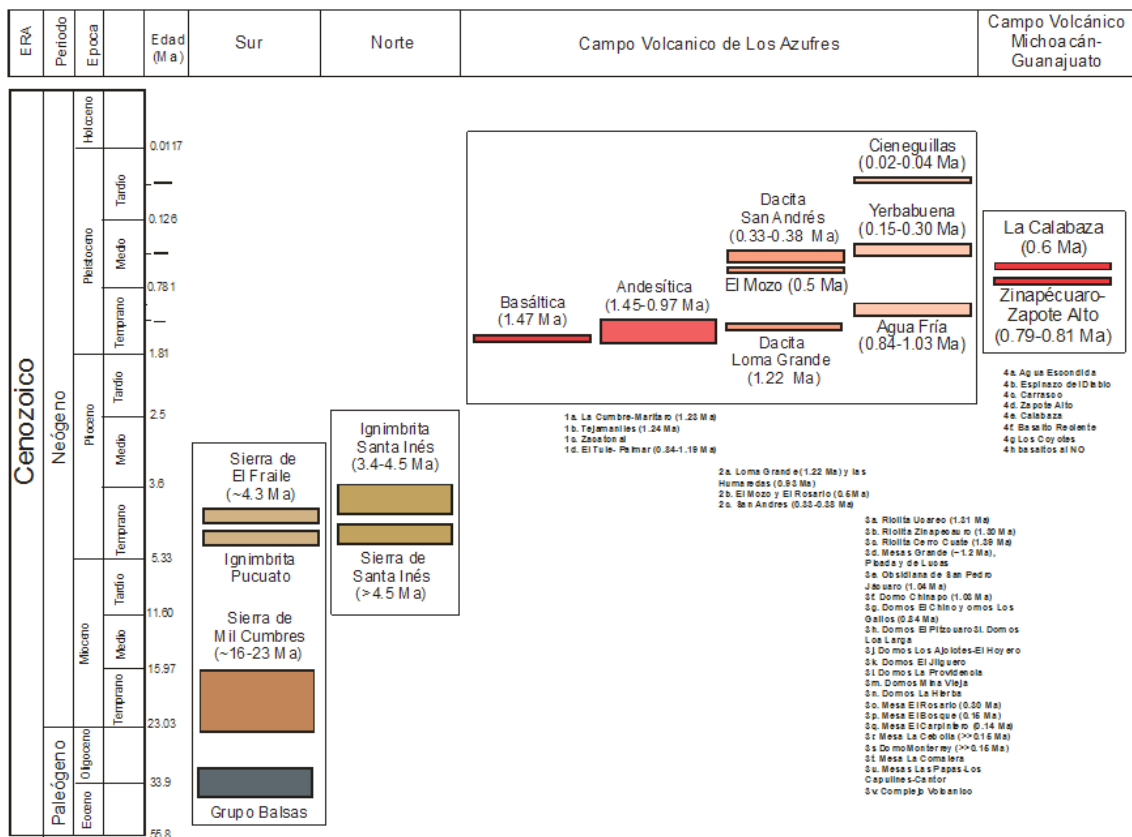


Figure 34: chronological sequence of the stratigraphically correlated volcanic events, occurred in the area of Los Azufres and surroundings (Pérez-Esquívias et al. 2010).

- At ~14.5 Ma there was the emplacement of a stratovolcano in the northern part of the studied area, which originated the Santa Inés Sequence. Nowadays, this sequence in the Santa Inés Mountain Range has an arcuate shape open toward the south, which seems to indicate that volcano were destroyed due to a high-magnitude eruption, associated with the formation of a caldera.
- The Activity continued at approximately 7 Ma with the effusion of andesitic lavas which are exposed above the Mil Cumbre Sequence in the W-SW of Figure 33.
- Lately, it is observed a volcanic activity return, with the explosive emplacement of the Santa Inés Ignimbrite at ~4.7 Ma, which fills the Santa Inés Range depressions, in the northern part of the area of Figure 33.
- At a later date, at ~4.3 Ma, the emplacement of Dacites and pyroclastic flows occurred, which formed the domes of El Fraile in the SE part of the area of Figure 33.

- The formation of the Los Azufres Volcanic field began approximately at 1.47 Ma. The magmatism was not centered in a unique place which would have given rise to the formation of a stratovolcano, but rather it was subordinated to the rise of magma through faults present in the area, generating temporally-random fissure effusions. In such a way, the magmatism began with basaltic emissions, followed by andesitic ones, with ages going from 1.47 to 0.97 Ma. Then it continued with dacitic lavas, with age between 1.22 and 0.33 Ma, and, finally, an evolution to rhyolitic emissions occurred, generating some important domes and plateaus, with ages comprised between 1.03 and 0.02 Ma. The products associated with this rhyolitic volcanism (domes and plateaus) stand undoubtedly above andesitic or andesitic-basaltic lavas, which correspond to apparatus belonging to the monogenetic volcanism of the Michoacán-Guanajuato Volcanic Field (MGVF), which is in turn part of the Western Sector of the TMVB. Those volcanos come across the periferical part of the area of Figure 33.
- At last, it must be said that the activity of the LAVF has not finished yet, as rhyolitic volcanic eruptions happened during the Late Pleistocene. Along with the volcanic activity, there are regional active faults which cut the volcanic complex. The major part of the domes of the field have an E-W structural geometry, like the Agua Fría fault which originated a south directed collapse of the domes themselves. In addition, dacitic lava domes and monogenetic volcanic apparatus were emitted through those regional E-W faults (and through other with NW-SE direction) .

A part from the mere volcanological history, what is really important for this work, are the geological map of the Los Azufres' area and surroundings (Figure 35), and the lithostratigraphic, volcanological and structural model for the LAGF (Figure 36), which were produced by Pérez-Esquívias et al. (2010).

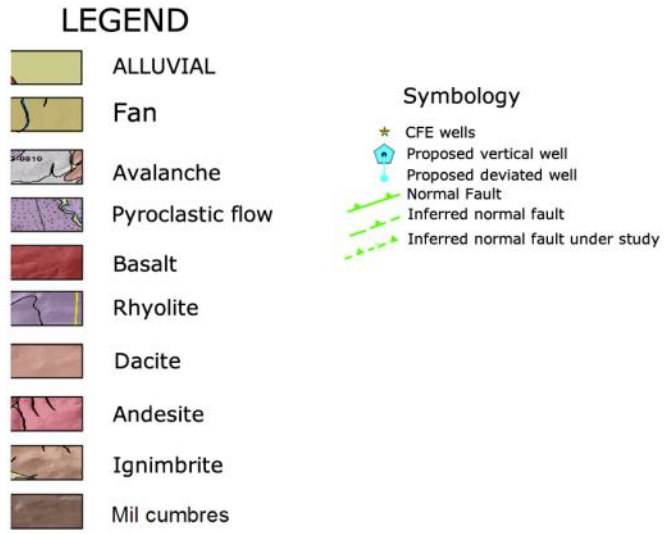
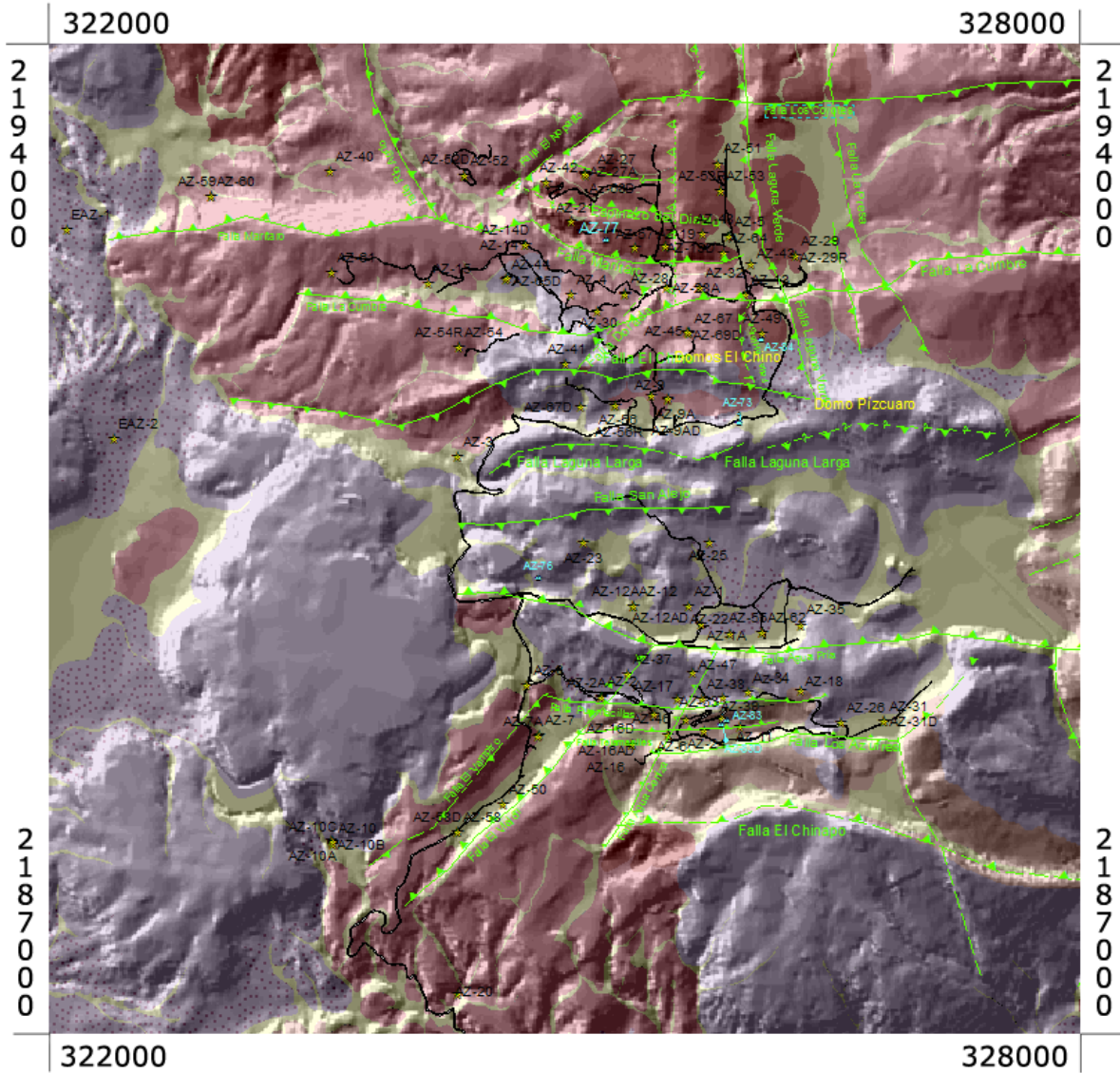


Figure 35: Structural and geological map of the investigated area in Perez-Esquívias et al. (2010)

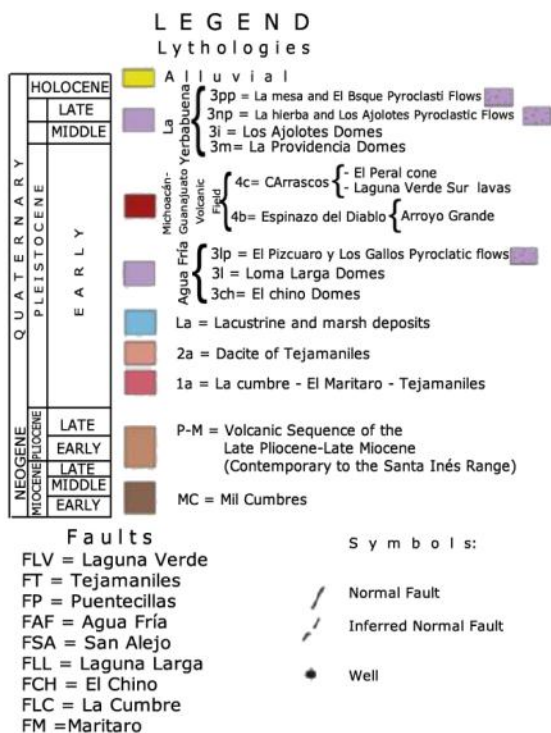
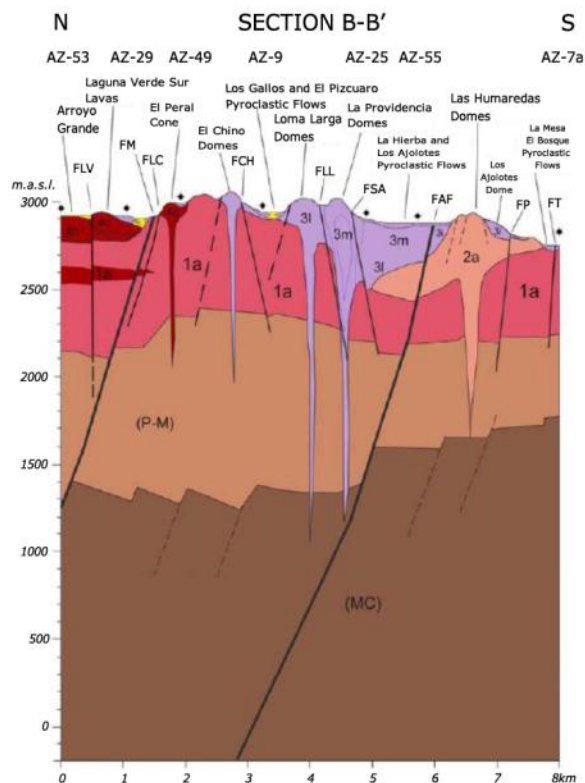
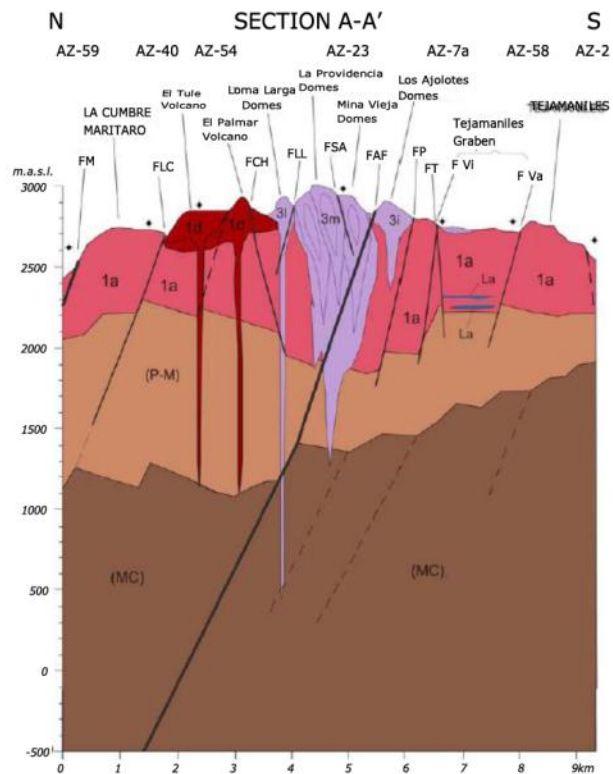
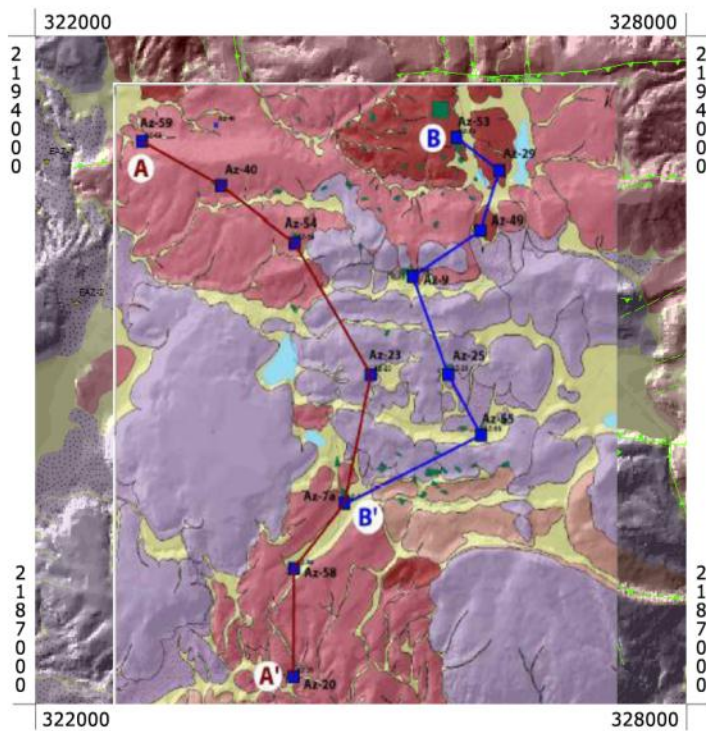


Figure 36: lithostratigraphic, volcanological and structural idealized model of the Los Azufres Geothermal Field Pérez-Esquívias et al. (2010).

In Figure 35, it is possible to note the presence of rhyolitic domes standing above andesitic lavas, and important alignments of E-W, NE-SW and N-S (or

NNW-SSW) direction. On the other hand, in the structural sections of the area (Figure 36), the main rock formations which are present in the Los Azufres underground are visible. The deepest one is the andesitic Mil Cumbre Formation (MC), overlain by another andesitic formation of Late Pliocene-Late Miocene age (P-M). In the upper part, it is visible the La Cumbre-El Maritaro-Tejamaniles andesite Formation (1a) overlain by Rhyolitic (3l, 3m) and Dacitic domes (2a). Also, it is possible to recognize the Maritaro Fault (FM) in the northern part and the Agua Fría Fault (FAF) in the southern one, reaching the Late Pliocene-Late Miocene complex (P-M) and the Mil Cumbre Formation (MC). A geothermal reservoir is present between ~2200 and ~700 m.a.s.l. and the interaction between main faults and lithological changes have made it profitable to exploitation (Pérez-Esquívias et al., 2010). Also the rhyolitic rocks result to be deeply fractured originating a reservoir, but the fracturing is with all probability only a superficial one with maximum depths of 500 m, excluding this formation from being exploitable for geothermal uses.

So, in the Los Azufres Geothermal field:

- a) The meso-structure direction corresponds to the regional fracturing, having direction NNW-SSE (or N-S), NE-SW and E-W where the main faults and fractures systems are observed.
- b) The inclinations of the fractures has a semi-vertical behavior in all the lithologies of the field, with a range that stands between 70° and 90°.
- c) The most intense fracturing is localized in the Santa Inés Range and in the Mil Cumbres Range, both of which are the hosting rocks of the geothermal reservoir and they are constituted by andesitic sequences. In the volcanic field the fracturing is much intense in major faults, which are the Marítaro and Agua Fría Faults.
- d) The geothermal reservoir is hosted in the most ancient units (Miocene-Pliocene), which have registered more deformation events. These units are suitable to localize future wells, which tend to intercept this deep formation. However, fracturing and faulting of the more recent rhyolites, reveals only superficial systems, not suitable for geothermal exploitation.

- e) In particular, quaternary rocks reach depth close to 500 m. Miocene rocks begin at depth varying from some 700 m in the south, until near 1200 m in the north, due to a stepped faulting. The actual results seem to indicate that the geothermal reservoir is closed-up by the quaternary volcanic rocks.
- f) Based on these assessments, two reservoir zones have been identified at different depth. The first ranges between 500 and 700 m depth from the ground level and is referred to the lithological change between Quaternary units (1.47 Ma) and andesitic rock of Pliocene Age (4.7 Ma), interacting with not very deep fractures and faults (i.e. Laguna Verde Fault FL, Puenteceillas Fault FP). The second zone is identified as the lithological change between Pliocene's rocks (4.7 Ma) and the Miocene's rocks of the Mil Cumbres Range ( 23 to 17 Ma) interacting with deep faults such as the Agua fría Fault and the Maritaro Fault.

Based on the available information, the research activity performed during this thesis work where devoted to formulate a proposal for a new productive well, called AZ-35A, to be drilled in the LAGF. An example of the kind of job that is necessary to carry out in order to drill a new well in a Geothermal Field is here presented: geological, geophysical, petrographical, geochemical and engineer skills must be taken into consideration in order to make it possible the drilling of a new production well.

## 5. METHODOLOGY

Aim of this thesis is to prepare a technical proposal for the drilling of a new production well.

On this purpose, the research activity consists of four main parts, summarized as follow:

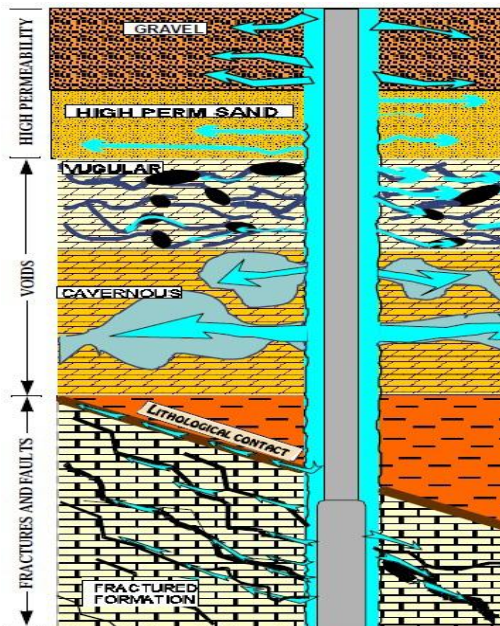
- Lost Circulation and Spinner Log analysis
- Structural Geology analysis
- Petrographic analysis
- Geophysics Electromagnetic analysis

Here after a short overview of the methodologies associated to each research step is described.

### 5.1 LOST CIRCULATION AND SPINNER LOG ANALYSIS

Lost Circulation is a loss of an appreciable part or entire volume of drilling fluid through borehole into cavernous, vugular and/or highly porous formation (Mohan Doshi, 2014). It can also indicate a faulted and fractured zone in a rock formation, or the lithological contact between two different rock formations (Figure 37). This is why circulation losses during drilling activities are so important, because they indicate the presence of a possible fractured zone able to host a geothermal reservoir. In a geothermal field, during the perforation of a new well, lost Circulation is measured in  $m^3/h$ .

*Figure 37: in this scheme it is shown a well that was drilled trough different rock formations and lithological contacts, each one of whom have the capability of losing circulation of perforation fluids. (modified from Mohan Doshi, 2014).*



Moreover, once the well has been already drilled, the presence of a Circulation Losses Zone, and the possible increasing or decreasing of the losses themselves during the years and so the efficiency of the well, can be detected through a device called *Spinner Flowmeter*. With this device it is also possible to detect eventual damages in the pipeline of the well.

The Spinner Flowmeter (Figure 38) is “A device for measuring *in situ* the velocity of fluid flow in a production or injection well based on the speed of rotation of an impeller, or spinner” (Shlumberger, 2015). The spinner can be helical (Figure 40), or like a vane, which is similar to a fan blade. In both cases, the speed of rotation is measured and related to the effective velocity of the fluid. There are several types of spinner flowmeter. The most common device uses a small vane-like spinner, about 1.5 in. [3.8 cm] in diameter, allowing the logging tool to pass through the tubing and other restrictions before reaching the reservoir interval. (Aziz et al., 2015). The Spinner is measured in Round Per Second (RPM) and a decrease in RPS indicates the escapement of fluids that is Circulation Loss, and so the presence of a permeable zone and the reservoir. Unexpected changes in the usual RPS vertical column usually indicates well’s damages.

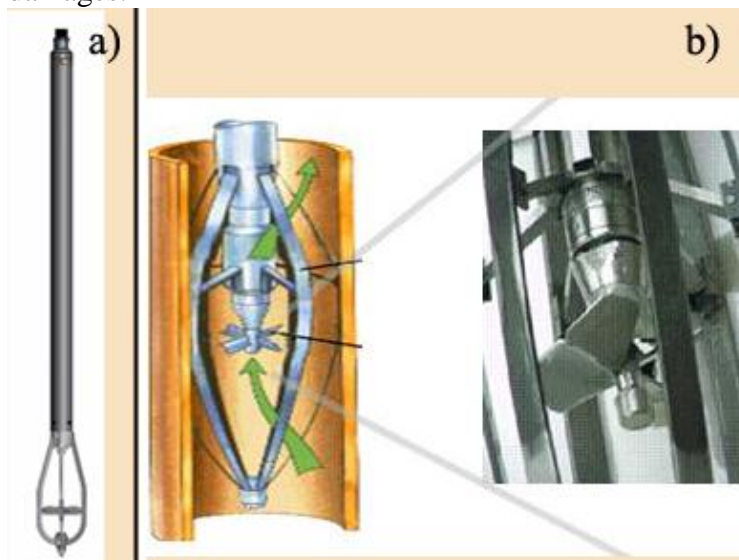


Figure 38: a) Example of Spinner Flowmeter probe for measuring impeller rotation caused by fluid flow in the borehole. B) Zoom on the helical probe of a Spinner flowmeter. (From Mount Sopris Instruments web site).

Comparing common Lost Circulations and Spinner Logs of different adjacent wells contributes to identifying the reservoir zones of a particular geothermal field area, section or volume.

## 5.2 STRUCTURAL GEOLOGY ANALYSIS

In order to define design, thickness and geometry of the faulting-fracturing system, as well as its dimensions, in the surroundings of a new well to be drilled, the finding of measurable and cartographable structural datum is carried on.

The method that is employed for the accomplishment of this goal consists in:

- Definition of an *Area of Investigation* in the surroundings of the well, usually including adjacent valleys or canyons where tectonic features are better visible
- *Strike and Dip Measurement of planar Structural Features* encountered inside the Area of Investigation, such as faults and fractures. In every Station of measurement (called *Structural Station*) geographical coordinates are taken with the use of a GPS device (Figure 39) and the position is marked in a topographical map showing the Area of investigation.

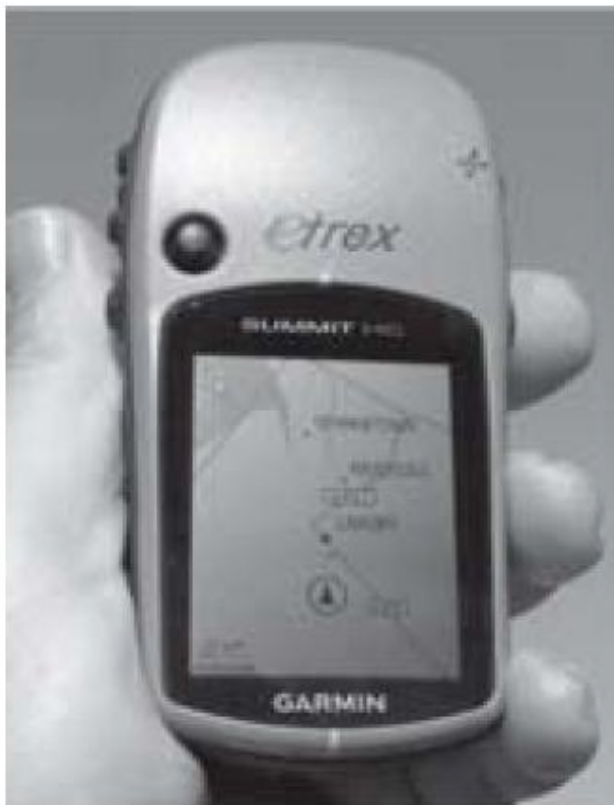


*Figure 39: example of GPS Garmin unit with ability to plot location onto a simple on-screen base map.*

*(from Lisle et al., 2011).*

Later, *Strike and Dip* of one or more structural features (Figure 40), encountered in every single Structural Station, are measured with the use of a Geological Compass (Figure 41).

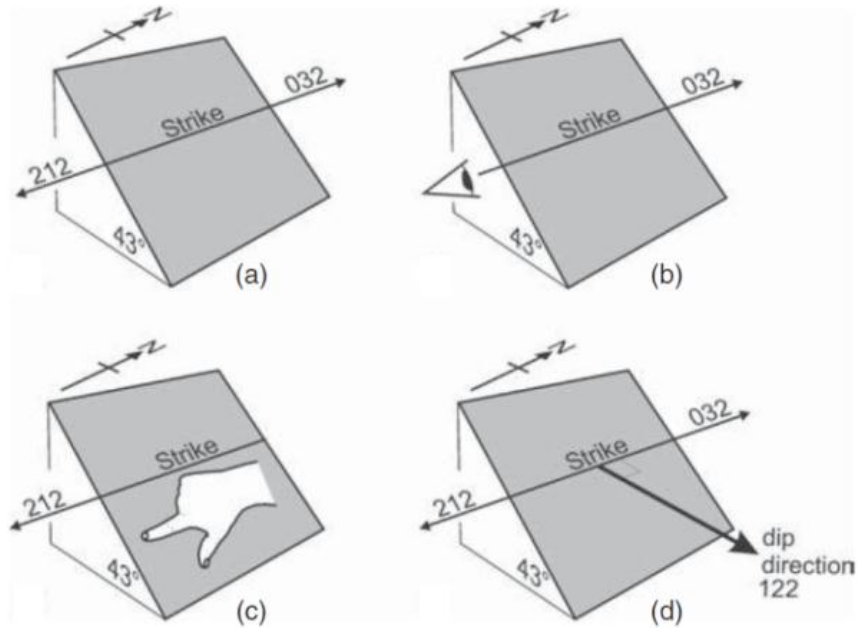
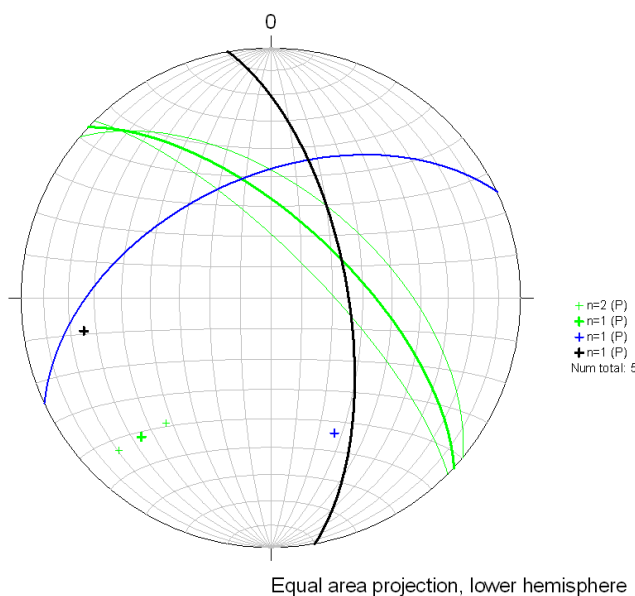


Figure 40: Conventions for recording strike and dip. (a) Strike/dip/quadrant of dip direction, that is, 032/43 SE (or 212/43 SE). (b) Strike/dip; the strike direction is chosen that, when used as a viewing direction, gives a dip to the right, that is, 032/43. (c) Strike/dip; the strike corresponds to the direction in which the index finger of the right hand points when the thumb points down dip, that is, 12/43. (d) Dip direction/dip, that is, 122/43 (from Lisle et al., 2011).



Figure 41: example of Compass designed for the geologist. In particular it is visualized a Finnish Suunto compass, similar to the Swedish Silva Ranger 15 TDCL. (from Lisle et al., 2011).

- Once Structural Features data have been collected, they are analyzed by:
  - *Graphing* the Strike and Dip datum measured in the field using the software *Stereonet* with the aim of producing a *Stereoplot* database. Usually, in the field surveys, for each Structural Feature, more than one measurement is done (usually five or ten), and they are all graphed along with their *Resultant*, which consists in the arithmetic average of strike and dip between all the measurements of the same structural feature (Figure 42).



*Figure 42: Example of a Stereoplot with marked Structural Datum*

- Elaborating a *Statistical Analysis above the Structural Datum*, identifying the main structural systems of the investigated area.
- Elaborating *Structural Profiles* crossing the area under investigation. In this way, different information about the wells standing in the same profile line, as well as the topography along it, can be graphed using the software *Grapher*.
- Finally, after an accurate examination of the profile, an *Area of Geothermal Interest Economically Exploitable* is defined, which is the final goal of each profile.

### 5.3 PETROGRAPHIC ANALYSIS

The Petrographic Analysis in a geothermal area aims to identify the main minerals related to presence of the geothermal reservoirs. For this purpose, specimens duly collected along the wells at disposal are used. The research activities can be summarized as follows::

- Identification of the *Lithostratigraphic Column* of the New Well under study. If the new well is going to be drilled in a completely new platform, the column can be inferred with the correlation between nearby wells' lithostratigraphic columns. On the contrary, if it is going to be drilled in an already existing platform, the column can be inferred from that of the platform's wells.
- *Identification of Minerals.* The adequate instrument for the accomplishment of this purpose is the *Polarized light Microscope* (Figure 43b), an instrument which allows to observe the enlarged image of a mineral or rock section and, through the light polarization, to study the optic properties of minerals to get to their identification (Bellieni et.al., 2004). Single minerals and rock must be previously brought, through the use of special abrasives, to the thickness of 30 micrometers. One of more pieces of rock are glued together, cut with a diamond saw until a thickness of 30 micrometers is reached and finally covered with a thin glass. From this process, *Thin Sections* (Figure 43a) analyses are made (Bellieni et.al., 2004).

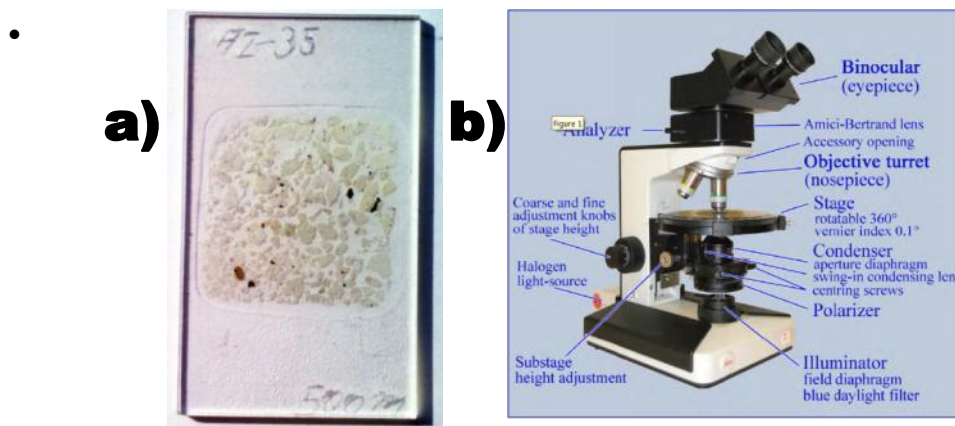


Figure 43: a), Thin Section; b) Polarized Light microscope. (from Raith et al., 2012)

- Thanks to Thin Section analyses with Polarized Light microscope, it is possible to recognize *alteration minerals* in the samples. These minerals are particularly important because they indicate specific temperature ranges of formation and stability. Apart from high intensity alteration, they're indicators of high permeability in the geothermal reservoir. It's for that reason that they are called Thermoindicator minerals and they are used as geothermometers for the identification of the reservoir temperature (Figure 44 - Lagat, 2010).

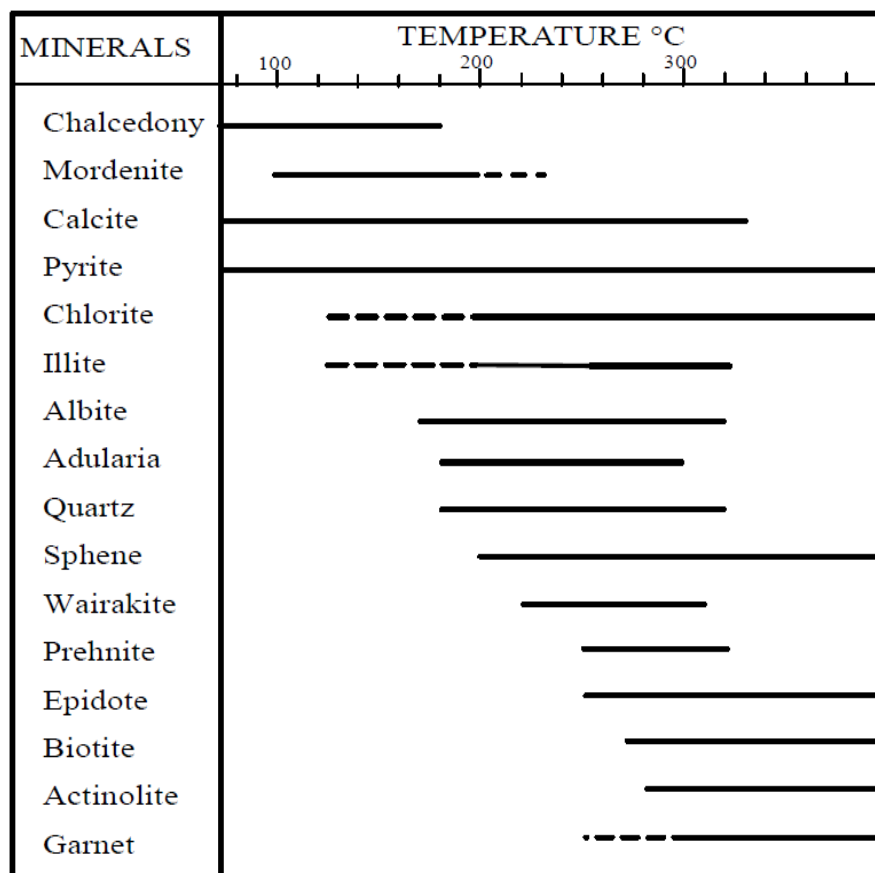


Figure 44: Common hydrothermal alteration minerals used as geothermometers and their temperature stability ranges. Dotted sections indicate mineral outside their usual stability ranges (modified from Lagat, 2010)

For example in Los Azufres field, well-crystallized Epidote indicates temperature of over 220°C. Presence of Chlorite and Epidote reveals temperatures of 220-340°C, while that of Actinolite-Tremolite occurs at 280-350°C. Garnet normally is an indicator of temperatures over 300°C, while

Smectite of less than 220°C. So normally the reservoir at LAGF is included between the presence of Epidote and Anfibol (Actinolite-Tremolite).

Considering the presence of Hydrothermal Minerals inside samples of the Petroteque, *Hydrothermal Zones* with different mineralogical association can be distinguished (CFE, 2014).

#### 5.4 GEOPHYSICS ELECTROMAGNETIC ANALYSIS

The transient electromagnetic method, TEM, allows to measure the electrical resistivity of the underground layers down to a depth of several hundred meters.

The electromagnetic geophysical methods are all based upon the fact that a magnetic field varies in time – the primary field – and thus, according to the Maxwell equations, induces an electrical current in the surroundings – e.g. the ground as a conductor. The associated electrical and magnetic fields are called the secondary fields. The TEM method applies an ungrounded loop as transmitter coil. The current in the coil is abruptly turned off, and the rate of change of the secondary field due to the induced eddy currents in the ground is measured in the receiver coil, usually an induction coil. The primary field is therefore absent while measuring (Sørensen et al., 2006) (Figure 45).

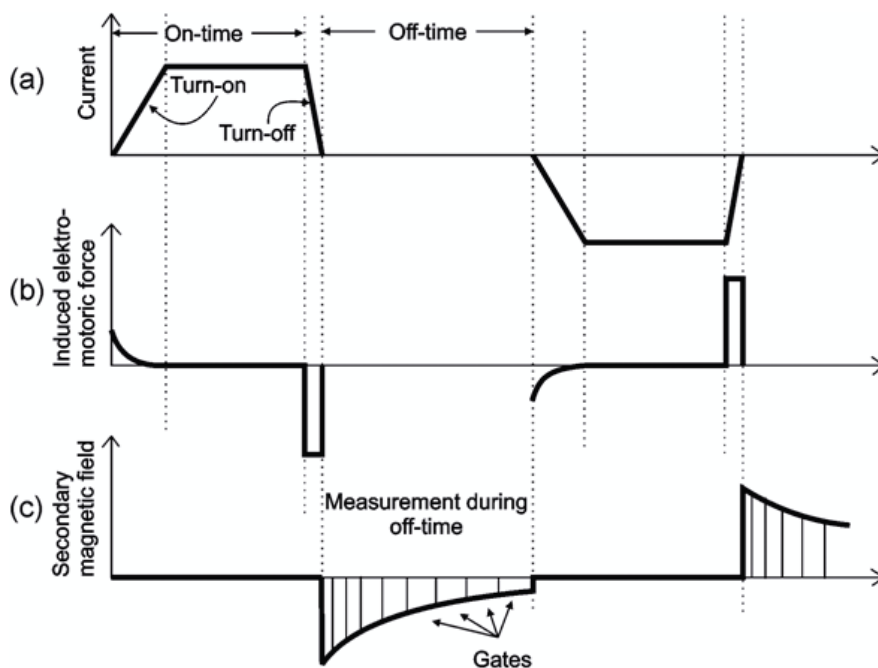


Fig. 45: Basic nomenclature and principles of the TEM method. (a) Shows the current in the transmitter loop. (b) is the induced electromotive force in the ground, and (c) is the secondary magnetic field measured in the receiver coil. For the graphs of the induced electromotive force and the secondary magnetic field, it is assumed, that the receiver coil is located in the centre of the transmitter loop (from Sørensen et al., 2006)

When performing fieldwork, a transient electromagnetic sounding can be conducted by placing a wire in a square loop on the ground as the transmitter coil, Tx-coil.

The measurements are carried out by ejecting a current in the Tx-loop (Figure 46). Just after the current in the Tx-loop is turned off, the current in the ground will be close to the surface, and the measured signal reflects primarily the resistivity of the top layers. At later decay-times the current has diffused deeper into the ground, and so the measured signal contains information about the resistivity of the deeper layers. Measuring the current in the Rx-coil will therefore give information about the resistivity as a function of depth. The configurations shown in Figure 46a have the receiver coil placed in the centre of the Tx-coil and is called a central loop or an in-loop configuration. The receiver coil can be placed outside the Tx-loop (Figure 46b) which results in an offsetloop configuration (Sørensen et al., 2006).

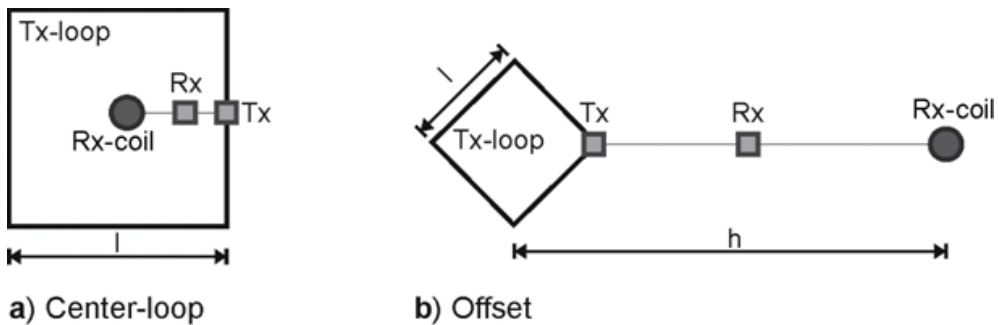


Fig. 46: Field setup of a TEM system: a) Shows a central loop configuration, b) an offset-loop configuration. Rx denotes the receiver, Tx the transmitter,  $l$  the side length of the loop and  $h$  the offset between Tx-coil and Rx-coil centres.

The acquired data is an observation of the decaying magnetic field, which is not very informative. For this reason, through inversion methods, the plot of magnetic decay is converted into a plot of apparent resistivity,  $\rho_a$ , which is more illustrative. The  $\rho_a$ -converted curves can be used as a data quality tool and as first estimate of the resistivity levels of the underground structure. (Sørensen et al., 2006).

## 6 ANALYSIS OF RESULTS

### 6.1 CASE STUDY

Within the production wells of the Los Azufres geothermal site (see Figure 14), the research efforts have been focused on the AZ-35 well (Figure 47). It was drilled at the beginning of the 1980's and was integrated in the energy production unit U-7 called Tejamaniles in 1988 (see Chapters 3.2-3.3 and Figure 16), for commercial generation of electricity. The well is located in the eastern part of the "Agua Fría" Fault (see chapter 4.3), characterized by an E-W direction, where optimum conditions for the steam production are encountered. The AZ-35 is located near the CFE camp of Los Azufres (650 m to the S-E), the well AZ-18 (697 m to the N) and the well AZ-62 (416 m to the NE) and has a total depth of 1240 (Izaguirre, 1983). Its coordinates are (Figure 47):

$$X = 326,731.94; \quad Y = 2,188,981.83; \quad Z = 2,870.82 \text{ m.a.s.l.}$$

This well has got a total depth of 1240 (Figure 47) (Izaguirre, 1983).

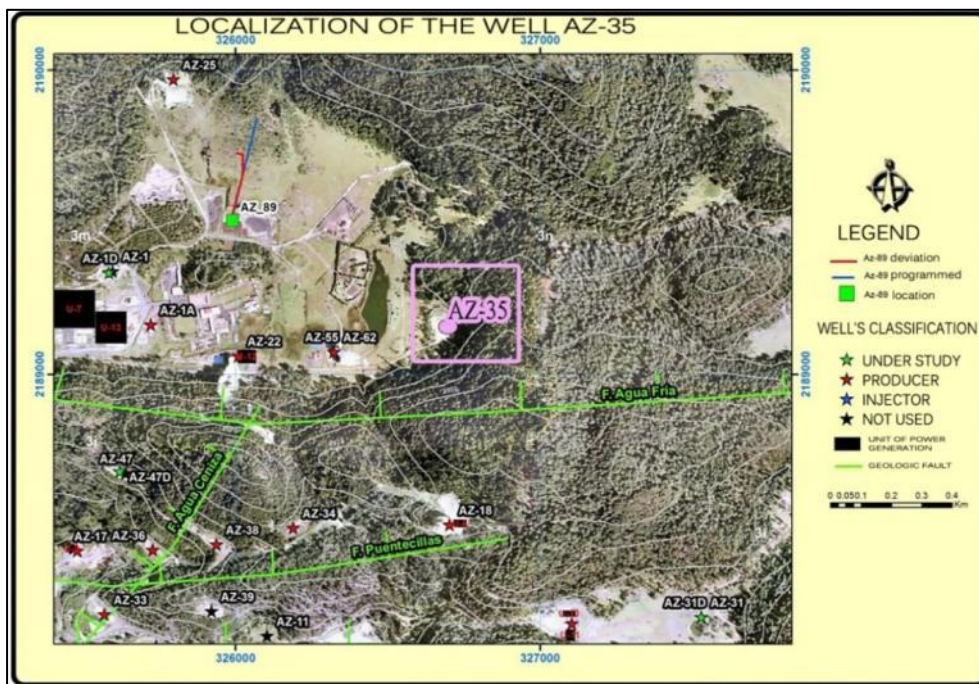


Figure 47: location of the well Az-35 (CFE, 2011).

At the end of September 2012, the U-7 had to be subjected to some maintenance operations, and in this contest the AZ-35 was subdue to a diminishing of its

production orifice from 4'' to 1'', in order to save vapor during the maintenance operations, when the well would have been out of the production system. However, after five days, some cracks with vapor emanations were detected in a considerably wide area surrounding the platform of the AZ-35, as well as the lifting up of the well shaft, the retention area around the drill hole and the steam-pipeline of approximately 10 cm above the natural ground level.

The problem required immediate attention by the personal of the Residence of Studies at the LAGF. The place was analyzed and evaluated to plan a possible solution. The first suggestion to solve the problem was that of coming back to the original conditions on which the well was originally integrated, in order to see if the emanations and the rising up of the wellshaft would return to their original positions. This operation gave good results at least for the steam-pipelines and the wellshaft, which returned to their original position, but the vapor emanations didn't stop. (Figure 48)



*Figure 48: Platform of the Well AZ-35, at the time when vapor emanations were discovered (CFE, 2012).*

Given that, the Areas of Geology, Geophysics, Geochemistry and Reservoir Engineering planned analysis for these anomalies, which emphasizes the presence of a mechanical damage in the pipeline of 9 5/8'' at 815 m of depth (CFE, 2015).

Furthermore, looking at the sheets concerning the well's perforation (Izaguirre 1983) and another register of P-T-S (Pressure-Temperature-Spinner) realized in 2000 (CFE, 2015), it was found out that during the same perforation, at the moment of covering the circulation loss zones, the cementation didn't fit well, which indicates that since then the well is badly cemented.

During the well perforation Circulation Losses were registered between 1110 and 1150 m of depth (Figure 49a). Comparing them with results of the Spinning Log registered in 2000 (Figure 49b) the same Lost circulation Zone is identifiable. In fact, between 1100 and 1150 m of depth the RPS number diminish drastically until reaching a value of 0, which means that the Spinner Flowmeter (see Figure 40) diminishes its rotation until stopping it, due to complete loss of fluid circulation inside the pipeline, because of the presence of an highly fractured zone. Moreover, looking in details to the Figure 49b, it is also possible to identify mechanical damages in the pipeline of 9 5/8'': the first damage zone is at 265 m of depth (RPS diminishing), and the second one begins at 740 m of depth, and it was lately identified to be at 815 m (CFE, 2015 (1)).

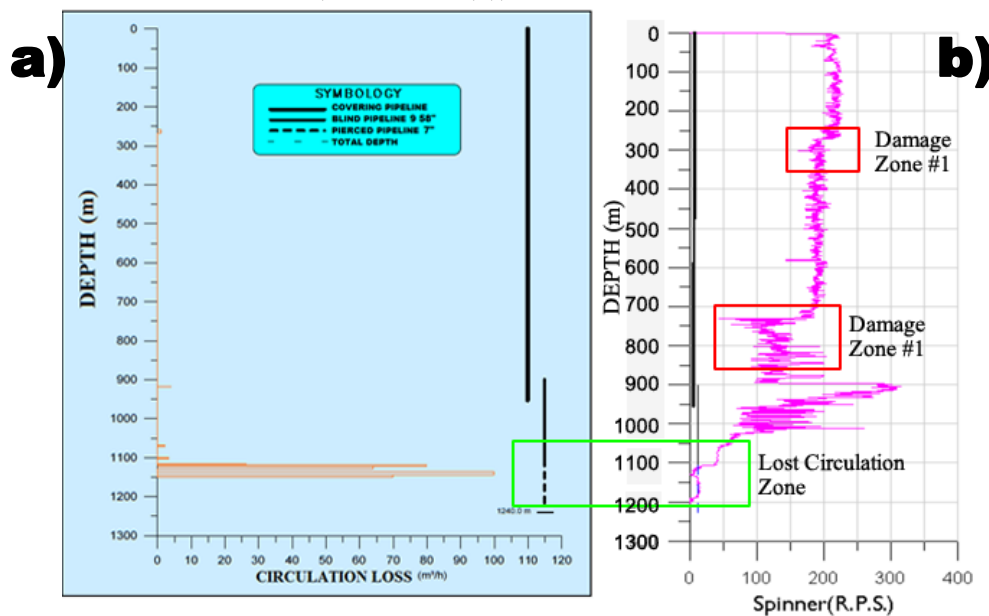


Figure 49: a) Original Circulation loss zones, encountered during the perforation. b), Spinner register (RPS=round per second) realized in 2000 (from CFE,2015 (1))

This means that in the year 2000 the damaging was already existent, probably dating from the time of construction, as the cement didn't fit well the fissures in the permeable zone (CFE, 2015 (1)).

After that, the Area of Geology and Geophysics planned the possibility of making a concrete-injection treatment, with the perforation of various boreholes at different depth around the well. In November 2012, it started the beginning of this treatment and gradually it was observed a notable gases emanation's decreasing on surface.

In spite of that apparent improvement in the well's conditions, the well required greater mechanical reparation. Therefore, given the age and use conditions of the AZ-35, a better option was to consider the drilling of a new twin well, called AZ-35A, that would stand in the same platform of the former one (Figure 50).

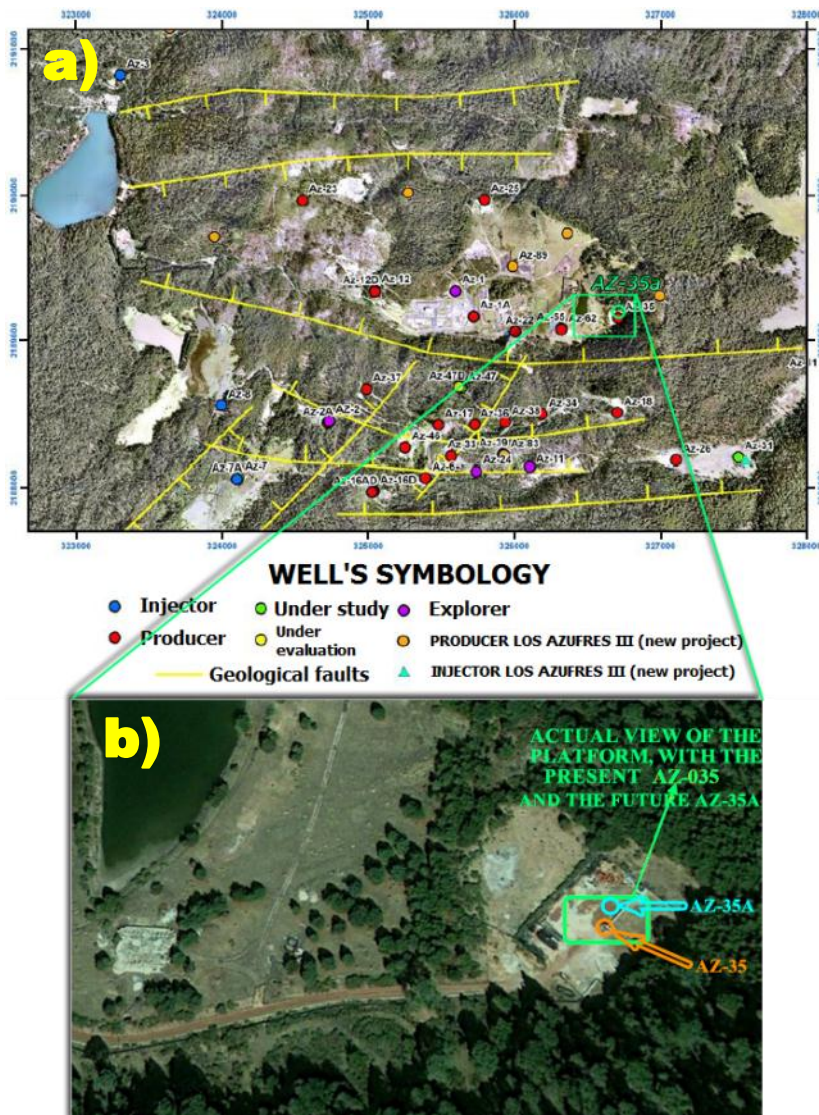


Figure 50: a) Geographic map of the south zone of the LAGF, in which it is possible to see the principal tectonic features and the location of the AZ-35. b) Google Earth image zooming into the platform of the AZ-35 showing the decided location where the new AZ-35A would be drilled.

The successive activities, which are the subject of the next chapters, concerned the analysis of all the available information and collection of new data, in order to identify the optimum conditions for the perforation of the new well AZ-35A.

The AZ-35A would be localized at the northern extreme of the platform, some 10-15 meters north of the AZ-35 (Figure 50b). This position is considered to be the best, because in this way the Agua Fria Fault System can be intercepted at greater depth, given its north-dipping inclination (see chapter 4.3).

The platform of the well AZ-35 is property of the CFE and it is free from vegetation. The UTM proposed coordinates for the new well AZ-35A are the following:

X=326712.0;      Y=2189169.9;      Z=2877 masl.

## 6.2 *LOST CIRCULATION AND SPINNER LOG RESULTS*

It is now presented an analysis on the well AZ-35 and different wells of the LAGF surrounding it, were Lost Circulation values measured during the perforation and Spinner Log analysis made after the well was drilled, are considered.

In both cases, the relative information belongs to the LAGF base camp, and have been made available by the CFE Studies Area.

Two sections oriented E-W and NW-SE were produced, in order to identify the possible correlation zones between the available wells standing along the same profile using data from the Lost Circulation values and Spinner log analysis.

### ***E-W Correlation***

The first section with E-W direction involves wells Az-12, Az-12D, Az-1A, Az-22, Az-62 and Az-35, where AZ-12 and AZ-12D reach the greater depth, over 1900 m (Figure 51).



Figure 51: E-W section for the proposed well AZ-35A, with wells indication.

The analysis of the circulation losses allows to detect three different intervals (Figure 52).

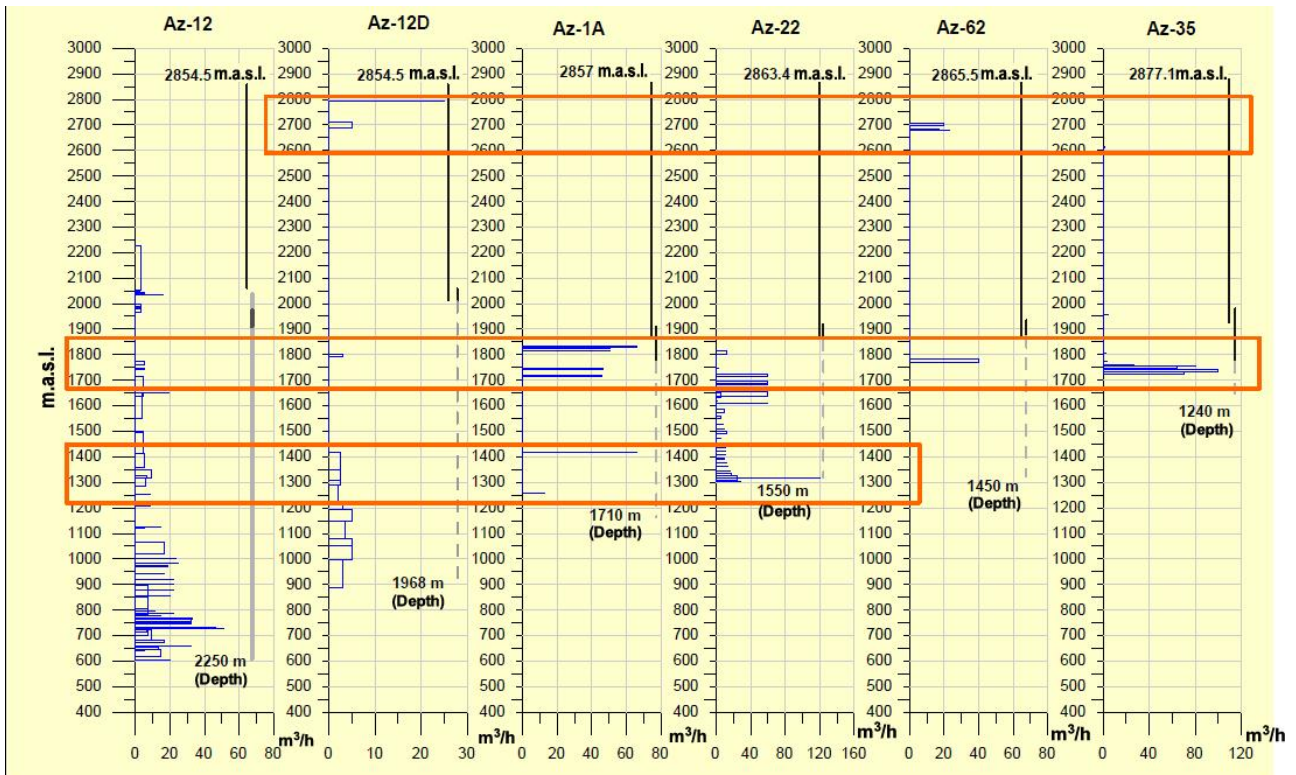


Figure 52: E-W section crossing the wells AZ-12, AZ-12D, AZ-1A, AZ-22, AZ-62 and AZ-35. Orange-contoured zones are given by the correlation between Circulation losses encountered during the wells drilling.

The first interval is observed at 2850-2650 m above sea level (m.a.s.l.), that is about 100-300 m of depth from the ground level. The circulation losses belongs to wells AZ-12D, AZ-62 and, in minimum quantity, AZ-35.

The second one is encountered in each well between 1900 and 1700 m a.s.l., about 1050-1250 m of depth. This is the most important interval as regards the permeability.

The third interval ranges between 1470 to 1250 m.a.s.l., that is about 1430-1700 m of depth, The AZ-62 well does not show circulation losses in its deepest zone, while the AZ-35 was not taken into account because its total length stops at about 1650 m a.s.l. Nevertheless, the existence of this circulation loss interval along the AZ-35 well column and, as a consequence, along the AZ-35A, is quite sure.

Spinner Log data registered by a Spinner Flowmeters are in agreement with the Lost Circulation analyses, identifying the same zones characterized by fracturing in the Geothermal reservoir (see chapter 5.1).

The RPS number of the Spinner Log, registered in wells AZ-1A, AZ-22, AZ-62, AZ-35 along the E-W section (Figure 53), shows a diminishing trend between 1900 and 1700 m a.s.l., about 1050-1250 m of depth, corresponding to the second interval of circulation fluid loss (Figure 52).

In wells AZ-1A and AZ-62, the presence of a deepest fractured zones is directly observed (CFE, 2015 (1)), while in wells AZ22 and AZ35, due to the lower total length of the wells (< 1300 m), the existence of the third interval is derived from the comparison with the other wells.

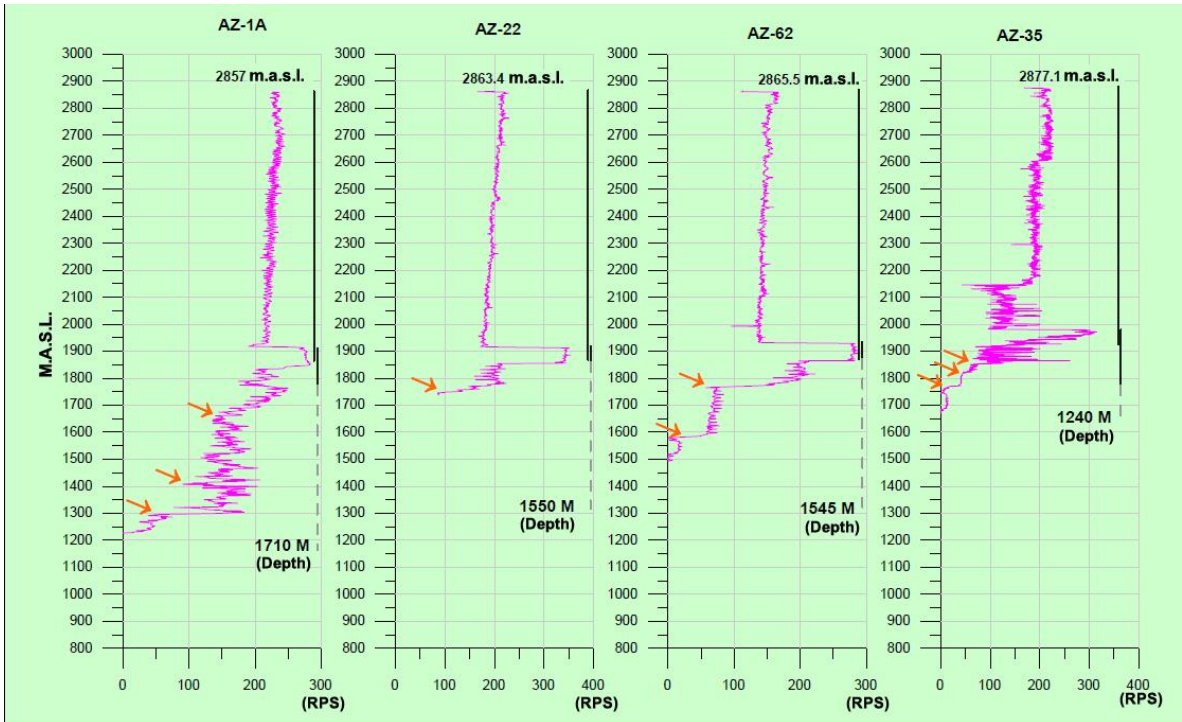


Figure 53: correlation of Spinner Logs for the proposed well AZ-35A, according to the E-W section (Figure 51). Great diminishing in the RPS number are indicated with orange-colored arrows.

### NW-SE Correlation

The second section has a NW-SE orientation and crosses nearby the wells AZ-25, AZ-89, AZ-35 and AZ-18 (Figure 54).



Figure 54: NW-SE section for the proposed well AZ-35A with the location of the correlated wells.

Like in the previous section, first the correlation between the different circulation losses intervals was carried out (Figure 55).

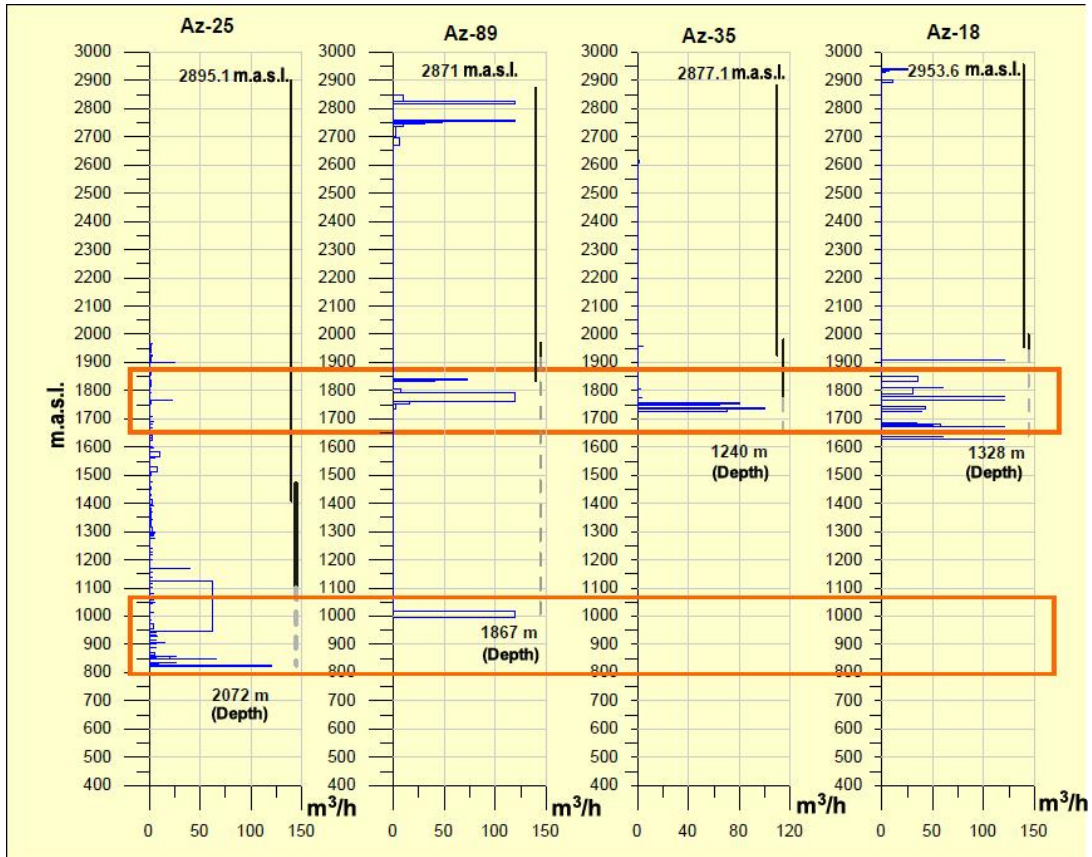


Figure 55: NW - SE section crossing the wells AZ-25, AZ-89D, AZ-35, and AZ-18. Orange-contoured zones highlight the existence of Circulation losses during the drilling of the wells.

Two intervals of weakness were detected for the NW-SE section: the first one between 1850 and 1700 m a.s.l., that is about 1000-1250 m of depth; the second one between 1100 and 850 m a.s.l., that is about 1850-2100 m of depth. Although the second interval is shown only in the deepest wells of the section (AZ-25 and AZ-89), it is reasonable extend it also under wells AZ-35 and AZ-18, that do not reach depth greater than 1350 m (CFE, 2015(1)).

Concerning Spinner Register correlation analysis, data were available only for wells AZ-25 and AZ-35. For well AZ-89 only the final phases of its perforation data, that is PT Register and Water Loss Test, have been used (Figure 56).

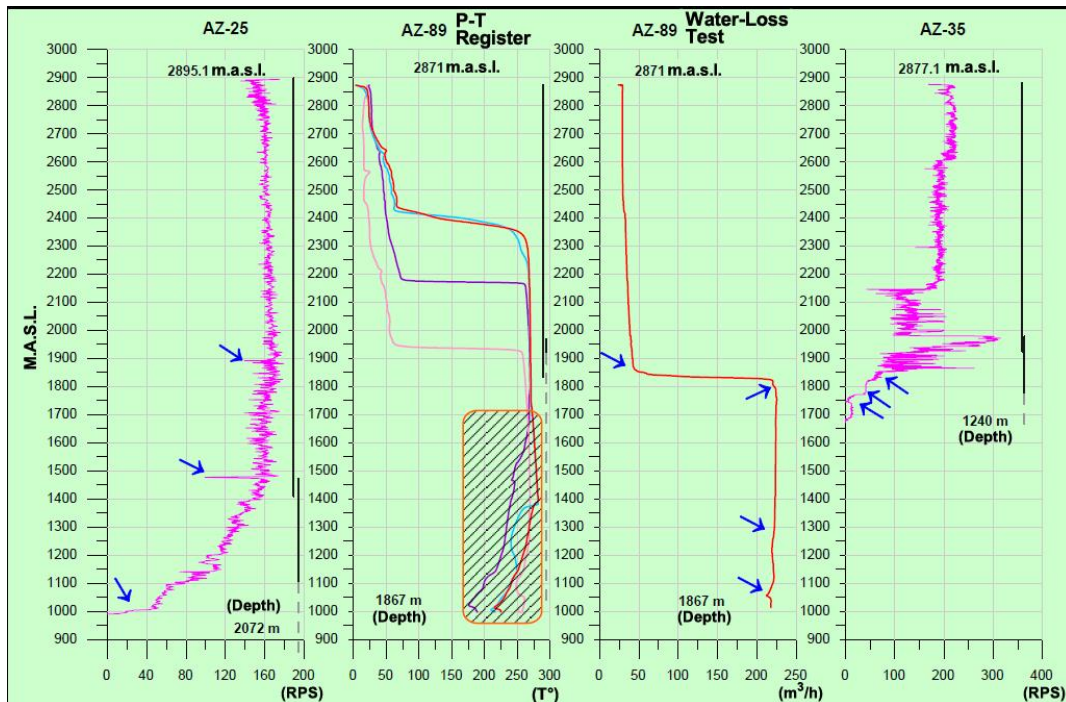


Figure 56: correlation of Spinner Logs, according to the NW-SE section (Figure 54). Great diminishing in the RPS number are indicated with blue-colored arrows.

Given that, it is possible to observe a correlation between contribution zones for the well AZ-89 and the wells AZ-25 and AZ-35 in the interval between 1900 and 1700 m.a.s.l (~1000-1200 m of depth).

It can be observed also a good correlation between Contribution Zones of wells AZ-25 and AZ-89 in the interval between 1500 and 1000 m.a.s.l, given that in well AZ-25 two Contribution Zones are shown and in well AZ-89 a large permeable interval is visible.

From the results exposed in the previous pages, it is possible to affirm that a good correlation exists between the E-W section's wells, either in terms of Circulation Losses and in terms of Spinner Log analysis. Wells Az-1A, Az-22, Az-62 and Az-35 are characterized by a fractured zone in the interval between 1900 and 1700 m.a.s.l. (~1050-1250 m of depth), corresponding to the geothermal productive section of the field. A good correlation exists, also, with the wells of the NW-SE sector, concerning both the Circulation Loss and Spinner Logs data. Wells AZ-25, AZ-89 and AZ-18 are productive and the most important zone of contribution and loss is located in the interval ranging from 1900 to 1600 m.a.s.l. (~1050-1350 m of depth).

So the new well AZ-35A is going to encounter at least this great Lost circulation zone, if it would maintain the same production activity of its twin well AZ-35.

On the other hand, if the new well will be drilled until greater depth, it is possible that other two Lost Circulation zones would be encountered: The first between 1470 and 1250 m.a.s.l. (1430-1700 m of depth) and the second one from 1100 to 850 m a.s.l. (~1850-2100 m of depth).

In conclusion, the proposal of perforation of the well AZ-35A, from the Circulation Losses point of view, is viable in agreement with the results of the analyzed information. In the two analyzed sections (E-W and NW-SE), the most important interval of production of the wells is encountered at 1900 -1600 m a.s.l (1050 to 1350 m of depth), that, in fact, is where the same wells are actually producing. Nevertheless, the information of the two sections and the correlations encountered in those sectors indicate, also, that there are good possibilities to encounter permeable and productive zones at greater depth. It is for this reason that from the beginning it is suggested to drill the new well until a depth of ~2000 m from the ground level. This would allow to reach the deepest liquid-dominant reservoirs, which are known to be more productive and long-lasting (see Chapter 3.2). It is suggested to take special care during the drilling, in order to preserve this important production interval in the south zone of the LAGF.

### 6.3 STRUCTURAL GEOLOGY ANALYSIS

#### *Field Survey*

A geological Field Survey was realized within an *Area of Investigation* of ~1.90 Km<sup>2</sup>, which is delimited by the following UTM coordinates (Figure 57):

$$X = 325178 - Y = 2189147; X = 327874 - Y = 2189427;$$

$$X = 325178 - Y = 2188584; X = 327874 - Y = 2188584.$$



For each Structural Station, the position was detected by a GPS device and usually 5 structural measurements of the same tectonic features were taken.

The processing of the rough data collected allows to obtain 30 structural Resultants (mean strike and dip determined for every Structural features of a Structural Station), distributed over 21 Structural Stations (Table 2).

Structural Station (EE <i>Estación Estructural</i> )	UTM coordinates	E- W system, Agua Fria Fault	NE-SW System	N-S system	NW-SE system
EE 01-14	325300.4 2188815	NW74 84°SW			
EE 02-14	325369.8 2188733.9			NW10 89°SW	
EE 03-14	325457.7 2188756.7		NE51 88°SE		
EE 04-14	325642 2188689	NW83 81°SW			
EE 05-14	326132 2188766				NW61 82°NE
EE 06-14	325470 2189027	NE70 75°NW			
EE 10-14	327603 2189158		NE44 35°NW		
EE 11-14	327592 2189118		NE49 50°NW	NE12 50°NW	
EE 12-14	327678 2189280		NE40 60°NW		
EE 13-14	327627 2189293	NE80 80°NW			
EE 14-14	327743 2189373	NE80 55°NW	NE65 50°SE		
EE 20-14	326163 2188685	NW71 80°NE		NW09 59°SE	
EE 21-14	326079 2188684		NE32 45°SE		NW38 55°NE
EE 22-14	326471 2188854	NE 75 47°NW			

EE 23-14	326696 2188827		NE65 50°NE	NW10 65°NE	NW50 65°NE
EE 24-14	326469 2188725	NE88 40°NW NW70 80°SW			NW40 55°NE
EE 25-14	326396 2188854	NE81 50°NW			
EE 30-14	3272122 2188720	NE72 62°NW	NE32 60°NW		
EE 31-14	327249 2188755			NE03 70°NW	
EE 32-14	327250 2188748		NE45 82°NW		
EE 33-14	327140 2188757				NW50 60°NE

Table 2: structural resultants for structural stations of 2014 field survey.

A statistical analysis of all the data collected, summarized in Table 2, reveals that:

- E-W system constitutes 37% (11/30) of the direction Resultants collected;
- NE-SW system represents 30% (9/30) of the direction Resultants collected;
- N-S system constitutes 16.5% (5/30) of the direction Resultants collected ;
- NW-SE system constitutes 16.5% (5/30) of the direction Resultants collected

It clearly results that the E-W and NE-SW systems are part of the Agua Fría Fault system and are the most important in this part of the LAGF. Moreover, the N-S and NW-SE fault systems must be taken into consideration to identify the optimum conditions in order to drill a productive AZ-35A well.

Lately, in order to better visualize the Structural datum measured in the field, all data were graphed using the software *Stereonet* (Figures from 59 to 63), with the color classification mentioned above.

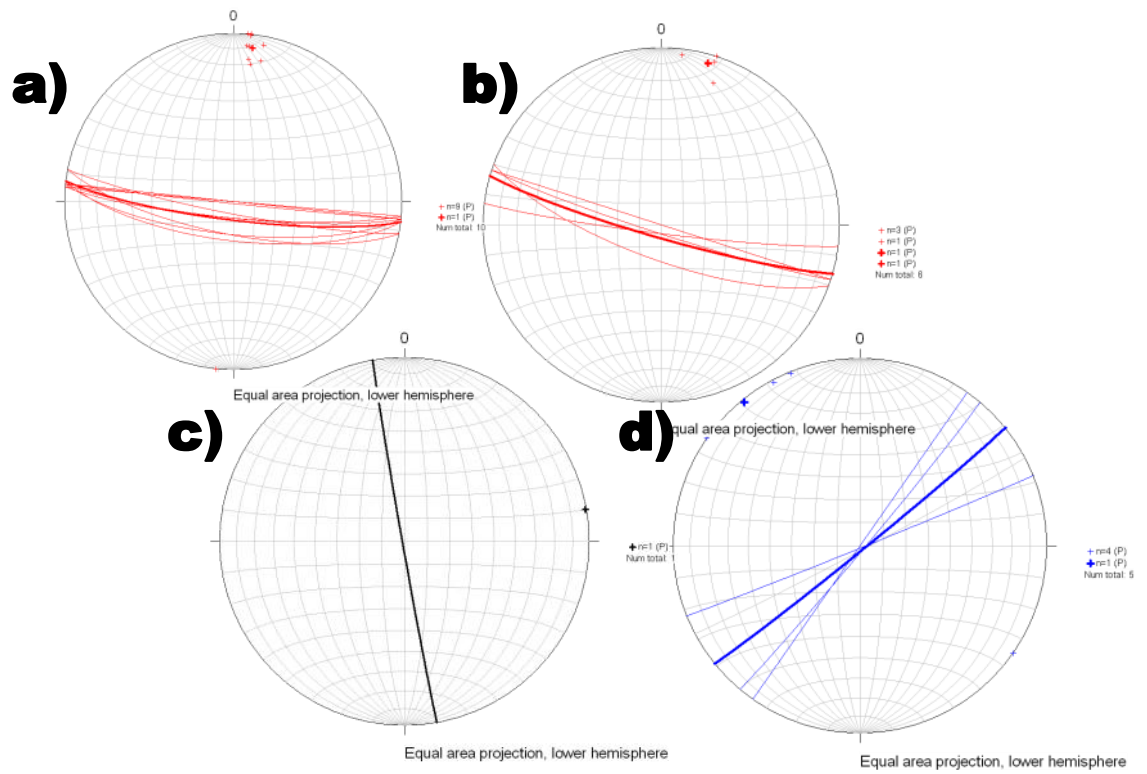


Figure 59: Stereoplots for the structural stations a) 01-14, b) 02-14; c) 03-14 and d) 04,14 (see table 2 and Figure 58)

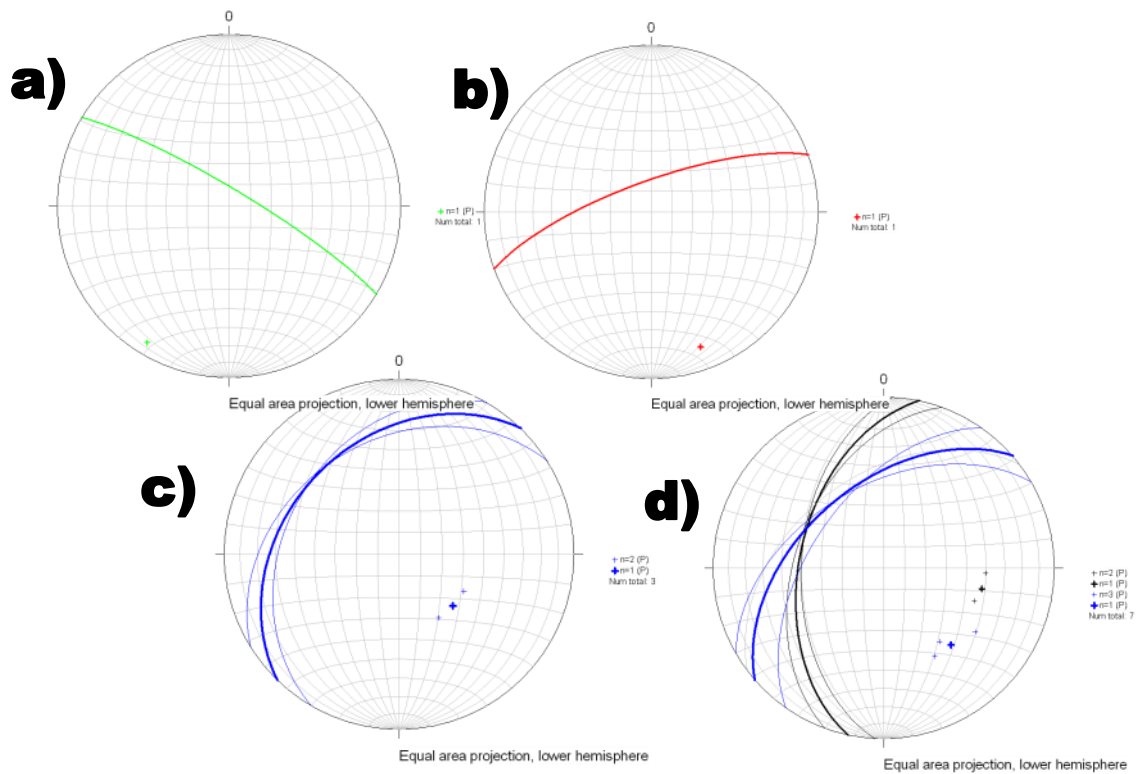


Figure 60; Stereoplots for the structural stations a) 05-14, b) 06-14; c) 10-14 and d) 11,14 (see table 2 and Figure 58)

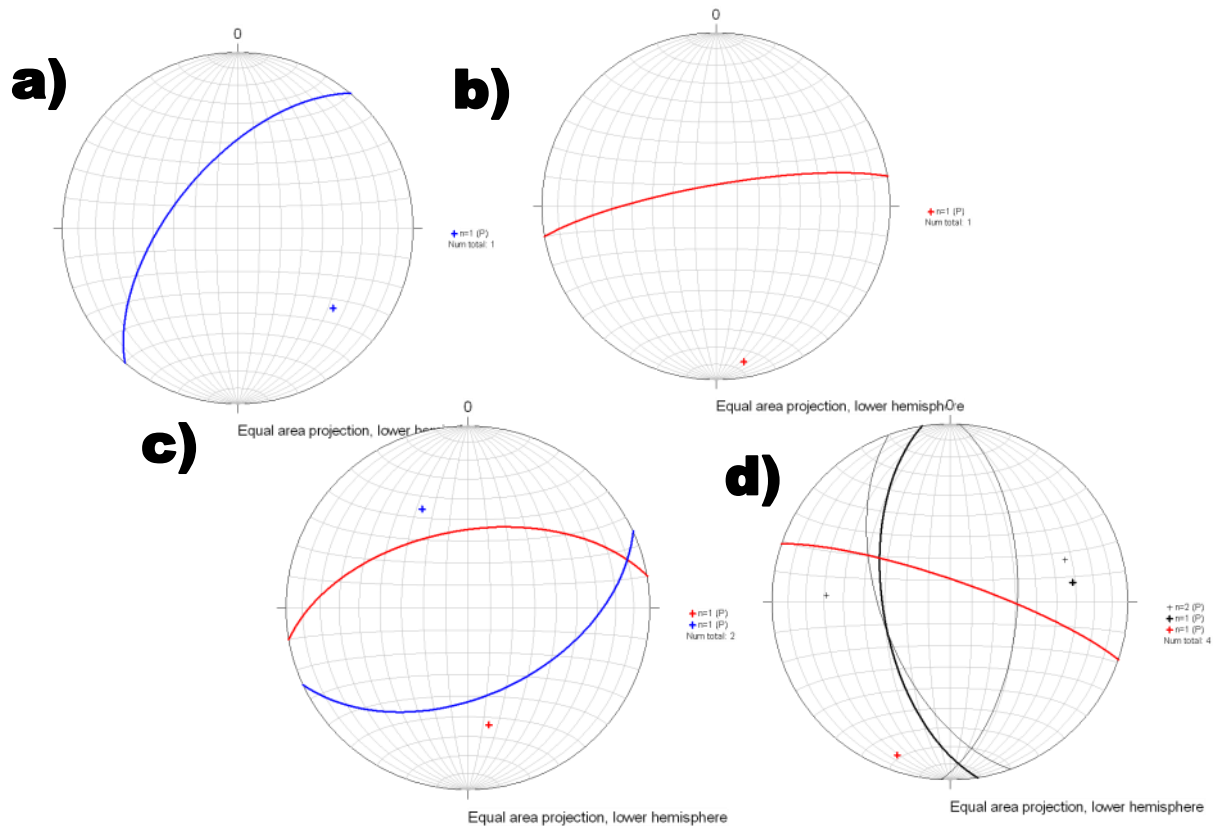


Figure 61: Stereoplots for the structural stations a) 12-14, b) 13-14; c) 14-14 and d) 20-14 (see table 2 and Figure 58)

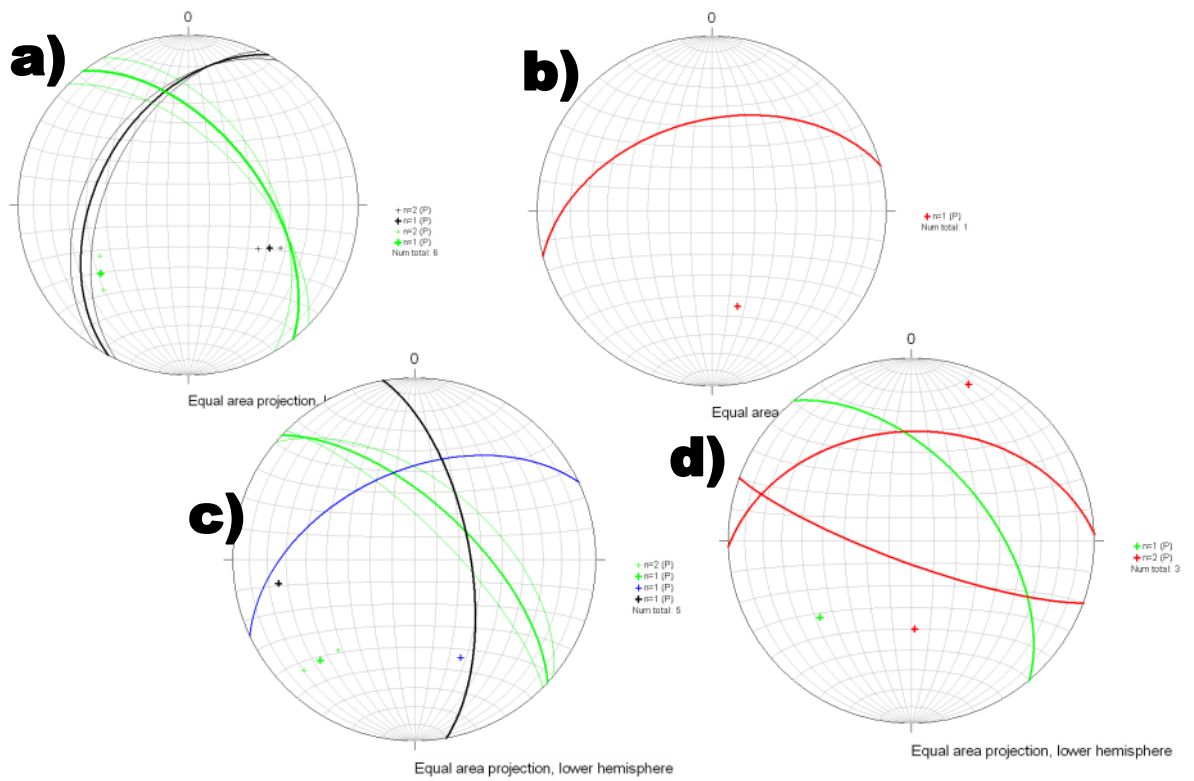


Figure 62: Stereoplots for the structural stations a) 21-14, b) 22-14; c) 23-14 and d) 24-14 (see table 2 and Figure 58)

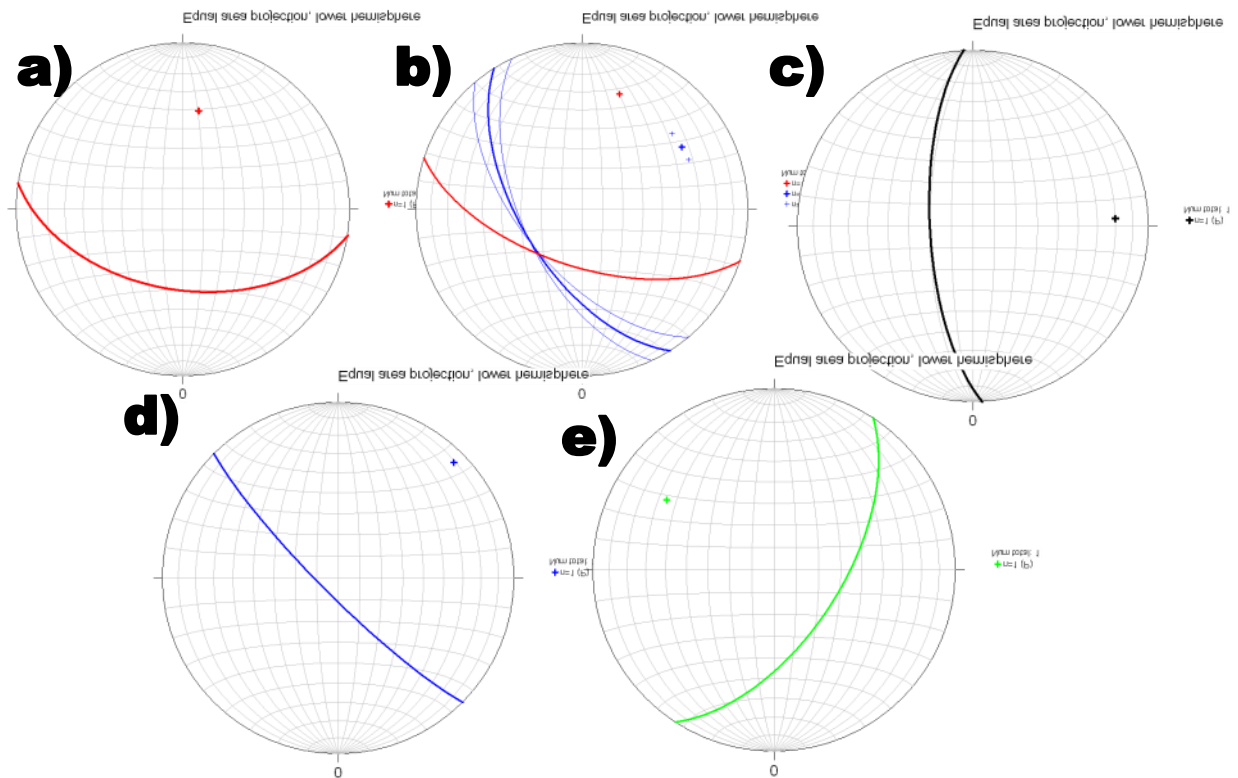


Figure 63: Stereoplots for the structural stations a) 25-14, b) 30-14; c) 31-14; d) 32-14 and e) 34-14 (see table 2 and Figure 58)

Finally, structural data from previous surveys performed on 2007 and 2012 (Table 4 - CFE 2007, 2012) were compared to those collected in 2014. From the literature data, 79 Resultants were extracted (Table 3).

Structural Station (EE <i>Estación Estructural</i> )	UTM coordinates	E- W system, Agua Fria Fault	NE-SW System	N-S system	NW-SE system
EE 01-12	326263 2188894			NE01 72°SE	
EE 02-12	326475 2188823	NE89 76°NW	NE55 77°NW	NW03 74°NE	NW54 77°NE
EE 03-12	326532 2188893	NW89 75°NE		NW20 78°NE	
EE 04-12	326587 2188934		NE62 74°NW	NW06 63°NE	
EE 05-12	326686 2188852	NE77 74°NW			NW31 72°NE

EE 06-12	326676 2188849				
EE 07-12	326676 2188890	NW74 72°NE		NE05 79°NW	
EE 08-12	326667 2188912	NW73 68°NE			
EE 09-12	327031 2188949		NE63 87°SE NE49 78°NW	NE24 76°NW	
EE 10-12	327222 2188726			NW06 76°SW	
EE 11-12	327481 2188920			NW11 74°NE	NW58 74°NE
EE 12-12	327507 2188932			NE18 74°SE	
EE 0703	326110 2188392		NE48 79°NW		NW58 81°NE
EE 0705	326119 2188504		NE54 75°NW		NW33 85°NE
EE 0706	326325 2188454				NW59 79°NE
EE 0709	326349 2188155		NE69 56°NW		
EE 0710	326486 2188101	NE87 88°NW	NE63 70°NW		
EE 0711	326455 2188108	NE83 64°NW			
EE 0712	326938 2188113	N 90 70°N			
EE 0714	327186 2188010		NE45 74°SE		
EE 0715	327696 2188046		NE27 67°NW		
EE 0718	326426 2188236	NW88 80°SW	NE59 74°NW		
EE 0720	326856 2188355	NW88 75°NE NE88 81°SE			

EE 0721	328331 2188580		NE52 84°NW		
EE 0725	326649 2189003	NW77 61°NE	NE31 60°NW		NW46 76°SW
EE 0726	326562 2188935	NE89 78°NW	NE63 68°NW	NE08 72°NW	
EE 0727	326749 2189099				
EE 0728	327372 2189336	NE78 75°NW	NE45 73°NW		
EE 0729	327396 2189354	NE77 83°NW			
EE 0730	327624 2189229		NE53 87°SE		NW37 76°SW

Table 3: structural resultants for structural stations of 2012 and 2007 field survey (CFE, 2007, 2012)

The location of the 79 Resultants of Table 4, is not always within the Area of Investigation, but it was decided to include also some important Structural Datum measured at the south and south-east of the same area. (Figure 64)

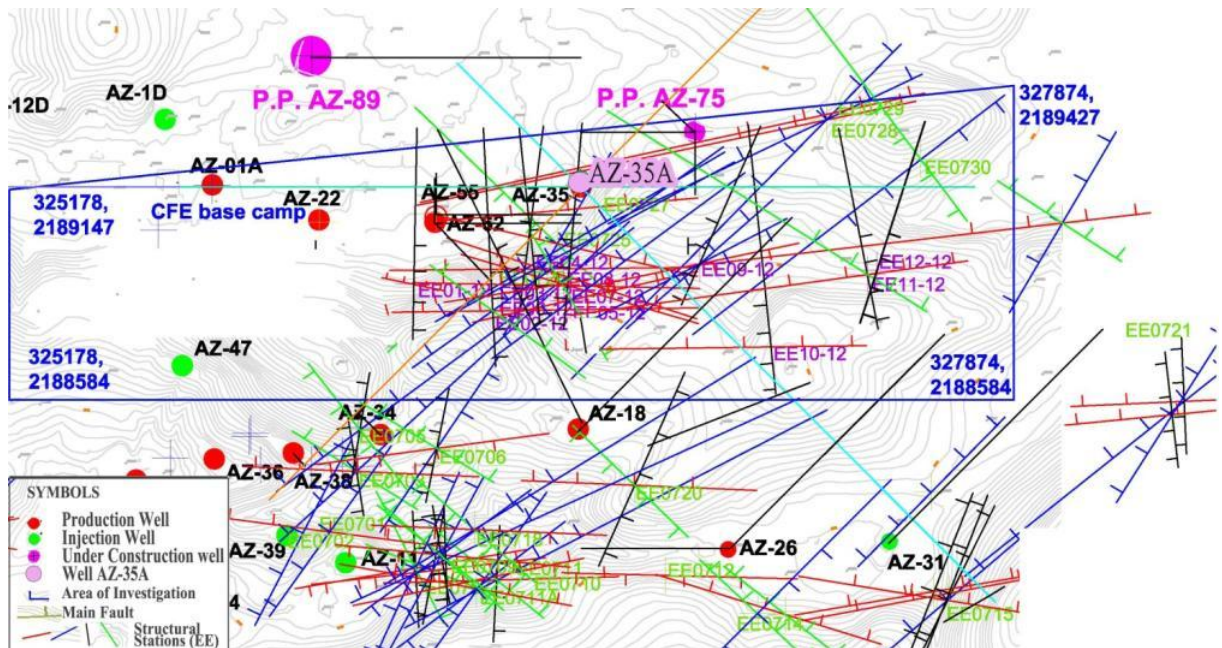


Figure 64: image showing the Area of investigation and the Structural Stations and Datum from brought from the measurement of 2012 and 2007 Field Surveys (CFE, 2007, 2012).

The same statistical analysis as that for Datum of Table 3, made on the Resultants of Table 3, shows that the:

A statistical analysis of all the structural resultants, summarized as in Table 2, reveals that (Table 3):

- E-W system constitutes 33% (26/79) of the direction resultants collected;
- NE-SW system represents 33% (26/79) of the direction resultants collected;
- N-S system constitutes 19% (15/79) of the direction resultants collected ;
- NW-SE system constitutes 17% (13/79) of the direction resultants collected

Comparing these percentages with those obtained in Table 2, it is evident that the E-W and the NE-SW systems are the most relevant, related to the most important geological structure of the zone, such as the Agua Fría Fault. However, the N-S and NW-SE systems are linked to the deep N-S fracturing systems, related to the deformation phase occurred between the Oligocene (33.7-23.8 Ma) and Miocene (23.8-5 Ma) (see Chapter 4.3). The intersection between The E-W and the N-S system at great depths is thought to be the principal fractured systems hosting the deep geothermal reservoir at the LAGF. (see Chapter 4.3).

Therefore the principal fault systems identified in the structural stations, have been associated with four colors, able to easily shown the strike direction on the structural maps:

- **Red** for the E-W system, which varies from NW90-NW70 and NE70-NE90, in the clockwise direction.
- **Blue** for the NE-SW system, varying from NE30 and NE70 in the clockwise direction.
- **Black** for the N-S system, varying from NW30 and NE30 in the clockwise direction.
- **Green** for the NW-SE system, varying from NW70 and NW30, in the clockwise direction.

## Structural Profiles

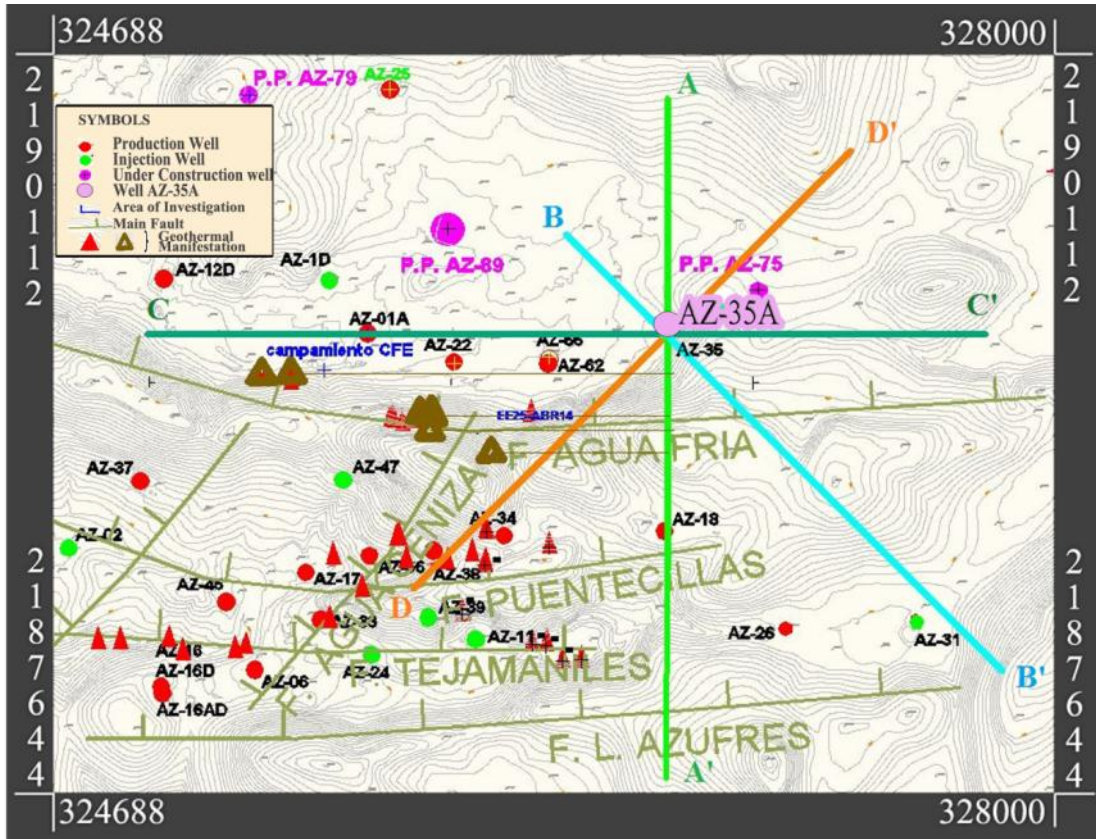


Figure 65: AutoCad 2010 map showing the direction of the four profile realized in this phase.

With the purpose of knowing the geometry of the structural systems at different depth, as well as defining the depth of the new well AZ-35A, the geological sections A-A', B-B', C-C' and D-D' were elaborated based on the Structural Datum of Tables 2 and 3 (Figure 65).

### *E-W STRUCTURAL SYSTEM (AGUA FRÍA FAULT)*

The most important structural system in the LAGF is the E-W fault system, belonging to the Agua Fría Fault (Figure 66).

This system has strike directions varying from NW90 and NW70 and from NE90 and NE70. Inclinations can vary, with the majority of data dipping toward N. In particular, NW-dipping data vary between 40° and 88°, while NE-dipping data vary between 61° and 80. Some structural data dip toward the SW with inclinations between 80° and 84°.

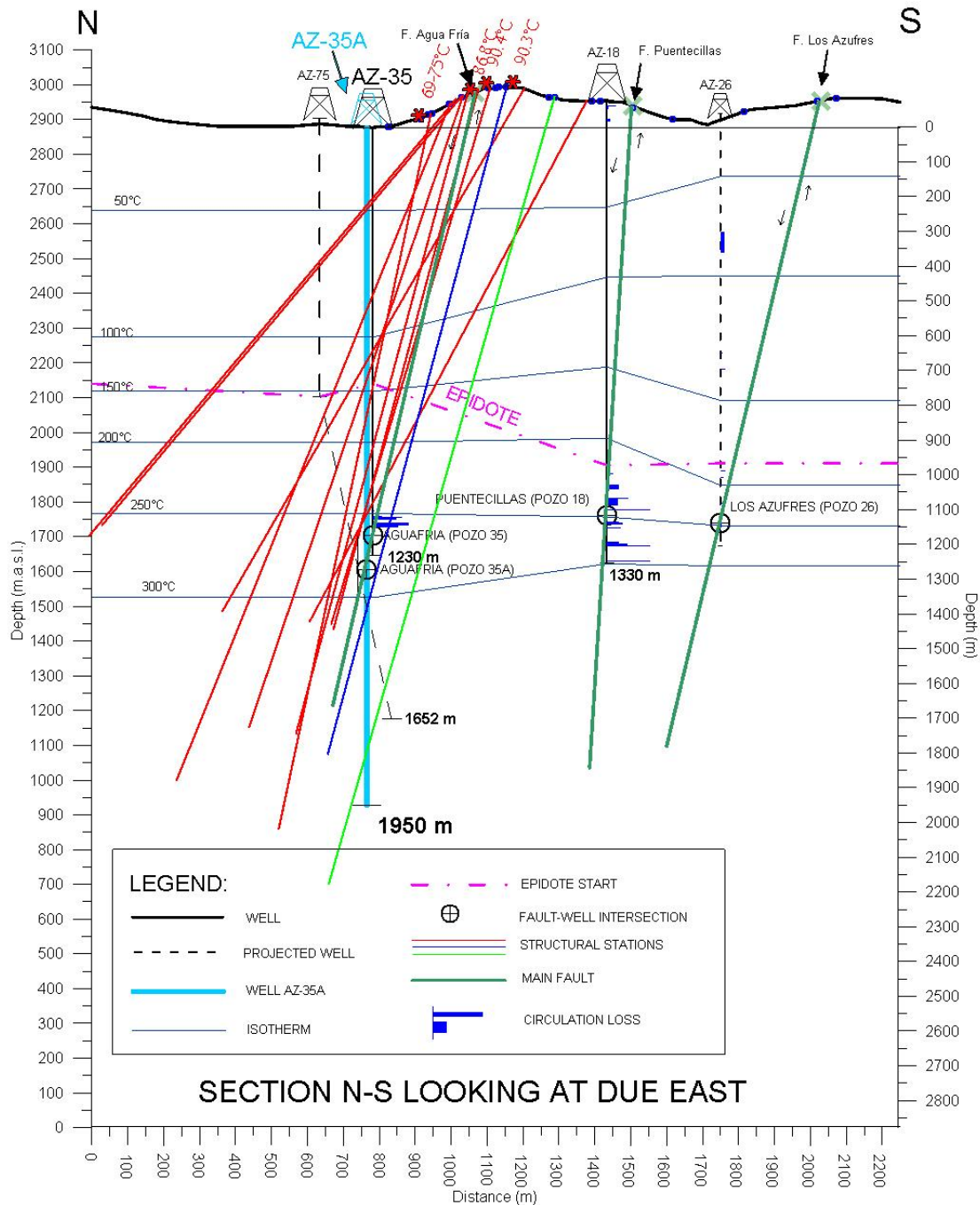


Figure 66: Profile A-A' of North-South direction, analyzing the East-West structural system.

In addition, the depth at which the Epidote (see Chapter 5.3) is encountered in the samples collected from well AZ-35 states the existence of a weathered and permeable zone in agreement with the beginning of the fracturing zone identified by the Lost Circulation data analysis of the same well (Figure 66).

In the profile AA', it can be noticed that, locating the new well AZ-35A approximately 15 m to the north with respect to its twin AZ-35, it is possible to cross the Agua Fría Fault at a depth of approximately 1250 m, that is around 100 m deepest than the current fault-crossing intersection for the well AZ-35. This fact could allow reaching a geothermal resource at temperature of around 300°C in this point.

Until now, a depth of 1950 m for the well AZ-35A can be inferred. The E-W structural stations does not reach this depth, but the projection of the structural stations EE02-12 of the NW-SE system (Green colored line) and the EE09-12 of the NE-SW (blue-colored line) indicate to us the presence of fracturing until this depth.

At the depth of 1950m, the liquid-dominant zone could be reached, which results to be more productive and long-lasting than the vapor-dominant zone, in which the AZ-35 is currently situated.

The profile allow to define the *Area of Geothermal Interest* standing between 750 and 1950 m of depth. The bottom coincide with the end of the last Structural Resultant crosses the well AZ-35A, while the top of this Area coincide with the depth at which the Epidote was firstly encountered during the perforation, meaning that we are in presence of a hydrothermal alteration within a Geothermal Reservoir. In this portion of the well, pierced pipeline would be placed.

#### *NE-SW STRUCTURAL SYSTEM*

The second most important system is the NE-SW (Figure 67). Also in this case, the majority of the data dip toward the NW with values of inclination comprised between 35° and 84°, while few structural datum dip toward the SE, with values of inclination comprised between 50 and 80°.

The two systems probably form a conjugate system. In the profile shown on Figure 61 the data dipping toward south are not shown because they do not cross the wells AZ-35 and AZ-35A.

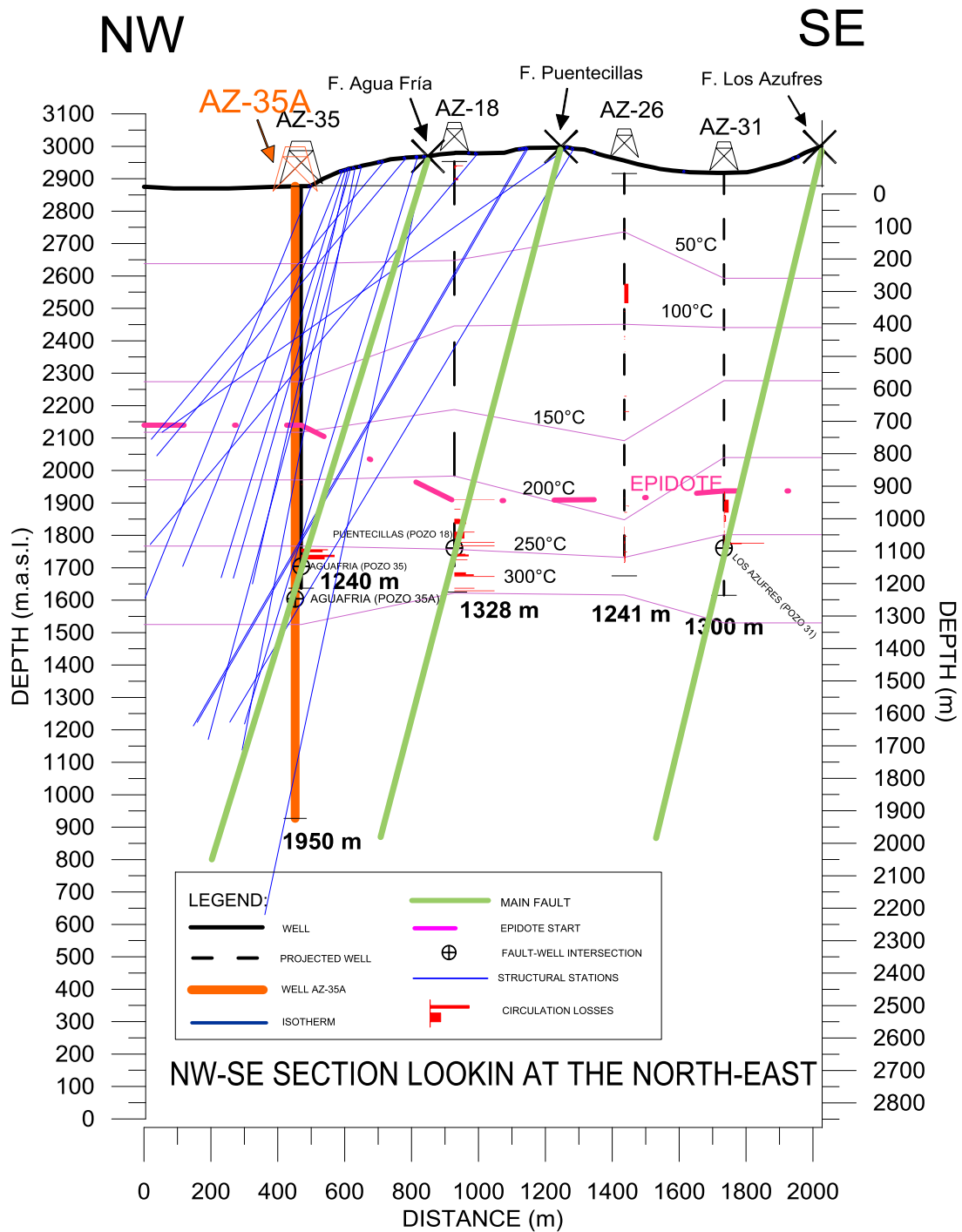


Figure 67: Profile B-B' of NW-SE profile analyzing the NE-SW system

The profile in Figure 67 highlights that the well AZ-35 is intersected by two important fracturing zones, characterized by good permeability. The first one is between 300 and 800 meters and it is not useful for geothermal purposes, because it has temperatures between 50° and 100°, so here the pipeline would be blind. The second zone is between 1000 and 1950 meters of depth, and, on the contrary, it can be considered an *Area Of Geothermal Interest*, because it allows assuming a drilling depth of the well AZ-35A reaching reservoir temperatures near to 300°C, characterized by vapor-dominant fluid. Moreover, the liquid-dominant zone of the reservoir could be reached at greater depth, because the presence of the NE-SW system (station EE09-12) shows a fractured zone at about 1950 m depth, useful for AZ-35A well.

#### *N-S STRUCTURAL SYSTEM*

The N-S system has also great importance because it is probably related with Miocene age fracturing present in the deepest formations, that are the Area of Geothermal interest already identified in the previous sections. The N-S system, when present, should be an indicator of deep reservoirs (Figure 68).

The strike directions obtained for this system vary between NW20 and NE24, while the dip value varies between 50° and 78° for the stations dipping toward the north, and between 59° and 89° for the stations dipping toward the south. In the profile of Figure 68, only the fracturing crossing the well AZ-35A are visualized.

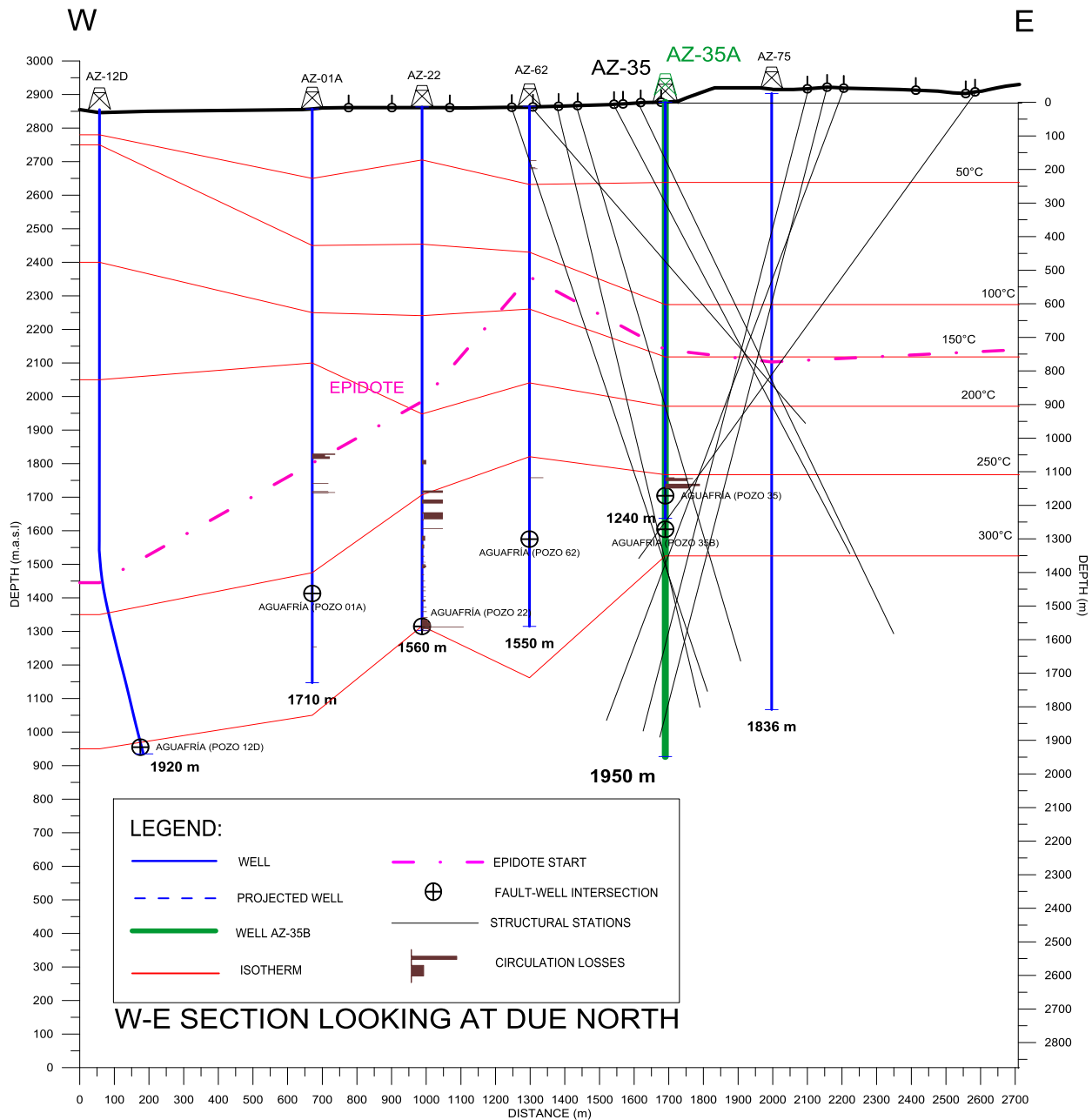


Figure 68: Profile C-C' of W-E profile for N-S structural stations.

Here the *Area of Geothermal Interest* is the one between 1250 and 1850 meters of depth. The presence of those fractures at a depth at which the temperature results to be 300°C or more is a good signal for inferring that the well AZ-35A could be more productive than its twin AZ-35 reaching a deeper liquid-dominant reservoir. Also in this case, the hypothesis of realizing the new well until a depth of 1950 m seems to be acceptable.

Moreover, thanks to this profile, it can be noticed that the crossing between the Agua Fría Fault and the wells goes deepening toward the west. The reservoir probably acts in the same way. Wells AZ-35A and AZ-35 seems to stand in the less deep zone of the same reservoir.

#### *NW-SE STRUCTURAL SYSTEM*

Finally, a profile for the NW-SE structural system was produced (Figure 69).

The encountered data were scarce in this case, with only 5 resultants crossing the wells AZ-35 and AZ35A.

The direction of fault and fracturing is, in this case, variable between NW61 and NW33, with distinction between north dipping inclinations ranging between 85° and 55°, and south dipping inclinations represented by a unique value of 76°. The two systems could be part of a fracturing conjugate system.

Though those few structural data crossing the wells AZ-35 and AZ-35A, two circulation loss zones can be indicated: a zone between 400 and 650 meters depth and another one comprised between 900m (depth at which the temperature is major than 220°C and Epidote is present) and 1950 meters (depth at which the well AZ-35A crosses the structural station 02-12, that is the deepest one). Of those two zones, only the second one can be referred as *Zone of Interest for Geothermal Purposes*, because it stands at a depth at which the temperature reaches and exceeds 300°C, in the case of well AZ-35. So, thanks to this profile it is correct to hypothesize that the well AZ-35A should have a depth of 1950 m.

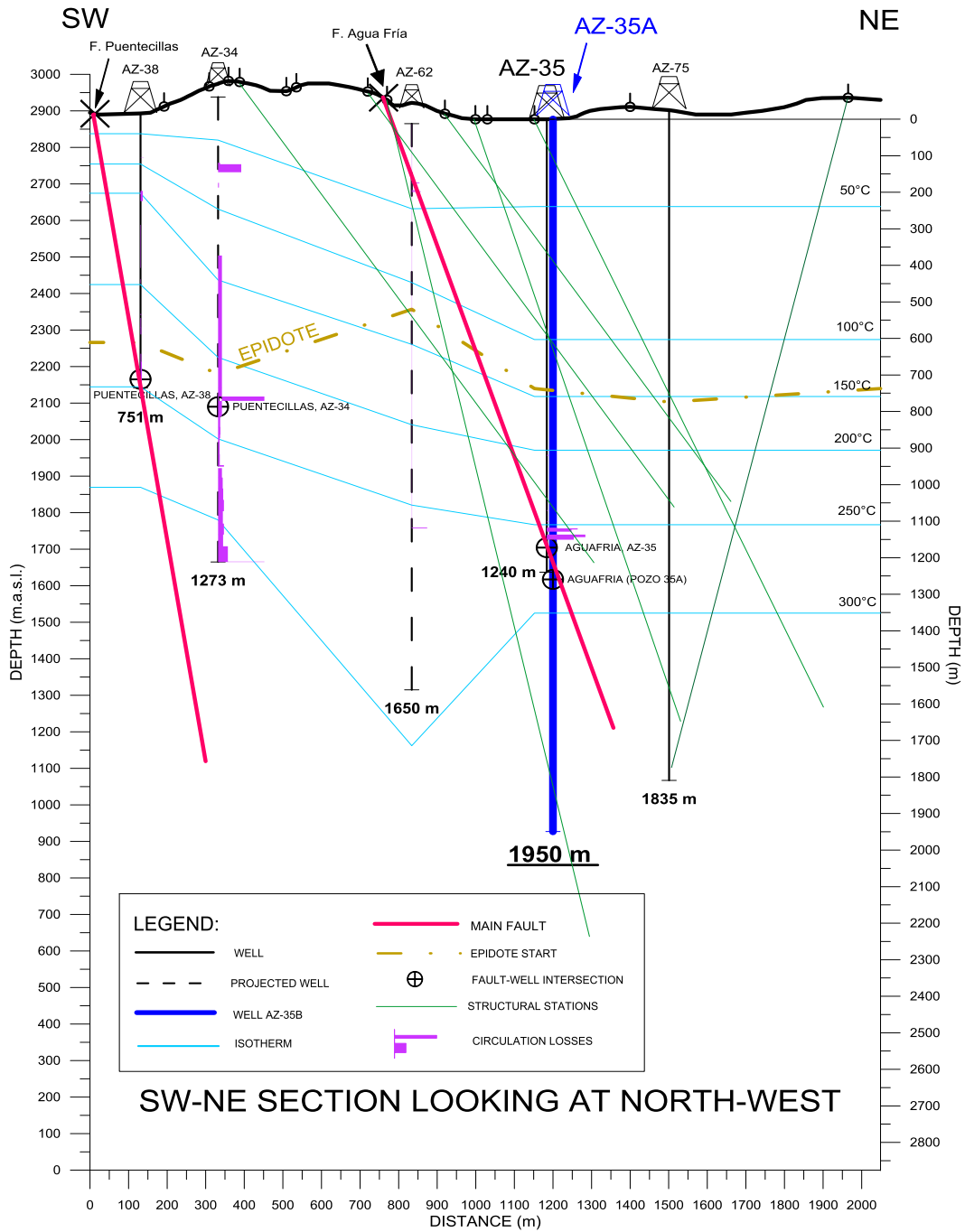


Figure 69: Profile D-D' of SW-NE profile for NW-SE structural stations.

After all the Structural Geology analysis discussed in this chapter have been carried out, it can be inferred that the Well AZ-35A can be drilled in the same platform of the AZ-35, with a depth of drilling of 1950 m. Structural Data are abundant for all the Structural System, but the most important systems are the E-W and the N-S. When the Resultants Structural data are projected in the realized profiles (Figure 66 to 69), they cross the well until ~1950 m, and so they indicate the presence of a deep Geothermal Reservoir and they can be taken as scientific

support for the drilling proposal. Moreover, at this depth higher temperatures and a sector of the reservoir with a major percentage of liquid are thought to be reached, which would make the well to be more productive. Apart of economic reasons, the well AZ-35A drilled until 1950 m would also be useful for exploring purposes, because it is going to be located in the eastern-most part of the Agua Fría Fault, where it would be the deepest well, giving new important information about the underground of the LAGF.

#### 6.4 PETROGRAPHIC ANALYSIS RESULTS

The lithostratigraphic column expected during the perforation of the well AZ-35A, is similar to that of the well AZ-35 and it is formed by magmatic rocks varying from acidic to intermediate composition (Figure 70).

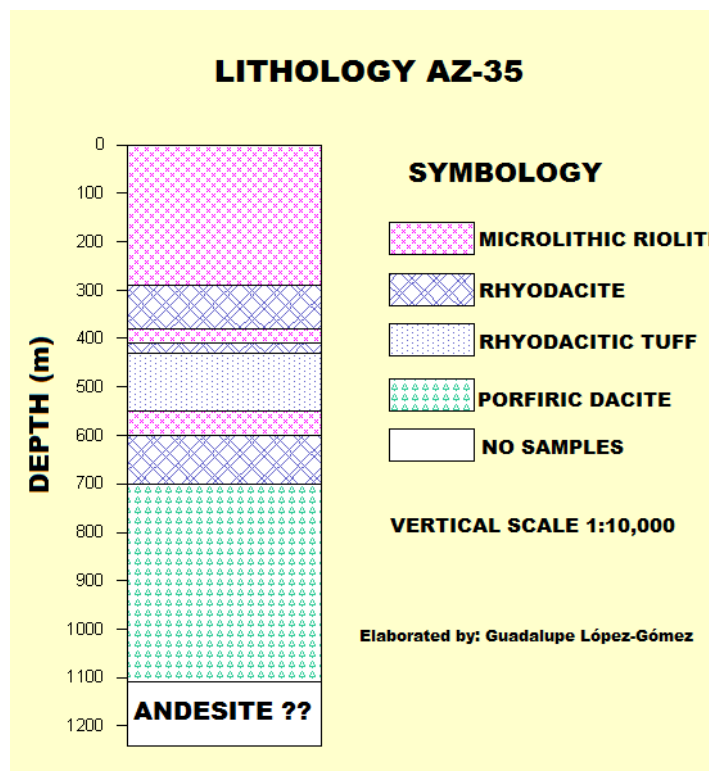


Figure 70: Lithostratigraphic column of the well AZ-35, which is presumed to be appropriate for the new well AZ-35A .

In order to analyze in details the rocks belonging to the AZ-35 lithostratigraphic column, samples from the Petroteque of the LAGF were collected. Precisely, samples belonging to the depths of 50, 250, 350, 500, 750 and 1050 m were collected, in order to have at least one sample for every type of rock indicated in Figure 70 (Figure 71, 72 and 73).



*Figure 71: Samples of Well AZ-35. On the left, 50 m depth sample (Rhyolite) . On the left, right m depth sample (Rhyolite). (CFE Petroteque at the Los Azufres Geothermal Field).*



*Figure 72: Samples of Well AZ-35. On the left, 350 m depth sample (Rhyodacite). On the right, 500 m depth sample (Rhyodacitic tuff). (CFE Petroteque at the Los Azufres Geothermal Field).*



*Figure 73: Samples of Well AZ-35. On the left, 750 m depth sample (Dacite). On the right, 1050 m depth sample (Dacite). (CFE Petroteque at the Los Azufres Geothermal Field).*

Lately, thin sections from the samples were made (Figure 74), in order to identify with the use of a Polarized Microscope the rocks minerals (see Chapter 5.3).

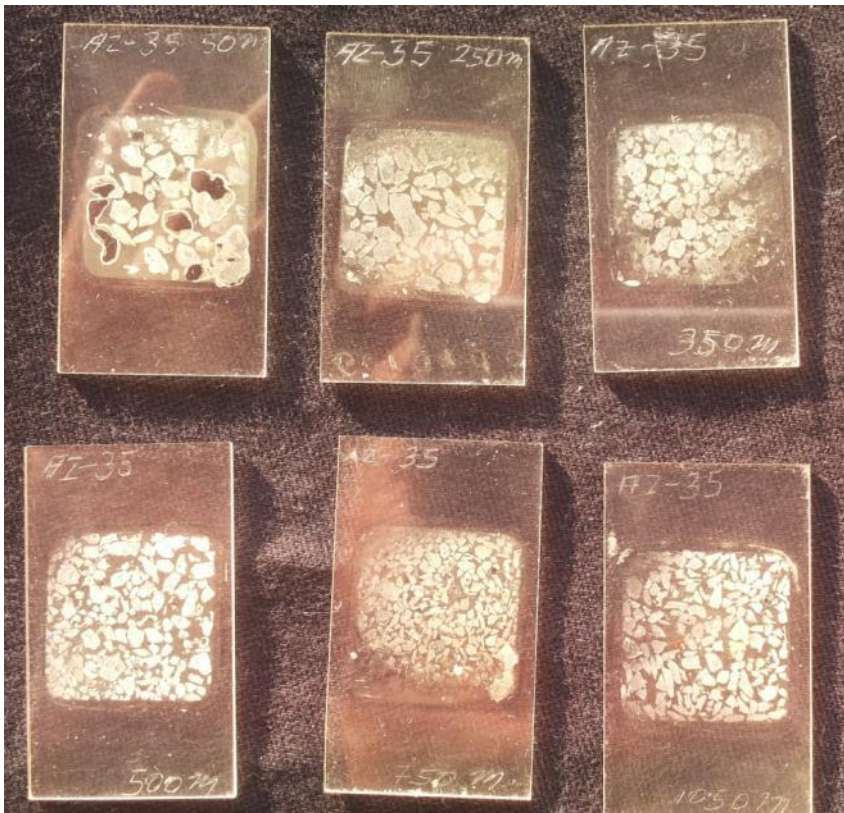


Figure 74:  
Thin sections realized with AZ-35 rock sample . (CFE Petrographic Laboratory at the Los Azufres Geothermal Field).

Petrographic analysis, made on these samples at the *Laboratorio de Petrografía* of the LAGF, allowed the redaction of the Table 4.

Depth	Present Minerals and Matrix	Lithology	Texture	Other things
50 m	Plagioclase, oxidated minerals (iron oxide and hematite), Quartz, sporadic argillitic minerals (Feldspar alteration products). Spherulites are present.	Rhyolite (Agua Fria)	Fluidal-spherulithic	Fluids penetrate the rock through superficial fracture and alterate it.
250 m	Quartz, Plagioclase, scarce Piroxene. Alrgillitic alteration is so present.	Rhyolite	Microlithic.	

350 m	Fragments of rhyodacite and scarcely of rhyolite. Abundant pyrite with iron oxides, calcite and argills. Glass and microlites matrix.	Dacite-Rhyolite	From microcrystalline to porphyric	No fractures.
500 m	30-40% of Alteration. Abundant Quartz and Plagioclase. Calcite is present in fractures.	Rhyodacitic tuff	From microcrystalline to porphyric	Calcite-filled Fracturing. It started to be seen a heavy alteration.
750 m	70-80% of Calcite-made matrix. Pyroxene, Quartz and Plagioclase are present. <b>Epidote</b> is present as Ca-Plagioclase alteration product.	Dacite	Microlitic	
1050 m	Almost 100% of the matrix is made of Calcite (high CO <sub>2</sub> content), Plagioclase, Quartz in minimum quantity. <b>Epidote</b> is present.	Dacite	Microlitic.	/

*Table 4: In this table it is presented the mineralogic-petrographic description of samples at different depth of the well AZ-35, which are thought to be appropriate for the new well AZ-35A.*

The results shown in Table 4 coming from the Polarized Microscope analyses, are in agreement with the lithostratigraphic column of Figure 70.

The main result is the presence of Epidote in the Dacite sample of 1050 m of depth. As we mentioned before (see Chapter 5.3, Figure 44) Epidote is a useful thermobarometer mineral because it is forming, as an alteration product of Ca-plagioclase, from a temperature greater than 220°C and shows the presence of a geothermal reservoir (Lagat, 2010).

The same presence of Dacite is a peculiarity of the area in which the wells AZ-35 and AZ-35A are located. Like it is possible to see in Figure 36 (Chapter 4.3),

Dacite is not abundant in the LAGF area, and it is only present approximately between the Agua Fría and the Tejamaniles Faults at the Las Humaredas Domes. During the drilling of the AZ-35A, Dacite is expected to be encountered at a depth of 700 m.

In addition, considering the presence of hydrothermal minerals which were identified inside the samples of the well AZ-35 (Table 4), it can be stated that the area where the well AZ-35A will be drilled is constituted by two main zones with different mineralogical association which are characterized in the following way:

ZONE I (Shallow) between 0 and 737 m of depth, composed by hematite + oxides + calcite + argils + pirite (anhedral) + quartz, identified as the top of the geothermal reservoir. → expected temperature <150°C.

Zone II (Deep) between 737 and 1240 m of depth, constituted by hematite + oxides + calcite + argils + pirite (euhedral) + quartz + epidote, representative of the geothermal reservoir. → expected temperature between 150°C and 300°C.

## 6.5 GEOPHYSICS ELECTROMAGNETIC ANALYSIS RESULTS

At the Los Azufres Geothermal Field, various TEM surveys (see Chapter 5.4) were realized in 2003, 2004, 2005, 2007, 2009 and 2010, covering the whole geothermal field (Figure 75).

The whole territory was divided in a regular grid where TEM surveys have been performed. The cables to acquire the signals were arranged in a square mesh of 330x330 m length, allowing to reach in this way a depth of approximately 2000 m.

2003-2005 TEM LOCATION PLAN, AT THE LOS AZUFRES GEOTHERMAL FIELD

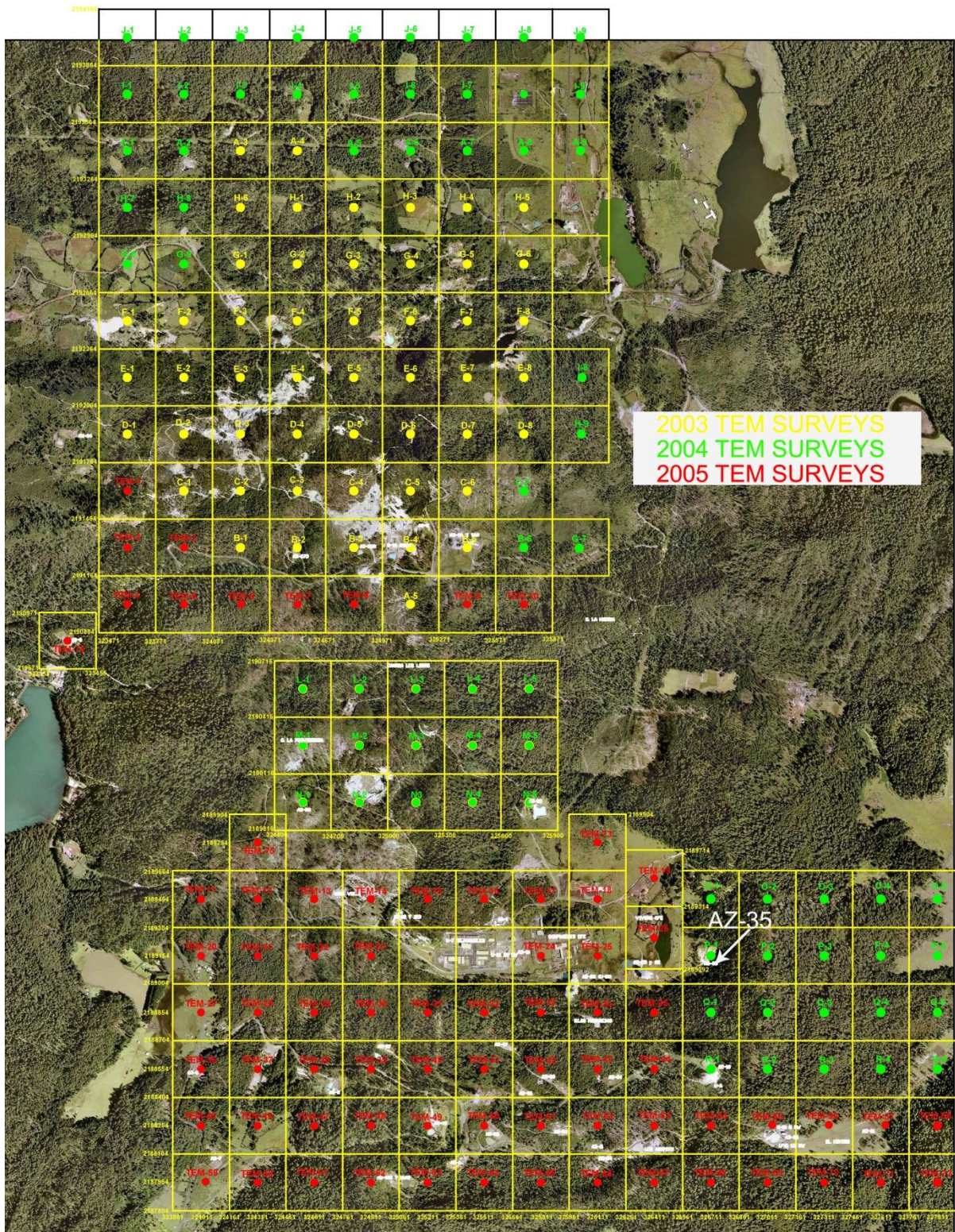


Figure 75: location of TEM survey performed at the LAGF between the years 2003 and 2005.

TEM measurements on site were performed by using the device SIROTEM "Mark III" (Figure 76).



*Figure 76: SIROTEM equipment.*

Processing the data with the Temixs software, based on the Occam algorithm, a 1-D model for each measurement station was obtained (Constable et al., 1987 and 1990; CFE, 2015 (2)).

Then, numerical code as Winglink software were used to interpolate the data and define the geoelectric behavior of the underground by means of longitudinal and transversal sections. Coupling the geoelectrical outcomes with the geological models of the area, allows to determine the electrical resistivity profiles of LAGF (CFE, 2015 (2)). For example, a geoelectric section N-S oriented covering the whole LAGF extension is shown in Figure 77.

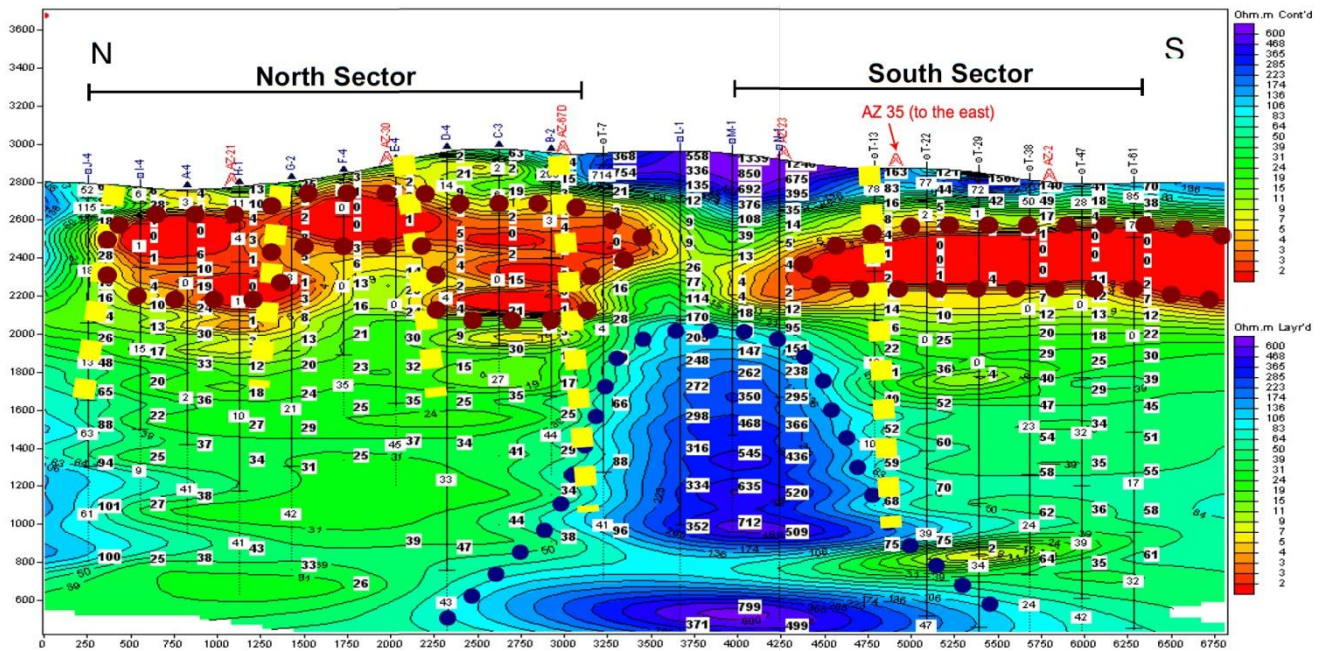
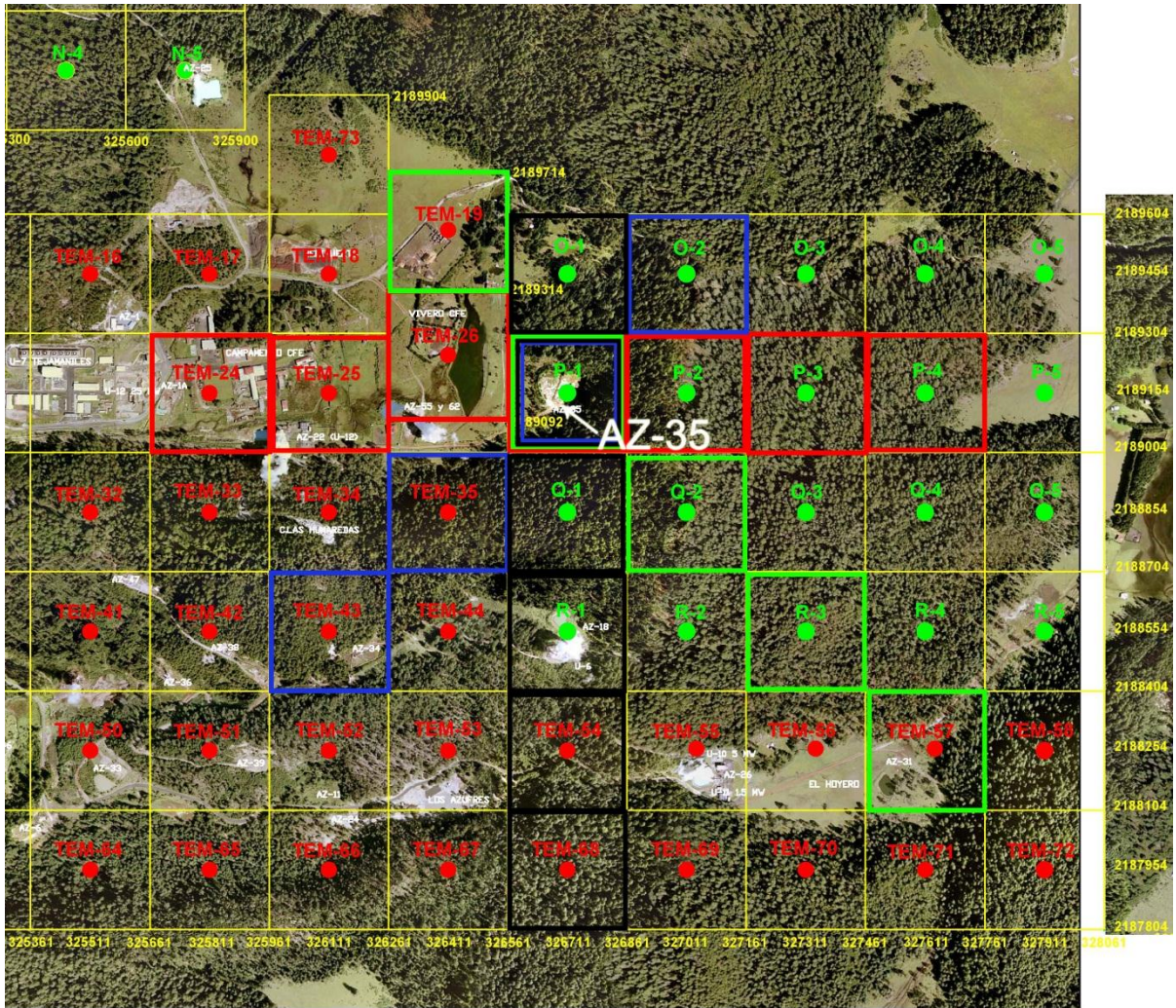


Figure 77: Resistivity section along N-S direction in Los Azufres geothermal field (modified from Molina-Martínez, 2013).

Here, it is possible to notice that low resistivity zones ( $0 < \rho < 200 \text{ Ohm}\cdot\text{m}$ , from red to light blue color) are concentrated in the northern and southern sectors of the section, while the central part is characterized by a high resistivity zone ( $\rho > 100 \text{ Ohm}\cdot\text{m}$ , from light blue to purple color). The low resistivity zones are related to the existence of hydrothermal fluids and a clay alteration zone representing the extent of the geothermal reservoirs, as confirmed also by drilling and temperature logs surveys (Molina-Martínez, 2013). The high resistive area, known as El Hoyo Dome, instead, is related to the presence of fresh rock not affected by hydrothermal fluids, showing a sector not exploitable for electric power generation purposes.

New geoelectrical sections oriented W-E, NW-SE, N-S and SW-NE were realized in the surroundings of AZ-35 well (Figure 78-79), in agreement with the main structural systems previously recognized (see Chapter 6.3), to verify the underground characteristics in order to define the suitable depth for the AZ-35A well.



- |                                                                                                                      |                                                                                                                      |
|----------------------------------------------------------------------------------------------------------------------|----------------------------------------------------------------------------------------------------------------------|
|  TEM surveys<br>for W-E section   |  TEM surveys<br>for N-S section   |
|  TEM surveys<br>for NW-SE section |  TEM surveys<br>for SW-NE section |

Figure 78: indication of TEM surveys used for AZ-35A geophysical analysis.

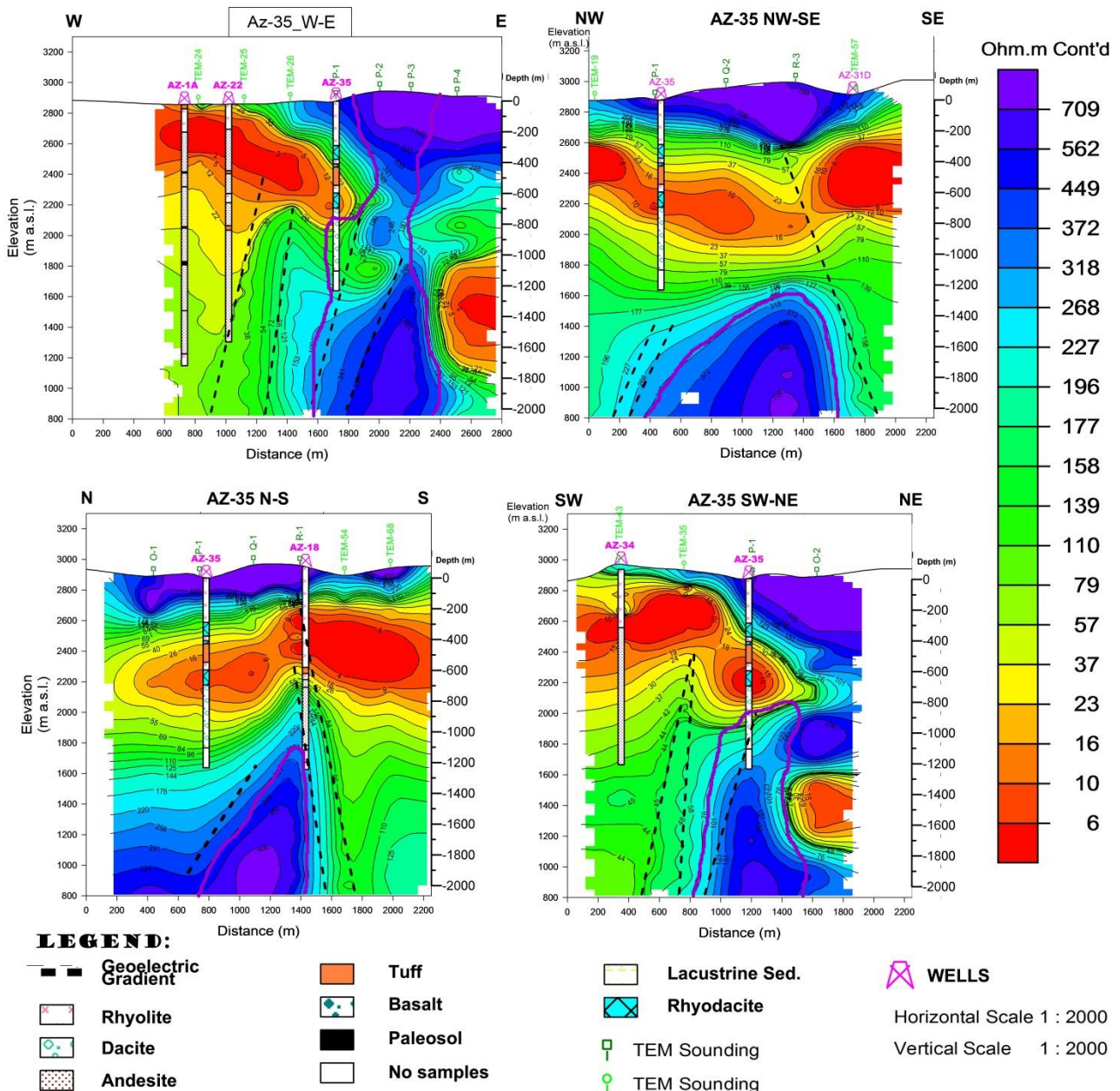


Figure 79: Geoelectrical profiles in the surroundings of well AZ-35.

In the profiles of Figure 79, it is possible to notice that:

- a high conductive zone (red-yellow color,  $0 < \rho < 35$  Ohm\*m) is present in the upper part of all the profiles, approximately between 0 and 750 m of depth. It is known that, in this zone, rhyolites act as cap rock at depths between 500 – 700 m from subsurface. This cap rock, suffering also hydrothermal alteration, prevents cold groundwater from infiltrating into the underlying high temperature reservoir.

- a *conductive zone* (yellow-light blue color,  $35 < \rho < 250 \text{ Ohm} \cdot \text{m}$ ) characterized by geothermal fluids circulation.
- a *high resistive zone* (dark blue-violet color,  $250 < \rho < 700 \text{ Ohm} \cdot \text{m}$ ) is present at the bottom of each profile as expected from previous studies outcomes (Figure 77). This area is part of the main resistive zone identified by Molina (Izaguirre, 1983; Molina-Martínez, 2013)..
- geoelectric gradients represented by black-dotted lines highlight the contact between high and low resistive zone, representatives of hidden faults in the underground, probably related to the four structural system previously identified.

From the correlation between the four profiles of Figure 79, a resistivity map corresponding to an elevation of 1400 m.a.s.l. (which in the zone of the well AZ-35 corresponds to a depth of 1477 m) was produced. (Figure 80)

This map clearly shows a sudden change of resistivity values between wells AZ-35-AZ62 and AZ-18-AZ34, highlighting the existence of a structural system with N-S direction that parts the *high resistivity* area from the *conductive* one. In addition, another hidden fault systems directed W-E (Agua Fría Fault systems) is recognized, involving mainly the *high conductive* and the *conductive* zones. When the two geoelectrical gradients crosses, a NW-SE geoelectric gradient is generated, indicating that the W-E system is affecting the N-S ones. As a consequence, the intersection between the two systems is potentially an excellent geothermal exploitation area. In fact, knowing that the main N-S fault system dip is verging towards west allows to exploit the *conductive* and the *high conductive* zones located on the west side of the geoelectrical gradient.

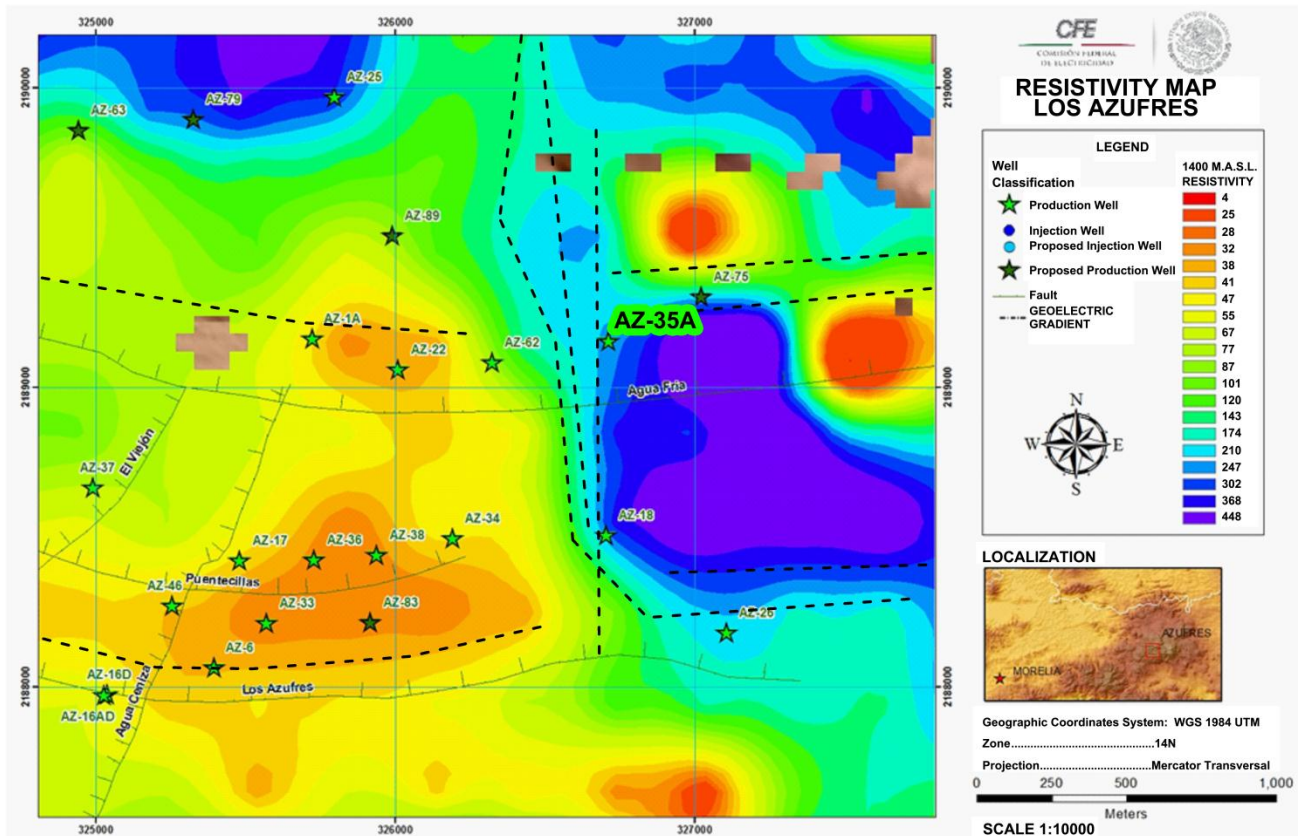


Figure 80: Resistivity Map of the LAGF area surrounding the AZ-35, at 1400 m.a.s.l. .

So, the new well AZ-35A, located at the edge between the *high-resistive* non-productive zone (El Hoyo Dome) and the *low resistivity* zone, considered the productive one, seems to be really productive and economically advantageous if deepened until a depth of about 2000 m. This consideration is supported also by the W-E, NW-SE and N-S sections (Figure 79), where is possible to see that deepening the well AZ35 until a depth of 1900-2000 m will affect mainly *the conductive zone*, more interested by the circulation of geothermal fluids..

## 6.6 ADDITIONAL BIBLIOGRAPHIC INFORMATION

### 6.6.1 GEOCHEMICAL DATA

#### *Geochemical Background*

At Los Azufres in the past years several geochemical analyses were performed on water and steam samples collected from available wells and from surface discharges manifestations (Molina-Martínez, 2013).

The main geochemical facies of water and steam samples is sodium-chloride and the pH is neutral (Molina-Martínez, 2013).

The dominant anion is chloride with concentration values ranging from 2,500 to 7,000 ppm. High concentrations of boron are typical of LAGF and are related to the water-rock interaction between parental fluid and the metamorphic regional basement (Figura 81, Molina-Martínez, 2013).

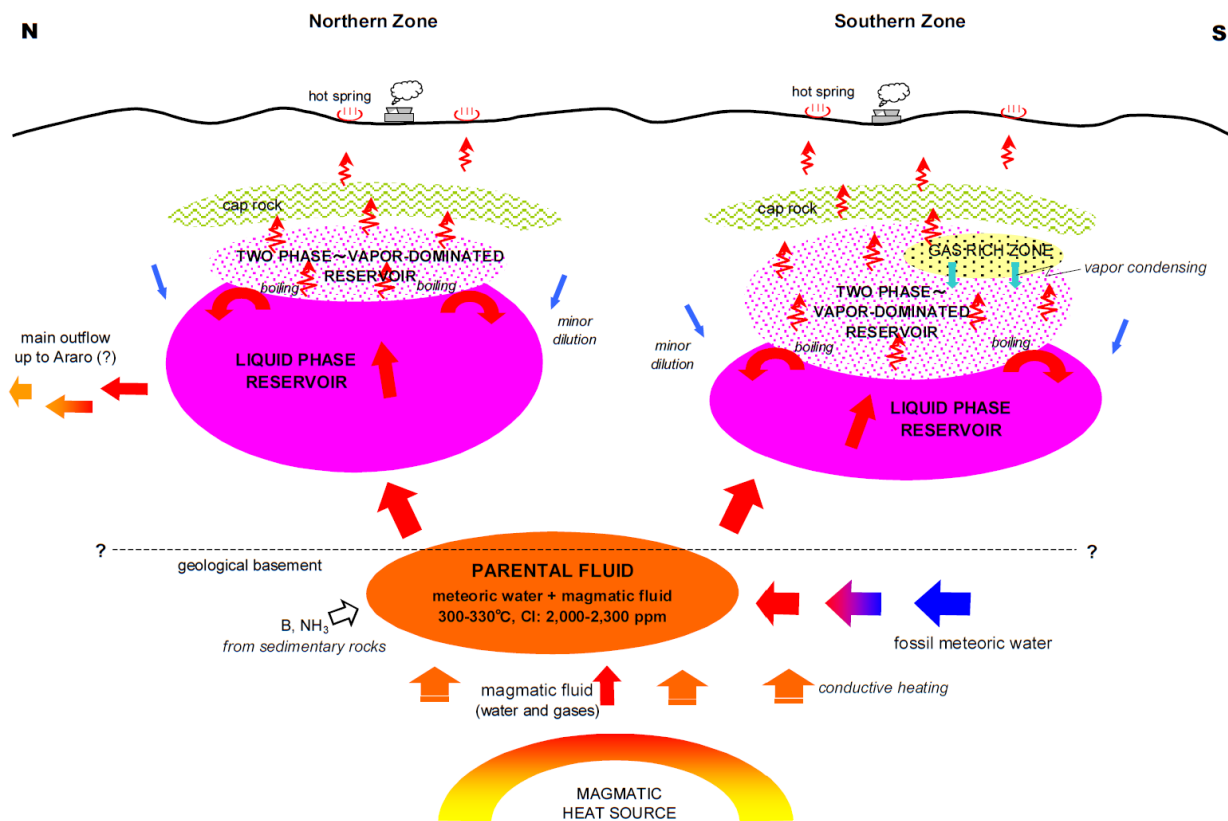


Figure 81: Fluid flow model of Los Azufres reservoir (modified from Molina- Martínez, 2013)

### *Geochemical Analysis for the proposed Well AZ-35A*

Thanks to the existing information about geochemical composition of separated water and steam in the production wells, the CFE personal of the Chemistry Area at the LAGF has determined temperatures and gas content derived from the analysis of LAGF southern sector samples collected in a specific database. To verify the potential productivity of well AZ-35A, the first 2014 bimester analyses were taken into account.

Temperatures of the production fluids were determined using geothermometer Na/K (Karingithi, 2009) on water well samples. Based on ions concentrations (Table 5) the T values were obtained using the following formula:  $T^{\circ}C = ((1217) / (1.483 + \log Na/K)) - 273.15$

Well	Date	Cl	B	HCO <sub>3</sub>	SiO <sub>2</sub>	SO <sub>4</sub>	Na	K	Li	Rb	Ca	Mg	As	Fe	T Na/K °C
		mg/L (ppm)													
Az-1A	24-feb-14	6168.82	538.47	0.00	561.67	26.24	3288.57	880.84	44.65	7.98	60.29	0.000	32.56	0.19	319.03
Az-2A	26-feb-14	5424.31	412.00	2.13	540.17	37.74	3103.04	408.50	27.38	3.20	195.21	0.001	3.77	0.11	241.74
Az-12D	25-feb-14	4821.61	461.55	2.66	1090.67	26.34	2605.64	787.14	39.31	6.41	27.52	0.000	32.51	0.13	334.48
Az-22	24-feb-14	3332.58	321.17	15.82	819.17	66.88	1968.18	460.40	25.98	4.27	26.63	0.000	133.83	1.89	302.55
Az-23	25-feb-14	3190.77	238.60	5.42	836.67	21.74	1732.69	418.40	26.94	4.34	15.83	0.000	24.44	0.12	306.34
Az-25	25-feb-14	2978.05	231.21	4.51	788.17	27.84	1633.27	384.65	23.66	3.95	14.30	0.000	23.44	0.10	303.36
Az-26	26-feb-14	3119.86	462.42	54.30	571.67	27.24	1620.27	375.88	17.56	3.18	82.65	0.000	38.59	0.31	301.57
Az-33	26-feb-14	6877.88	536.30	10.95	626.67	35.94	3669.68	746.99	34.06	5.26	326.39	0.009	8.31	0.11	286.57
Az-47D	25-feb-14	5991.56	482.84	13.88	602.17	28.24	3211.60	693.00	31.02	5.27	255.15	0.000	7.25	0.19	293.16
Az-62	24-feb-14	3119.86	268.58	35.61	681.67	14.74	1741.34	409.54	23.37	3.60	20.19	0.000	57.63	0.48	303.19
Az-83D	05-nov-13	7108.33	655.58	23.87	910.17	45.27	3909.47	911.25	37.44	6.84	133.21	0.000	41.33	0.27	302.13
Az-89D	25-feb-14	4608.89	468.07	3.71	930.17	27.24	2480.00	647.77	37.23	6.20	28.91	0.000	30.79	0.19	315.90

Table 5. Temperature of productions wells of the LAGF, Michoacán, calculated through the Na/K Geothermometer (Fournier)

Then, the temperature values have been used to generate a map of isothermatures in the surroundings of well AZ-35A, using a Geographical Information System (GIS) (Figure 82). (Legg, 2007)

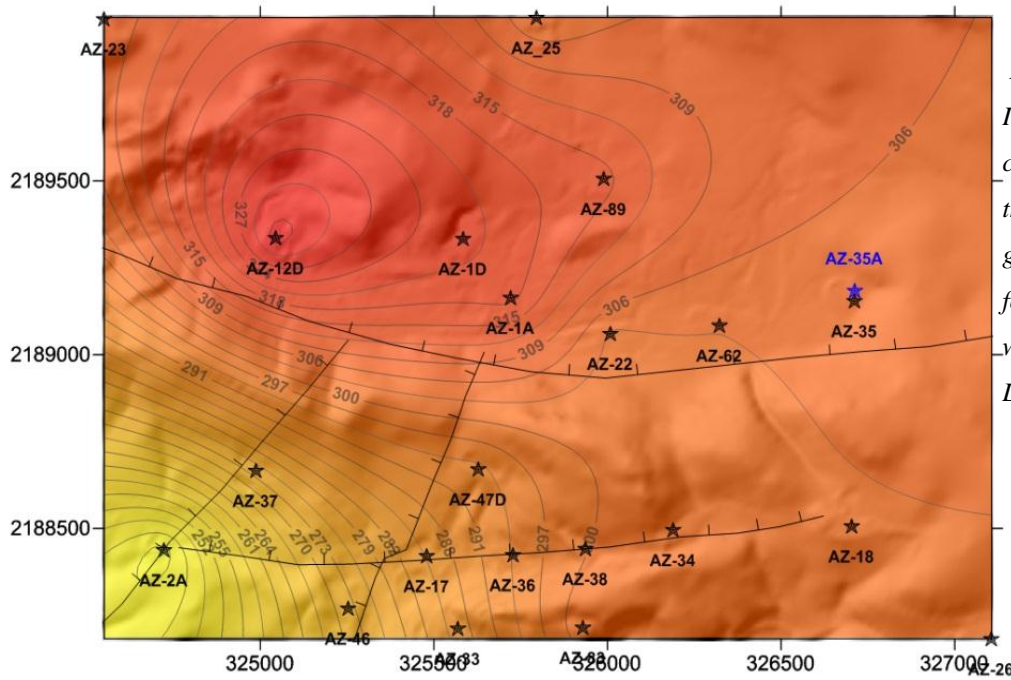


Figure 82: Isotherms calculated through the Na/K geothermometer, for production wells of the LAGF, Mich.

Based on this map, the fluids temperature that can be reached by AZ-35A is estimated of about 304°C.

Instead, the total gas content (%  $W_i$ ) of the production wells' samples show that the main gases present in the southern sector are CO<sub>2</sub>, He, Ar, N<sub>2</sub>, O<sub>2</sub>, CH<sub>4</sub>, CO<sub>2</sub>, H<sub>2</sub>S and NH<sub>3</sub> (Table 6). The total gas content of each well sample is done by the sum of the singular gas species (%  $W_i$ ).

Well	Date	He	H <sub>2</sub>	Ar	N <sub>2</sub>	O <sub>2</sub>	CH <sub>4</sub>	CO <sub>2</sub>	H <sub>2</sub> S	NH <sub>3</sub>	Total Gas (%Wt)
		%W <sub>i</sub>									
AZ-01A	24-Feb-14	0.00010	0.0282	0.1199	1.0141	0.0000	0.0053	95.97	2.843	0.015	0.905
Az-02A	26-Feb-14	0.00120	0.0279	0.7657	50.5914	0.0000	0.0000	46.45	2.109	0.060	1.820
Az-006	26-Feb-14	0.00014	0.0102	0.0100	0.7770	0.0000	0.0122	98.49	0.622	0.076	5.703
Az-12D	25-Feb-14	0.00007	0.0344	0.1331	1.2517	0.0000	0.0049	96.09	2.454	0.034	0.882
Az-016	17-Feb-11	0.00007	0.0150	0.0319	2.6581	0.0000	0.0125	96.00	0.642	0.641	2.110
Az-16AD	26-Feb-14	0.00126	0.0234	0.4926	40.0145	0.0000	0.0000	57.98	1.470	0.019	8.312
Az-017	26-Feb-14	0.00000	0.0380	0.0714	5.9207	0.0000	0.0144	92.72	1.056	0.176	2.899
Az-018	26-Feb-14	0.00000	0.0059	0.0046	0.2551	0.0000	0.0311	99.09	0.579	0.039	8.366
Az-022	24-Feb-14	0.00010	0.0148	0.0413	0.5618	0.0000	0.0198	97.81	1.402	0.152	2.303
Az-023	25-Feb-14	0.00004	0.0386	0.0764	1.3415	0.0000	0.0228	94.58	3.796	0.147	0.794
Az-025	25-Feb-14	0.00000	0.0341	0.2913	0.9900	0.0000	0.0212	94.56	3.787	0.321	0.601
Az-026	26-Feb-14	0.00017	0.0066	0.0066	0.3005	0.0000	0.0466	99.03	0.548	0.060	9.783
Az-033	26-Feb-14	0.00043	0.0079	0.0058	0.3880	0.0000	0.0214	98.74	0.792	0.042	3.657
Az-034	26-Feb-14	0.00021	0.0098	0.0082	0.6636	0.0000	0.0344	98.77	0.484	0.031	8.000
Az-035	24-Feb-14	0.00007	0.0196	0.0358	0.6773	0.0000	0.0474	97.52	1.511	0.190	1.708
Az-036	26-Feb-14	0.00007	0.0090	0.0068	0.3495	0.0000	0.0228	98.56	1.005	0.046	3.456
Az-037	26-Feb-14	0.00021	0.0619	0.1406	9.0324	0.0000	0.0084	88.88	1.515	0.364	3.037
Az-038	26-Feb-14	0.00009	0.0075	0.0050	0.3091	0.0000	0.0302	98.91	0.704	0.030	4.800
Az-47D	25-Feb-14	0.00008	0.0187	0.2522	0.4977	0.0000	0.0096	96.75	1.935	0.534	1.052
Az-046	26-Feb-14	0.00000	0.0304	0.0735	4.3507	0.0000	0.0040	94.42	1.067	0.051	3.344
Az-062	24-Feb-14	0.00008	0.0102	0.0266	0.3455	0.0000	0.0394	98.47	1.022	0.081	2.504
Az-83D	05-Nov-13	0.00008	0.0081	0.0223	0.3425	0.0000	0.0127	98.76	0.767	0.090	2.942
Az-89D	25-Feb-14	0.00007	0.0366	0.3102	1.0598	0.0000	0.0184	95.67	2.835	0.073	0.702

Table 6: Gas content %W<sub>i</sub> of production wells' fluids of the LAGF, Mich.

The spatial analysis of the total gas content (Wt) value obtained by GIS shows isolines distribution of equal %  $W_t$  in the area surrounding AZ-35 (Figure 83).

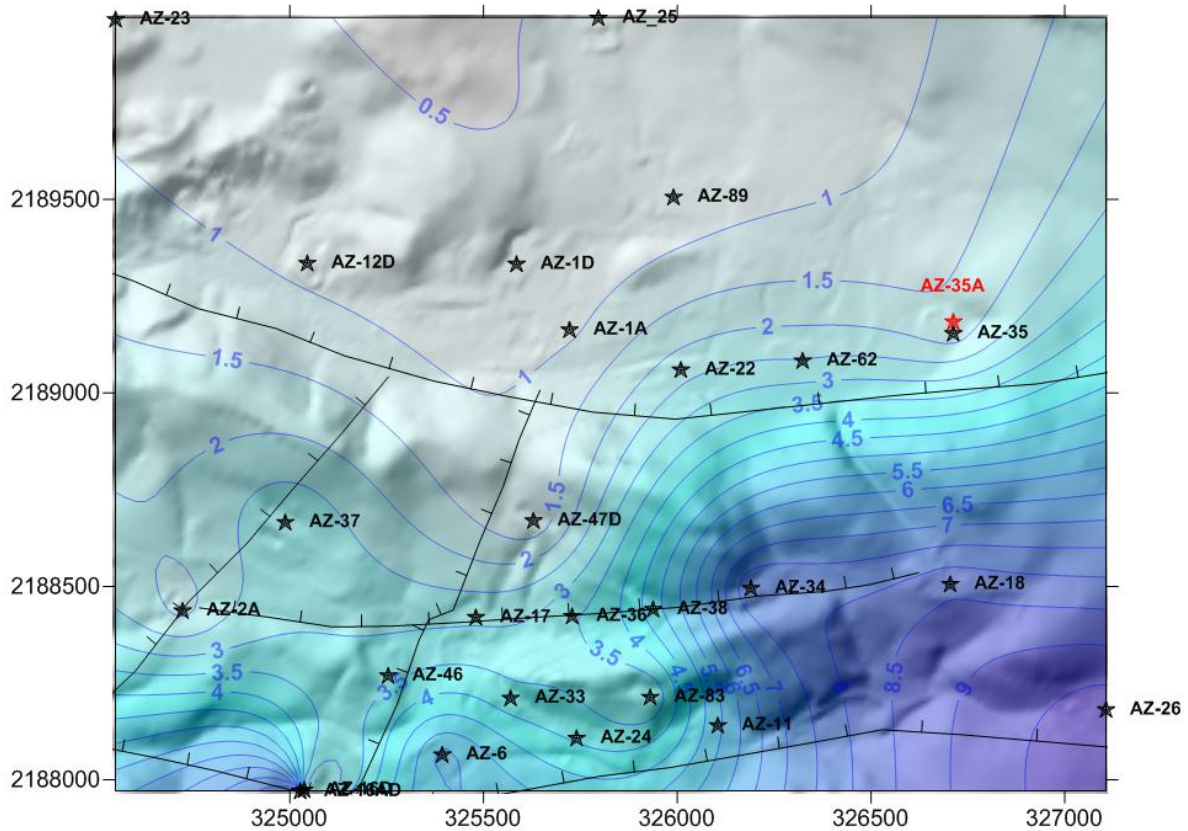


Figure 83: Isolines of Gas content % $W_t$  for production wells of the LAGF south zone, Mich.

The map reveals that the gas content expected for the well AZ-35A is about 1.7 % $W_t$ .

Therefore, since the expected T and % $W_t$  of extracted fluids in the AZ-35A location are estimated to be about 300°C and 1.7%, it follows that the exploitation perspectives for the well AZ-35A are positive and that the condensation cycle will be the most productive for this site.

### 6.6.2 THERMODYNAMIC DATA

From the thermodynamic point of view, the Production Depletion, Pressure drawdown, Fluid Mixture Quality and Production in  $t/h$  analyses for the southern sector of LAGF, where the proposed well AZ-35A is located, have been summarized in several maps by the CFE personal of the Reservoir Engineering Area at the LAGF (CFE, 2014) (Figure 84).

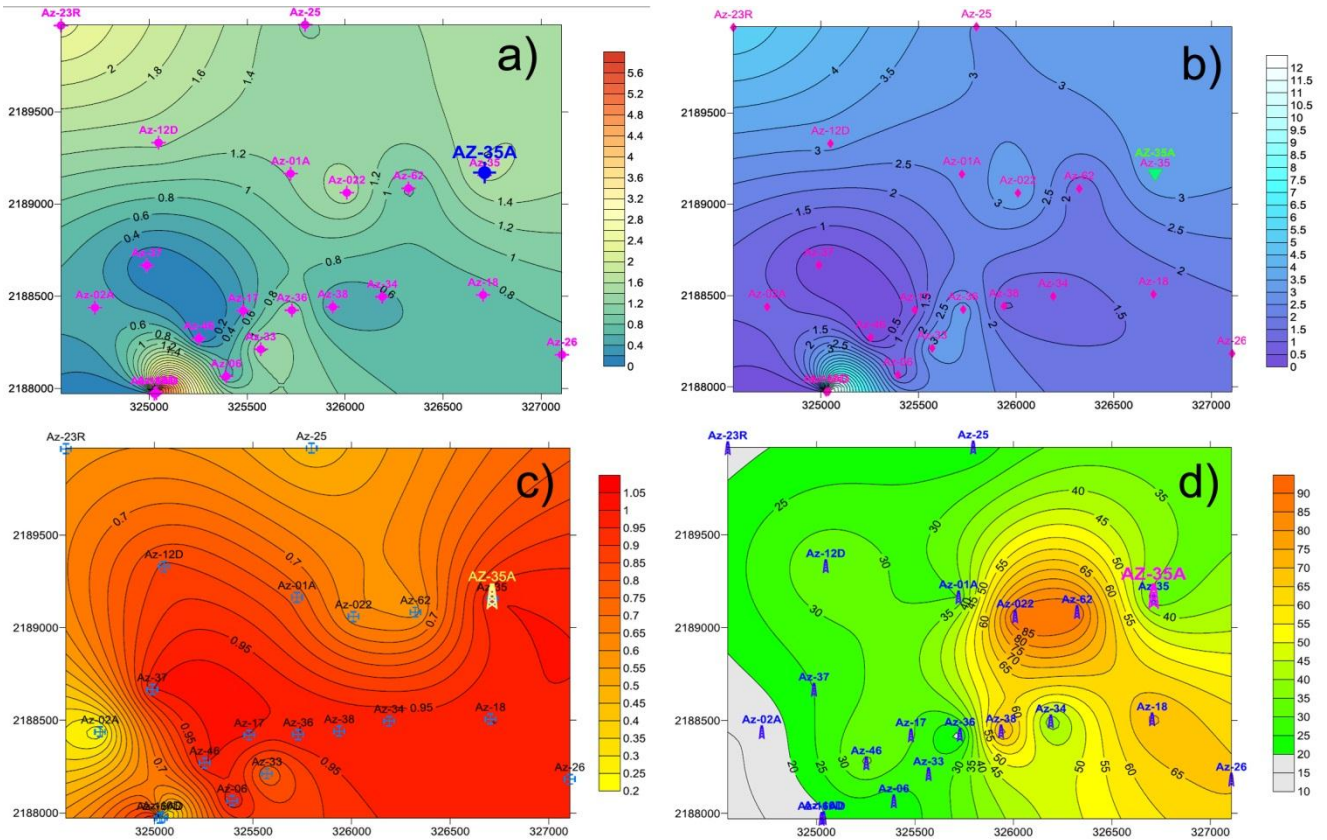


Figure 84: a) Production Depletion, b) Pressure drawdown test, c) Fluid Mixture Quality and d) Production in  $t/h$  maps for the south zone of the LAGF (CFE, 2015 (1))

The main results obtained near the location proposed for well AZ-35A are:

- ***Production Depletion*** (Figure 84a) the Annual Production Depletion percentages is comprised between 1.4 and 2 % per year, a low value inside the LAGF.
- ***Drawdown Pressure*** (Figure 84b), the Annual Drawdown Pressure percentage is between 3 and 4 % per year, which is considered a medium value inside the LAGF.
- ***Fluid Mixture Quality:*** (figure 84c) the Fluid Mixture Quality ranges between 0.95 and 1.00, which means that the Liquid phase in this zone of the LAGF geothermal reservoir is almost 100%.
- ***Production in t/h:*** (Figure 84d) the production should be of 35 to 40  $t/h$ , which is considered as an optimum value in the LAGF

Then, the obtained results support the decision to drill the new well from the Reservoir Engineering point of view (CFE, 2015 (1)).

## 7 DISCUSSION

In order to define the definitive and most correct alternative for the realization of the well AZ-35A, hereafter, the main results obtained from the Circulation Losses (see Chapter 6.2), the structural analyses (see Chapter 6.3), the petrographic analyses (see Chapter 6.4) and the Geophysics Electromagnetic soundings (see chapter 6.5) are displayed simultaneously (Figures 85 to 88). Aim of this action is to show the *Area of Geothermal Interest* which represents the *Economically Exploitable area* for the well AZ-35A.

In the N-S profile (Figure 85), representative of the E-W structural system, it can be noticed that the *Area of Geothermal Interest* is located between 800 and 1950 m of depth, where the concentration of structural features and the circulation losses are high.

The existence of the Epidote area reveals the existence of fluids with  $T^{\circ}$  ranging between 200 and 300 °C at a depth of 700-1000 m and greater below.

From the geoelectrical point of view, an important geoelectric zone is visible between 200 and 700 m of depth. This is a *high conductive zone* (red-yellow color,  $0 < \rho < 35 \text{ Ohm} \cdot \text{m}$ ) related to alteration of the Rhyolitic-Dacitic cap rock due to Quaternary age faulting (Agua Fría fault) and the presence of meteoric water. The Fault is known to reach important depth, and so intersecting ancient rock formations where the N-S fracturing is present (see figure 80). Hydrothermal reservoirs are supposed to be present in the *conductive zone* (35-250  $\text{Ohm} \cdot \text{m}$ ; from yellow to light blue color) between 800 and 1950 m.

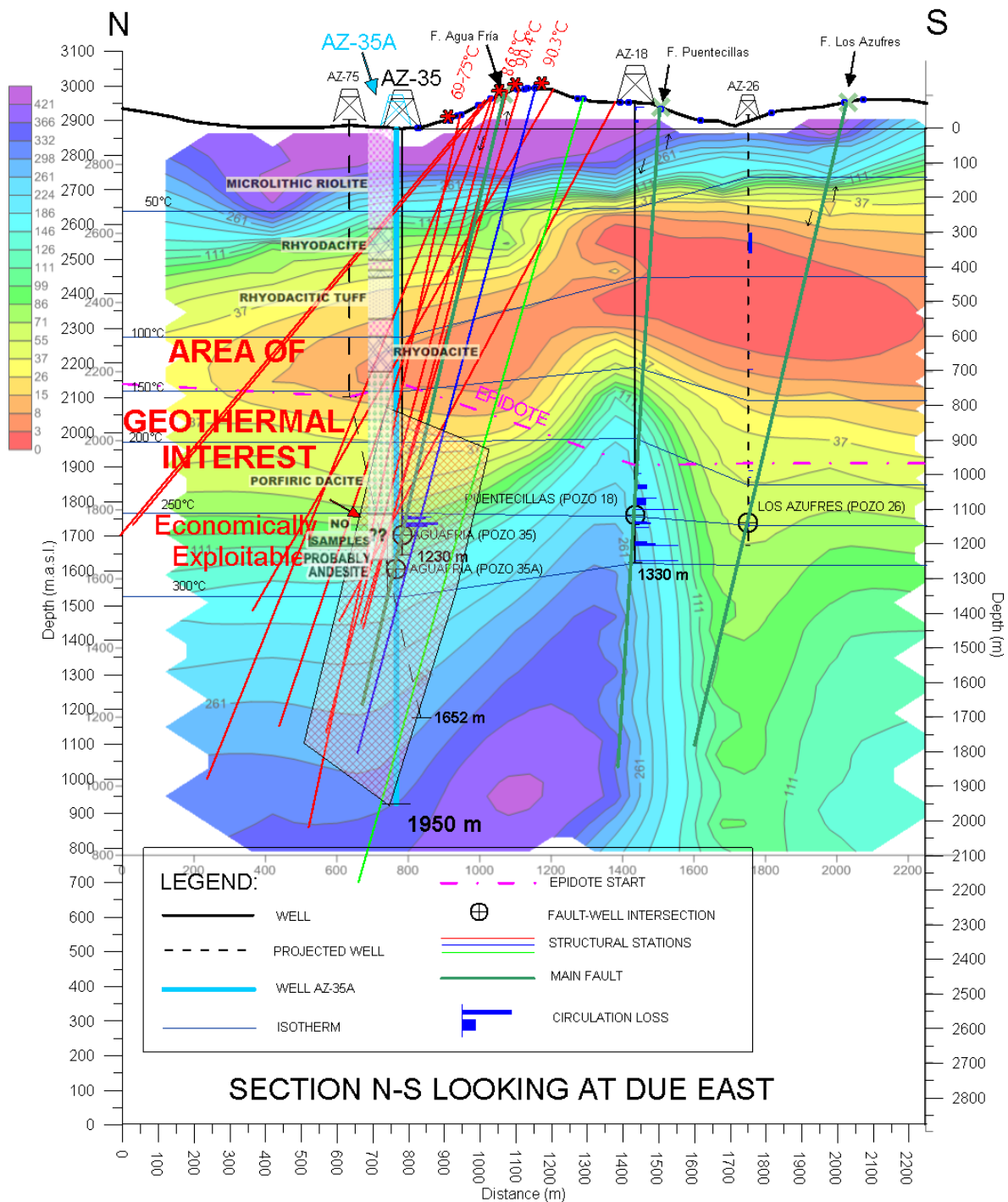


Figure 85: N-S profile, investigating the E-W structural System, with displayed Area of Geothermal Interest, circulation losses, lithostratigraphic column, structural datum and geoelectrical profile.

In the NW-SE profile (Figure 86), valid for the NE-SW structural system, the Area of Geothermal Interest is located again at a depth ranging between 900 and 1950 m below ground level, where the structural features and the Epidote zone are already

detected. Temperatures in this area are between 220 and  $>300^{\circ}\text{C}$ , and so this zone is economically exploitable.

Circulation losses are concentrated in the same zone as the majority of the structural features are.

Like in previous case, there are two main geoelectric zones associated with fracturing that can be intercepted by drilling the AZ-35A. The shallower geoelectric zone, that is the *high conductive* one (red-yellow color,  $0 < \rho < 35 \text{ Ohm}\cdot\text{m}$ ) between 200 and 800 m of depth, like before, coincides with the Rhyolitic-Dacitic cap rock which is known to be altered by fluids entering the zone through the Agua Fría Fault System. This interval is not economically advantageous for power production because the temperatures are lower than  $200^{\circ}\text{C}$  and so not good for the condensation cycle. The deeper geoelectric zone is the *conductive* one ( $35\text{-}250 \text{ Ohm}\cdot\text{m}$ ; from yellow to light blue color) and it coincides with the Area of Geothermal Interest between 800 and 1950 m of depth. In fact, hydrothermal reservoirs are supposed to be here because the E-W Agua Fría Fault is known to be reaching deep formations, intersecting with the N-S system (see Chapter 4.3).

In the W-E profile (Figure 87), produced to visualize the N-S structural System, the *Area of Geothermal Interest* is located between 1000 and 1950 m of depth,.

Also in this case, the Area of Geothermal Interest coincides with that of major faulting and fracturing, at a depth where the Epidote zone appears.

Circulation losses are concentrated in two zones; the first one is the same of the previous cases, between 1050 and 1250 m of depth, where the majority of the structural features cross the well. The second one is between 1430-1700 m of depth, and it is important because it proves the possibility of drilling the AZ-35A until 1950 m of depth.

Again, two principal geoelectric zones are present:

The *high conductive zone* (red-yellow color,  $0 < \rho < 35 \text{ Ohm}\cdot\text{m}$ ), between 0 and 800 meters below ground level, in the western part of the profile. This represents the Rhyolitic-Rhyodacitic altered cap rock, not economically exploitable.

The *conductive zone* (35-250 Ohm\*m; from yellow to light blue color), between 800 and 1950 m below ground level, represents the deep reservoir where the Agua Fría Fault system intersects the N-S system, making this zone of the underground suitable for exploitation. This zone coincide with the Area of Geothermal Interest and temperatures here are between 200 and >300°C, making the zone economically exploitable.

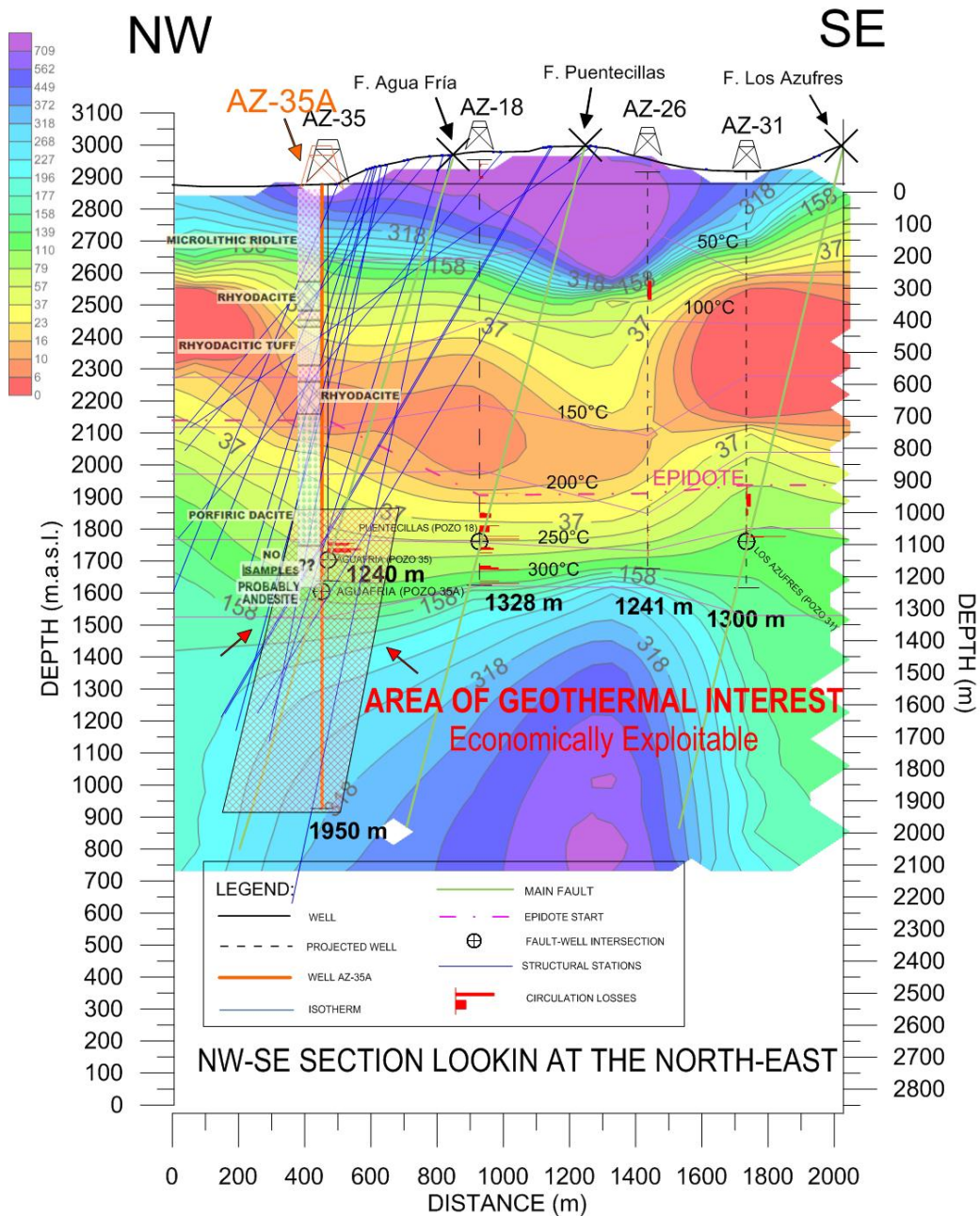


Figure 86: NW-SE profile, investigating the NE-SW structural System, with displayed Area of Geothermal Interest, circulation losses, lithostratigraphic column, structural datum and geoelectrical profile.

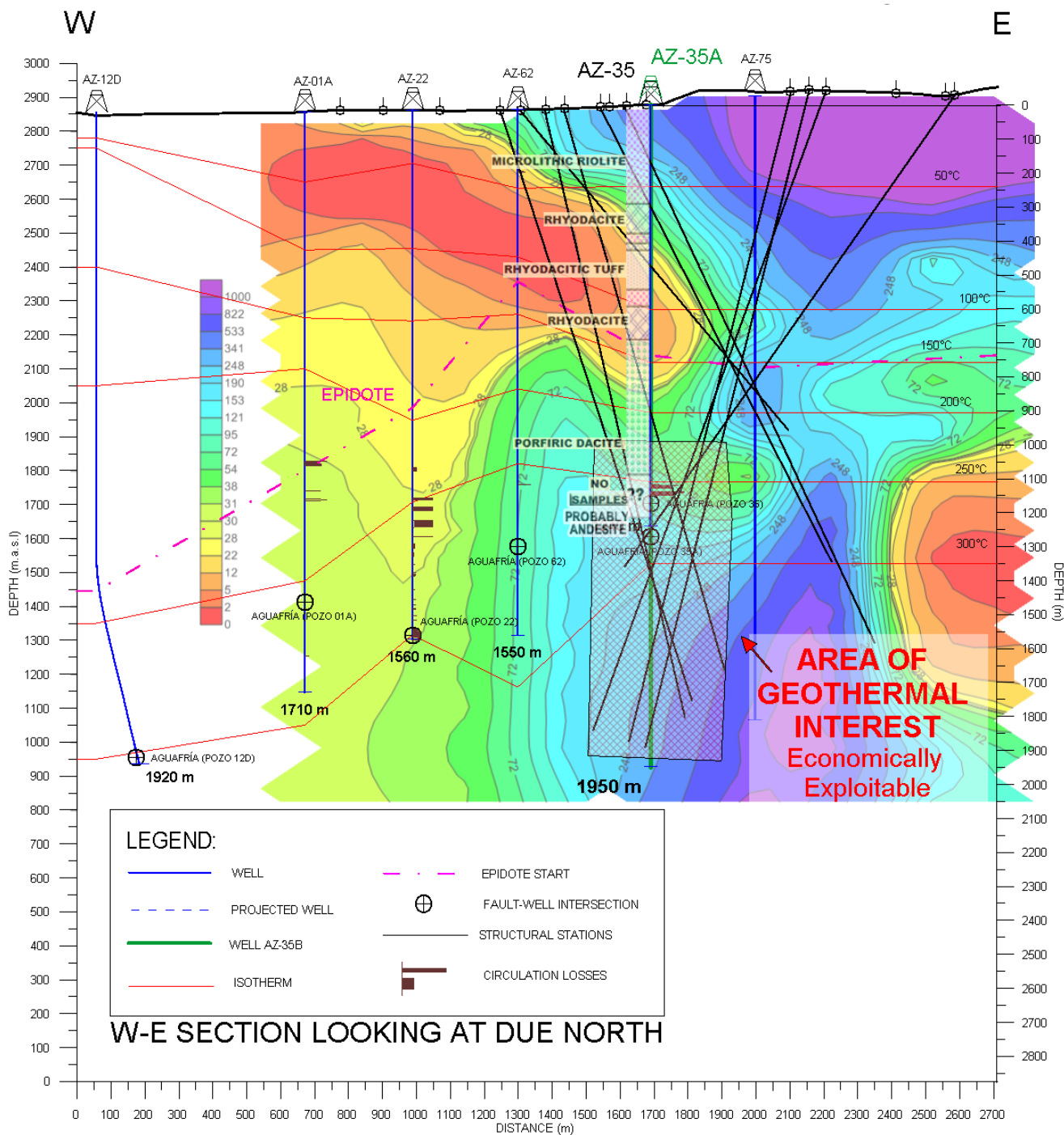


Figure 87: W-E profile, investigating the N-S structural System, with displayed Area of Geothermal Interest, circulation losses, lithostratigraphic column, structural datum and geoelectrical profile.

Finally, a profile of SW-NE direction related to the NW-SE structural system was produced (Figure 88).

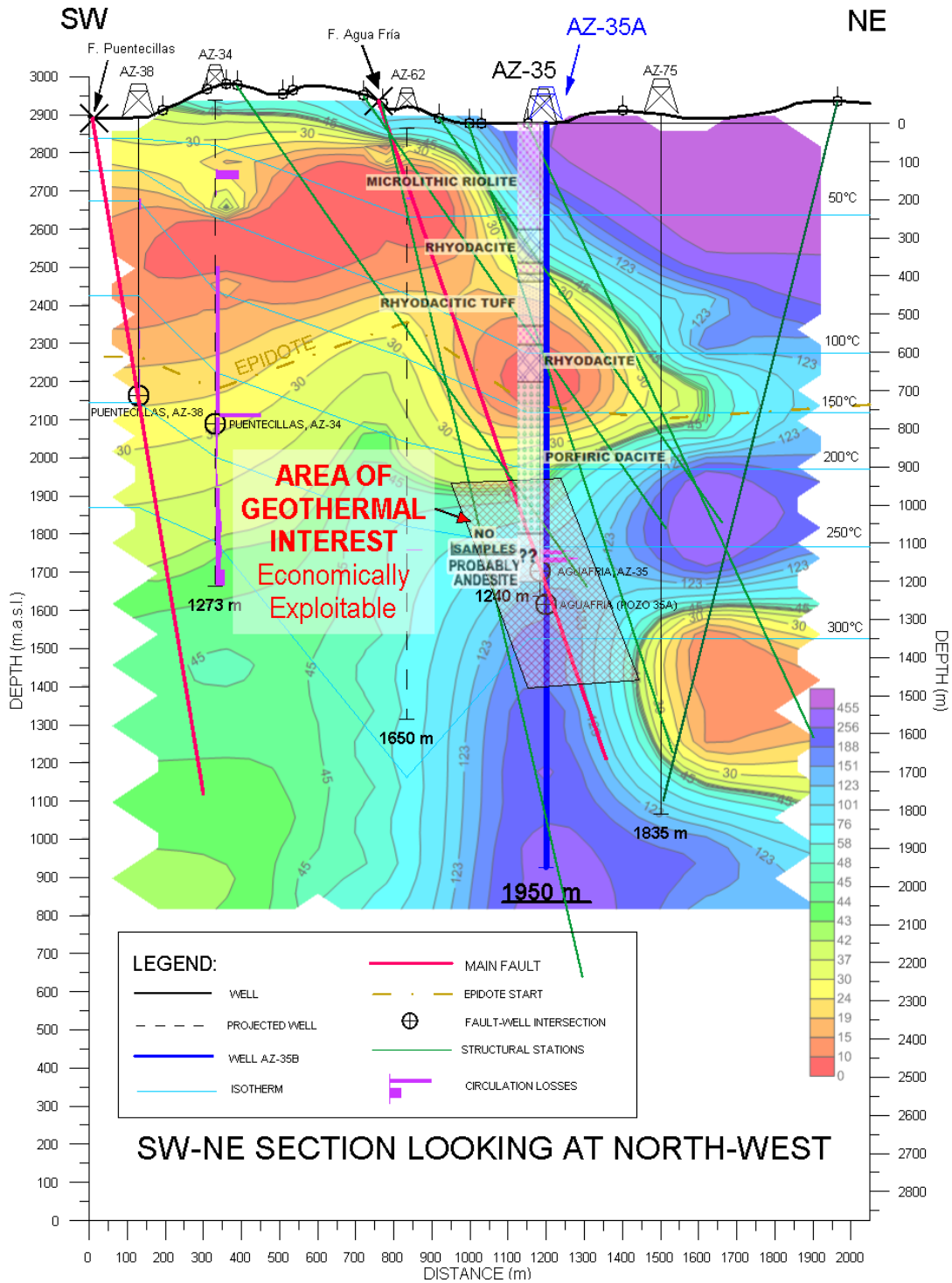


Figure 88: SW-NE profile, investigating the NW-SE structural System, with displayed Area of Geothermal Interest, circulation losses, lithostratigraphic column, structural datum and geoelectrical profile.

In this case, the *Area of Geothermal Interest* extends just between 1000 and 1500 m of depth.

The geoelectrical section indicates that, in the Area of Geothermal Interest, the conductive zone is present and the zone is economically favorable for the exploitation of the geothermal fluid, with temperatures between 200 and 300°C. Differently from the previous cases, at depths major than 1500 m, the *high resistive zone* is entered, which is not suitable for exploitation. The *high conductive zone* between 100 and 800 m below ground level, which is the Rhyolitic–Dacitic altered cap rock is not exploitable as well, due to temperature <200°.

Even though Circulation Losses and Epidote are present in the Area of Geothermal Interest, the geoelectrical results, along with the scarcity of fracturing and faulting features (detected in situ) of this structural system, seem to not favor the idea of drilling the well AZ-35A until depths major than 1500m. Anyway, this is considered to be the less important of all the structural systems and so it can be taken into scarce consideration.

So finally, considering all the results from Circulation Losses, Resultant Structural Data, Petrographic analysis and Geophysical analysis, and with the purpose of defining a unique proposal for all the structural systems, it can be affirmed and confirmed that **the zone of interest is between 750 and 1950 m of depth**. It is comprised in a zone where the rock is characterized by a strong hydrothermal alteration, fractured by two main systems N-S and E-W oriented. Therefore, we should expect a good permeability, with reservoir temperatures increasing from 180°C to 300°C with depth. Lost Circulation are supposed to appear between 1050-1350 m of depth (~1900 and 1600 m.a.s.l.), between 1430-1700 m of depth. (1470 and 1250 m.a.s.l) and probably also from 1850-2100 m of depth. (1100 to 850 m.a.s.l) .

Therefore, the proposal of perforating the well AZ-35A until a depth of 1950 m is advanced, localizing it 15 m to the north with respect to the AZ-35, using the same platform in its northern corner. Considering that the platform stands at an altitude of 2877 m.a.s.l., the new well AZ-35A should end at 927 m.a.s.l.

Therefore, the well would be vertical with pierced pipeline starting at 737 m of depth), when the Epidote zone appears.

The reasons why it is proposed to perforate the well until a depth of 1950 are the following:

1. The Agua Fría Fault system is wide and data collected either at the north or at the south of this Fault state this fact. The fault footwall reaches greater depths, with respect to the 1240 m reached by well AZ-35. Therefore, the new well can intercept a greater amount of geothermal fluid.
2. Due to the dip of the Agua Fría Fault system, the drilling of the AZ-35A well north to the AZ-35, allows to intercept a greater thickness of geothermal reservoir (low conductive zone) and to meet the fault plain at a greater depth (at 1272 m of depth instead of 1172 m). In this way the geothermal fluids will have a greater temperature, with benefits for the production cycle.
3. Drilling the well more in depth will allow to intersect more than one Lost Circulation zones, increasing the availability of fluid circulating in the permeable zones created by the intersection of different fault systems.
4. At greater depth the geothermal fluid will be characterized by a greater liquid dominant phase, which is more productive and long-lasting for power production.

## 8 CONCLUSION

The obtained results indicate that the proposed well AZ-35A would be drilled in a zone of high geothermal potential. In fact, *Structural Geology* analyses allowed to understand that two main N-S and E-W structural systems are intersecting at great depth, making the geothermal reservoir of the Los Azufres Geothermal Field particularly interesting for geothermal exploitation in this area. The fractured area seems to be uninterruptedly present from 800 to 1950 m of depth. In confirmation of this, *Lost Circulation* analyses showed that three zones of high geothermal fluid circulation should be encountered below 800 m of depth during the perforation, corresponding with high fracturing targets, and *Petrographic* Analyses collected during the AZ-35 well drilling, permitted to identify the presence of hydrothermal alteration minerals which indicate the presence of hydrothermal fluids and so the exploitability of the fractured zone. In addition, *Geoelectrical Resistivity* analyses confirmed the presence of saline conductive fluids below 800 m of depth, where low resistivity is present. Completing the study, Geochemical and Thermodynamic Data of LAGF production wells proved that the geothermal reservoir is liquid-dominant with suitable temperatures, pressure and yield for the application of the Condensation Cycle useful for electric power production.

Given all these information, the well AZ-35A is proposed to be drilled until a depth of 1950 m, with pierced pipeline starting at about 800 m of depth. In such a way, the exploitation of the geothermal fluid would be maximized and the productivity would be long-lasting, due to the high quantity of hydrothermal fluids which were detected with the analyses. Temperatures of geothermal fluids are expected to increase from 180 to more than 300°C in the zone between 800 and 1950 m of depth. It is recommended to integrate the New Well in the reinjection pipeline system of the LAGF, which would increase the long-lasting quality of the reservoir even more.

From this study, the suitability of the multidisciplinary and simplified approach adopted at the Los Azufres Geothermal Field has been proven and it can be affirmed that this method is replicable in others field of the world.

At this point, it is desirable that the collaboration between the CFE and the University of Padua could continue in the future. This would be important for the sharing and improvement of knowledge in the geothermal exploitation field, either for Italian academic students with the high enthalpy geothermal interest, who desire to have a work experience in a consolidated institution such as the CFE, or for Mexican Students who intend to learn about the scientific advances made by Italian institutes of research, such as the University of Padua, in the geothermal field.

Moreover, the sharing of knowledge and information between different important institutions working on Geothermal Energy is important because allows the improvement of the RES sector in the broad sense, and contributes to the development of a greener world. To work on geothermal energy is not only an economic opportunity, but also an opportunity to safeguard the planet from the environmental depletion and pollution caused by the use of carbon-fossil fuels.

## BIBLIOGRAPHY

Aguayo J.E., Trápaga R. *Geodinámica de México y Minerales del Mar*, 1996.

Alemán-Nava Gibrán S. Casiano-Flores Victor H., Cárdenas-Chávez Diana L., Díaz-Chavez Rocío, Scarlat Nicolae, Mahlkecht Jürgen, Dallemand Jean-Francois, Parra Roberto. *Renewable energy research progress in Mexico: A review*. *Renewable and Sustainable Energy Reviews* 32 (2014) 140–153.

Bellieni G., Predonzan R., Sambo M., Ravagnan C. *Manuale di ottica dei minerali delle rocce cristalline*. Il Leggio libreria editrice. 2004

CFE 2007. *Structural Datum of Field Survey*. Campo geotérmico de Los Azufres. Área de Geología.

CFE. 2011. Subdirección de Generación, Gerencia de Proyectos Geotermoeléctricos, Subgerencia de Estudios. *M.I.A. Manifestación De Impacto Ambiental, Modalidad Particular, Proyecto Geotermoeléctrico Los Azufres III 75MW*. Octubre 2011.

CFE 2012 (1). Photographs of well AZ-35. Campo geotérmico de Los Azufres. Área de Geologia.

CFE 2012 (2). *Structural Datum of Field Survey*. Campo geotérmico de Los Azufres. Área de Geologia.

CFE. 2014. “*Análisis de la declinación de la producción de los pozos productores del CGLA*”. Campo geotérmico de Los Azufres. Área de Ingeniería de Yacimientos.

CFE. 2015 (1). *Propuesta de Reposición del Pozo AZ-35A*. Campo geotérmico de Los Azufres. Área de Ingeniería de Yacimientos.

CFE. 2015 (2). *Como realizamos sondeos transitorios electromagneticos (TEM) y su utilidad*. Internal report.

Constable Steven C., Parker Robert L., and Constable Catherine G. *Occams' inversion: A practical algorithm for generating smooth models from electromagnetic sounding data*. *Geophysics*, Vol. 52, No. 3 (March 1987): P 289-300.

Constable Steven C., De Groot-Hedlin C. *Occams' inversion to generate smooth, two-dimensional models from magnetotelluric data*. *Geophysics*, Vol. 55, No. 12 (December 1990): P. 1613-1624.

Di Pippo Ronald. *Geothermal Power Plants, Principles, Applications, Case Studies and Environmental Impact*. Second Edition. 2007.

Ferrari L., Garduño V.H., Pasquaré G. and Tibaldi A. *Geology of Los Azufres caldera, Mexico, and its relationships with regional tectonics*. *Journal of Volcanology and Geothermal Research*, 47 ( 1991 ) 129-148 Elsevier Science Publishers B.V., Amsterdam

Ferrari L., Morán-Zenteno D., González-Torres E.A., 2007, *Actualización y adaptación de la Carta Geologica de la Republica Mexicana*, escala 1:2,000,000 publicada por el Instituto de Geologia de la UNAM y el Consejo de Recursos Minerales (Ortega-Gutiérrez et al., 1992)

Ferrari, L., M. López-Martínez, G. Aguirre-Díaz, and G. Carrasco-Nuñez, 1999. *Space-time patterns of Cenozoic arc volcanism in central Mexico: from the Sierra Madre Occidental to the Mexican Volcanic Belt*. *Geology*, No. 27, pp. 303-306.

Ferrari L., Orozco-Esquivel T., Manea V., Manea M., 2012, *The dynamic history of the Trans-Mexican Volcanic Belt and the Mexico subduction zone*. *Tectonophysics* 522–523 (2012), 122–149.

Flores Alcalá Luis Alberto. *Generación eléctrica con el Ciclo pressured water Generation (pwg)*. T e s i s, Universidad nacional Autónoma de México, Facultad de ingeniería. Que para obtener el titulo de: Ingeniero eléctrico y electrónico. 2012.

Grant Malcolm A., Bixley Paul F. *Geothermal Reservoir Engineering*. 2<sup>nd</sup> edition. 2011.

Gutierrez-Negrin Luis C. A.. *Update of the Geothermal Electric Potential in Mexico of the Mexican Geothermal Association (AGM)*, Morelia, Mich., Mexico. GRC Transactions, Vol. 36, 2012.

Iglesias Eduardo R., Dominguez a. Bernardo, Aragón A. Alfonso. *The Los Azufres, Mexico, Geothermal Reservoir: a Case History*. Revista Brasileira de Geofísica; Vol. 5 pp 335-346. 1987

Izaguirre Avila Oscar A., Ingeniero de la CFE, Superintendencia de Estudio, Area de Geologia. *Informe Geologico del Pozo Azufres No. 35*. 1983.

Karingithi Cyrus W., *Chemical Geothermometers for Geothermal Exploration*. Kenya Electricity Generating Company Ltd. (KenGen). Presented at Short Course IV on Exploration for Geothermal Resources, organized by UNU-GTP, KenGen and GDC, at Lake Naivasha, Kenya, November 1-22, 2009.

Lagat, John K., *Hydrothermal Alteration Mineralogy in Geothermal Fields with case examples from Olkaria Domes Geothermal Field, Kenya*. Geothermal Development Company, Kenya. Presented at Short Course V on Exploration for Geothermal Resources, organized by UNU-GTP, GDC and KenGen, at Lake Bogoria and Lake Naivasha, Kenya, Oct. 29 – Nov. 19, 2010.

Legg Christopher, C3P Consultant. *An Introduction to Geographic Information Systems (Gis) For the Crop Crisis Control Project using Diva Gis*. March 2007.

Lisle Richard J., Braham Peter J., Barnes John W. *Basic Geological Mapping*. 5<sup>th</sup> edition, 2011.

López-Gómez J. Guadalupe, Molina Martínez Abraham Ill, Hernández Pérez Adriana y Sandoval Medina Alejandro. *Resultados Geológicos, de Perforación y Producción del Pozo AZ-89, del Campo Geotérmico de Los Azufres, Mich.* Geotermia – Revista Mexicana de Energia. Volumen 28, No.1 Enero- Junio 2015.

Mohan Doshi. *Lost circulation – the Basics*. Unpublished presentation, Deputy General Manager at ONGC (Oil and Gas National Corporation), Bangalore, India. 2014.

Molina Martínez Abraham III. *Case History of Los Azufres – Conceptual Modelling in a Mexican Geothermal Field*. Presented at “Short Course V on Conceptual Modelling of Geothermal Systems”, organized by UNU-GTP and LaGeo, in Santa Tecla, El Salvador, February 24 - March 2, 2013.

Ormad Abraham. *Actualidad sobre el Campo Geotérmico Cerritos Colorados, México*. ThinkGeoEnergy News. September 30, 2014.

Ortega-Gutiérrez Fernando, Mitre-Salazar L. M., Alaniz-Álvarez. Susana, Roldán-Quintana Jaime, Aranda-Gómez J. J., Nieto-Samaniego Á. F., Y Morán-Zenteno, D. J., 1991, *Geologic provinces of Mexico -a new proposal and bases for their definition*: Universidad Nacional Autónoma de México, Instituto de Geología; Universidad Autónoma de Hidalgo. Instituto de Investigaciones en Ciencias de la Tierra; Sociedad Mexicana de Mineralogía; y Secretaria de Educación Pública. Subsecretaría de Educación Superior e Investigación Científica, Convención sobre la evolución geológica de México y Primer Congreso Mexicano de Mineralogía, Pachuca, Hidalgo, Memoria, p. 143- 144.

Ortega-Gutiérrez Fernando, Mitre-Salazar L. M., Alaniz-Álvarez. Susana, Roldán-Quintana Jaime, Aranda-Gómez J. J., Nieto-Samaniego Á. F., Y Morán-Zenteno, D. J., 1992, *Carta Geológica de la Republica Mexicana, escala 1:2,000,000, 5ª edición*. Compilada por el instituto de Geología de la UNAM y auspiciada por el Consejo de Recursos Minerales.

Pérez Esquivias Héctor, Macías Vázquez José Luis, Garduño Monroy Víctor Hugo, Arce Saldaña José Luis, Tenorio Felipe García, Govea Renato Castro, Layer Paul, Saucedo Girón Ricardo, Martínez Carlos, Jiménez Haro Adrián, Valdés Gabriel, Meriggi Lorenzo y Hernández Ramón. *Estudio vulcanológico y estructural de la secuencia estratigráfica Mil Cumbres y del campo geotérmico de Los Azufres, Mich.* Geotermia, Vol. 23, No.2, Julio-Diciembre de 2010.

Raith Michael M., Raase Peter & Reinhardt Jürgen. *Guide to Thin Section Microscopy*. Second Edition. ISBN 978-3-00-037671-9 (PDF). 2012.

Robin, C., and Pradal, E. 1993. *The Los Azufres caldera, Mexico—Comment on the paper by Ferrari et al., –An attempt to understand the volcanic structure–*. Journal

of Volcanology and Geothermal Research, No. 56, pp. 339-344. Torres-Rodriguez V. *Geothermal Chart of Mexico, scale 1:2,000,000/2000*. Unidad de Geotermia, Instituto de Investigaciones Eléctricas a.p. 1-475, Cuernavaca, Morelos, Mexico. 2000.

SENER. Secretaría Nacional de Energía. *Prospectiva de Energías Renovables 2012-2026*. Published in 2012.

Sørensen Kurt PhD, Christiansen Anders Vest PhD, Auken Esben PhD. *The Transient Electromagnetic Method*. Groundwater Geophysics. 2006, pp 179-225.

Urrutia-Fucugauchi, J., Flores-Ruiz, J., 1996. *Bouger gravity anomalies and Regional crustal structure in central Mexico*. International Geology Review 38, 176–194.

Waldron J., *Introduction to the stereographic projection*. From Lesson Lab 3 of the course EAS 233 “Geologic Structures and Maps”. Winter 2009. Academic Year 2008-2009 Department of Earth & Atmospheric Sciences. Faculty of Science. University of Alberta.